





EX LIBRIS
UNIVERSITATIS
ALBERTENSIS

The Bruce Peel
Special Collections
Library



Digitized by the Internet Archive
in 2025 with funding from
University of Alberta Library

<https://archive.org/details/0162014888562>

University of Alberta

Library Release Form

Name of Author: **Carmen Vanessa Rieder**

Title: **Expression of the Na⁺/H⁺ Exchanger Isoform 1 in Development**

Degree: **Master of Science**

Year this Degree Granted: **2001**

Permission is hereby granted to the University of Alberta Library to reproduce single copies of this thesis and to lend or sell such copies for private, scholarly or scientific research purposes only.

The author reserves all other publication, and other rights in association with the copyright in the thesis, and except as herein before provided, neither the thesis nor any substantial portion thereof may be printed or otherwise reproduced in any material form whatever without the author's prior written permission.

University of Alberta

**Expression of the Na^+/H^+ Exchanger Isoform 1
in Development**

by

Carmen V. Rieder 

A thesis submitted to the Faculty of Graduate Studies and Research in partial fulfillment of the requirements for the degree of Master of Science.

Department of Biochemistry

Edmonton, Alberta

Fall 2001

University of Alberta

Faculty of Graduate Studies and Research

The undersigned certify that they have read, and recommend to the Faculty of Graduate Studies and Research for acceptance, a thesis entitled Expression of the Na^+/H^+ Exchanger Isoform 1 in Development submitted by Carmen Vanessa Rieder in partial fulfillment of the requirements for the degree of Master of Science.

*For my husband, Manuel, whose love, encouragement and support
have been my strength*

And for Mom, Dad & Tyler, who have always believed in me

Abstract

Developmental regulation of the Na^+/H^+ exchanger isoform 1 (NHE1) promoter activity and protein expression was investigated. Examination of NHE1 transcription in GFP reporter gene transgenic mouse embryos revealed that NHE1 transcription is highest in the heart and liver of the youngest embryos examined (E12 and E15). Also, NHE1 transcription decreases in these organs from E12 to E18 and plateaus thereafter. Therefore, NHE1 is likely to play a significant role in early heart and liver development. Western blotting with an anti-NHE1 monoclonal antibody was used to measure NHE1 protein levels in wild type 18-day-old embryos, neonates and adults, and in AP-2 α and COUP-TFI gene disruption mice. It was concluded that NHE1 is subject to developmental and tissue-specific regulation because protein levels varied with age, and were found to differ between tissues at one age. Also, AP-2 α and COUP-TFI are not likely involved in NHE1 protein expression at E18 or older.

Acknowledgements

First and foremost, I would like to thank Dr. Larry Fliegel for introducing me to research (beginning as a summer student in 1995), for the opportunity to further pursue research as a graduate student, and for his patient supervision of this project.

Next, I would like to acknowledge the past and present members of the Fliegel lab, who have frequently shared their knowledge and encouraged me: Brenda Booth, Bonnie Bullis, Dr. Pavel Dibrov, Dr. Francoise Fernandez-Rachubinski, Dr. Xioju Li, Anice Lowen, Dr. Andrea Moor, Dr. Rakhilya Murtazina, Lena Salvadorov, Dr. D. Singh, Christine Wiebe, Bryan Yu.

I owe many thanks to individuals that have helped me with technical aspects of this project. I am indebted to Dr. Nasrin Mesaeli and Dr. Kim Nakamura, who provided tips and techniques on the care and use of mice; and to Dr. Peter Dickie, who generated the transgenic mice. Also, I am grateful to Dr. Bagnall, Dr. Chlumecky, Dr. Sun, and Dr. Young for sharing their microscopy expertise and equipment.

I would also like to thank the many members of the Health Sciences Lab Animal Services (HSLAS) facility who frequently provided invaluable mouse management assistance, especially Holly Demare, Keith Hussen, Brenda Roszell and Michelle Schrader.

Finally, I am grateful for the financial support of the Alberta Heritage Foundation for Medical Research.

Table of Contents

Chapter I: Introduction

I-1.	Physiological Roles of the Na⁺/H⁺ Exchanger.....	2
I-2.	The Na⁺/H⁺ Exchanger Family.....	3
I-3.	Structural Features of the Na⁺/H⁺ Exchanger.....	5
I-4.	Regulation of the NHE1 Protein.....	6
	<i>Phosphorylation</i>	7
	<i>Regulatory Proteins</i>	9
	<i>Acidosis, Hormones, Growth Factors and ATP</i>	10
I-5.	NHE1 Expression in Development and Differentiation.....	12
	<i>NHE1 Expression in Cellular Proliferation and Development.....</i>	12
	<i>NHE1 Expression in Cellular Differentiation.....</i>	13
I-6.	The NHE1 Promoter and Related Transcription Factors.....	16
	<i>The NHE1 Promoter.....</i>	16
	<i>The AP-2 Transcription Factors.....</i>	19
	<i>The Chicken Ovalbumin Upstream Promoter Transcription Factors (COUP-TFs).....</i>	20
I-7.	Phenotype of NHE1 Disrupted Mice.....	21
I-8.	NHE1 and Disease.....	24
	<i>Heart Disease.....</i>	25
	<i>Primary or Essential Hypertension.....</i>	28
	<i>Diabetes.....</i>	30
	<i>Cancer.....</i>	31
I-9.	Transcription Reporter Genes.....	33
	<i>The Green Fluorescent Protein.....</i>	34
	<i>The β-Galactosidase Protein.....</i>	36
I-10.	Thesis Objectives.....	37

Chapter II: Materials and Methods

II-1.	Materials.....	41
II-2.	Construction of Transgenic Mice with Reporter Genes.....	42
	<i>Assembly of Reporter Gene Constructs.....</i>	<i>42</i>
	<i>Construction of Transgenic Mice.....</i>	<i>44</i>
II-3.	Assay of Reporter Gene Activity in Mammalian Cells.....	45
	<i>Transfection of NIH 3T3 Cells.....</i>	<i>45</i>
	<i>Microscopy of GFP-transfected NIH 3T3 Cells.....</i>	<i>46</i>
	<i>Luminometer Assay for βgal Activity.....</i>	<i>46</i>
II-4.	Genotyping by Step-down PCR.....	47
II-5.	Preparation and Microscopy of GFP-positive Embryos.....	49
II-6.	Quantification of GFP Fluorescence.....	50
II-7.	X-Gal Staining of β-Galactosidase Reporter Embryos.....	51
II-8.	NHE1 Immunoblot Analysis.....	52
	<i>Preparation of Crude Microsomes from Mouse Organs.....</i>	<i>52</i>
	<i>NHE1 Immunoblots.....</i>	<i>53</i>
	<i>Immunoprecipitation of NHE1.....</i>	<i>54</i>
II-9.	Rat Heart Metabolic Experiments.....	55
	<i>Preparation of Rat Neonatal Myocyte Primary Cultures.....</i>	<i>55</i>
	<i>Treatment of Primary Myocyte Cultures with Different Metabolic Conditions.....</i>	<i>56</i>
	<i>Preparation of Microsomes from Myocyte Cultures.....</i>	<i>57</i>
	<i>NHE1 Immunoblots of Myocyte Microsomes After Different Metabolic Treatment.....</i>	<i>58</i>
II-10.	Genotyping of AP-2α Knock-out Mice.....	58

Chapter III: NHE1 Promoter Activity During Mouse Development

III-1.	Introduction.....	73
III-2.	Results.....	74
	<i>Development of NHE1 Promoter-Reporter Constructs and Creation of Transgenic Mice.....</i>	74
	<i>Analysis of the NHE1-promoter GFP-reporter Transgenic mice.....</i>	76
	<i>Analysis of the NHE1-promoter βgal-reporter Transgenic mice.....</i>	78
III-3.	Discussion.....	79

Chapter IV: NHE1 Protein Expression in Late Mouse Embryogenesis to Adulthood

IV-1.	Introduction.....	109
IV-2.	Results.....	110
	<i>NHE1 Protein Expression in the Late Embryo to the Adult.....</i>	110
	<i>NHE1 Protein Expression in Mice Lacking the Transcription Factors AP-2α or COUP-TFI.....</i>	113
IV-3.	Discussion.....	115

Chapter V: Summary and General Conclusions

V-1.	Summary and General Conclusions.....	145
V-2.	Future Experiments.....	148

Chapter VI: References

VI-1.	References.....	151
--------------	------------------------	------------

List of Tables

Chapter II: Materials and Methods

Table II-1	Recipes for Rat Neonatal Myocyte Culture Solutions.....	70
Table II-2	Media Recipes for Rat Myocyte Metabolism Experiments.....	71

List of Figures

Chapter I: Introduction

- Figure I-1** Schematic of the putative topology of NHE1 and the proposed regulatory mechanisms.....39

Chapter II: Materials and Methods

- Figure II-1** Construction of NHE1 Promoter-Reporter Gene Plasmids.....61

Chapter III: NHE1 Promoter Activity During Mouse Development

- Figure III-1** Schematic diagram of the NHE1 promoter-reporter gene DNA constructs used to generate the transgenic mice.....87

- Figure III-2** Nucleotide sequence of the 3.8-kb NHE1 promoter region.....89

- Figure III-3** Expression of the NHE1 promoter-reporter gene constructs in transiently transfected NIH 3T3 cells.....93

- Figure III-4** Genotyping Mice by Step-down PCR.....95

- Figure III-5** Activation of the NHE1 promoter in GFP-positive embryos at 12-, 15-, and 18-days-old.....97

- Figure III-6** Quantification of NHE1 promoter activity in the heart, liver and lung of 12-day-old embryos.....99

- Figure III-7** Activation of the NHE1 promoter in 12-day-old embryos hearts visualized at high magnification.....101

- Figure III-8** Quantification of NHE1 promoter activity in the heart, liver and lung of 15-day-old embryos....103

Figure III-9	Quantification of NHE1 promoter activity in hearts of: 18-day-old embryos, 1-day-old neonates, 14-day-old neonates and adults.....	105
Figure III-10	Activation of the NHE1 promoter in βgal-positive embryos at 12-days-old.....	107

Chapter IV: NHE1 Protein Expression in Late Mouse Embryogenesis to Adulthood

Figure IV-1	Optimization of Western blot analysis for the Na^+/H^+ exchanger protein from mammalian heart and kidney.....	123
Figure IV-2	Comparison of NHE1 protein expression levels in various organs from 18-day-old embryos, 1-day-old neonates, 2-day-old neonates, 14-day-old neonates and adults.....	125
Figure IV-3	Comparison of NHE1 protein expression levels in heart, lung, liver, kidney and brain at various ages.....	129
Figure IV-4	Comparison of NHE1 protein expression levels in rat cardiomyocytes treated with control, high glucose or high fat media.....	133
Figure IV-5	Analysis of NHE1 protein expression in 1-month-old mice lacking the AP-2α transcription factor.....	135
Figure IV-6	Analysis of NHE1 protein expression in 18-day-old embryos lacking the AP-2α transcription factor.....	139
Figure IV-7	Analysis of NHE1 protein expression in 18-day-old embryos lacking the COUP-TFI transcription factor.....	143

Abbreviations

Ad	Adult mouse
AP-2	Activating protein 2
AP-2α	Activating protein 2 α isoform
ATP	Adenosine triphosphate
B	Brain
βgal	B-Galactosidase gene
BSA	Bovine serum albumin
CaM	Calmodulin
C/EBP	CCAAT / enhancer binding protein
CHP	Calcineurin homologous protein
COUP-TF	Chicken ovalbumin upstream promoter transcription factor
COUP-TFI	Chicken ovalbumin upstream promoter transcription factor I isoform
Ctrl or C	Control
D1	1-day-old neonatal mouse
D14	14-day-old neonatal mouse
DMA	5-(N,N-dimethyl) amiloride
E12	Embryonic day 12
E15	Embryonic day 15
E18	Embryonic day 18
EIPA	Ethylisopropyl amiloride
FITC	Fluorescein isothiocyanate
G16	GFP mouse line number 16
G34	GFP mouse line number 34
GFP	Green fluorescent protein
H	Heart

HMA	5-(N, N-hexamethyl) amiloride
HMG	High mobility group
hsp70	Heat shock protein 70
K	Kidney
Liv	Liver
Lu	Lung
MAPK	Mitogen-activated protein kinase
NHE	Na ⁺ /H ⁺ exchanger
NHE1	Na ⁺ /H ⁺ exchanger isoform 1
NHE1P	Na ⁺ /H ⁺ exchanger promoter
P-buffer	Phosphate buffer
PCR	Polymerase chain reaction
PIP₂	phosphatidylinositol 4,5-bisphosphate
PKA	Protein kinase A
PKC	Protein kinase C
PMA	Phorbol 12-myristate 13-acetate
RA	Retinoic acid
RPM	Revolutions per minute
SHR	Spontaneously hypertensive rats
swe	Slow-wave epilepsy
VSMC	Vascular smooth muscle cell(s)
W2	2-week-old neonatal mouse
wt	Wild type
X-Gal	5-bromo-4-chloro-3-indoyl-β-D-galactopyranoside
+/-	Heterozygous for mutation
-	Homozygous for mutation

Chapter I

Introduction

I-1. Physiological Roles of the Na^+/H^+ Exchanger

Cellular metabolism generates a significant intracellular acid load; therefore, the active extrusion of acid equivalents is vital to maintain homeostasis. The cell is equipped with several plasma membrane transporters that regulate intracellular pH by facilitating acid efflux (Na^+/H^+ exchangers (NHE), ATP-driven proton pumps, $\text{Na}^+/\text{HCO}_3^-$ cotransporters) or acid entry ($\text{Cl}^-/\text{HCO}_3^-$ exchangers) into the cell.¹ The Na^+/H^+ exchanger is activated in acidic intracellular conditions; therefore, NHE is involved in physiological pH restoration following cellular acidification.¹

The Na^+/H^+ antiporter catalyzes the electroneutral exchange of one intracellular H^+ for one extracellular Na^+ . This activity is driven by the inwardly directed Na^+ gradient; however, ATP is necessary for optimal exchange.² The velocity of the reaction depends on the external Na^+ concentration in a manner that can be described by Michaelis-Menten kinetics.² However, if the Na^+/H^+ exchange activity only depends on the ever-present extracellular Na^+ gradient, why is NHE not constitutively active in physiological conditions? To answer this question, a proton modifier site on the cytoplasmic face of the protein has been hypothesized.³ This proton modifier site is suggested to be distinct from the H^+ binding site for transport, and is responsible for allosteric regulation of the antiporter.³ Furthermore, the existence of this site would explain the fact that NHE is exquisitely sensitive to changes in intracellular pH.³

In addition to maintenance of cytosolic pH, NHE plays an important role in cell volume regulation in response to osmotic shrinkage. In theory, the replacement of one intracellular H^+ for one extracellular Na^+ would not alter the osmolarity; however, active metabolism quickly generates more H^+ , and thus a net Na^+ gain results. The elevated Na^+ levels increase cellular osmolarity, which obligates water to enter the cell and correct the shrinkage.³ By a similar mechanism, NHE is also responsible for Na^+ reabsorption across intestinal and renal epithelia.²

I-2. The Na^+/H^+ Exchanger Family

The Na^+/H^+ exchanger family currently encompasses at least seven integral membrane proteins that share the ability to transport sodium and hydrogen ions. Sardet et al.⁴ isolated the first Na^+/H^+ exchanger isoform, NHE1, using a genetic complementation approach. In this procedure, hamster fibroblasts were chemically mutagenized and then selected for the inability to survive an intracellular acid load. Next, human genomic DNA segments were transfected into the selected fibroblasts, and the cells were subjected to an intracellular acid load. DNA was isolated from transfected fibroblasts that acquired the capacity to withstand the acid challenge. This DNA was characterized and resulted in the identification of NHE1.

Six other transmembrane proteins have been added to the Na^+/H^+ exchanger family since the discovery of NHE1, and are referred to as NHE2 – NHE7.^{2,5} The Na^+/H^+ exchanger proteins range in size from 74 - 99 kDa (calculated molecular weights).^{5,6,7,8} NHE1 – NHE5 have 34-60% amino acid identity while NHE6 shares only 20% identity with the others.² The most recently discovered Na^+/H^+ exchanger, NHE7, is 70% identical to NHE6 in primary structure but only 25% similar to NHE1 - NHE5.

An eighth member may soon join the Na^+/H^+ exchanger family. Rajendran et al.⁹ have identified and characterized the Cl-dependent Na^+/H^+ exchanger (Cl-NHE). As implied by its name, Cl-NHE is uniquely dependent on chloride ions for antiport activity. The primary structure of this protein has not yet been reported, thus it cannot be compared to the aforementioned Na^+/H^+ exchangers.

All NHE isoforms have the capacity to transport Na^+ and H^+ ions; however, they differ with respect to cellular localization, tissue expression and pharmacology. NHE1- NHE4 and Cl-NHE reside in the plasma membrane while the localization of NHE5 is unclear at this time.^{9,10} NHE6 and NHE7 are found in the membranes of cellular organelles; NHE6 in the mitochondria, and NHE7 in the *trans*-Golgi network.^{2,5} NHE1 is expressed in all cell types and is therefore known as the "housekeeping" isoform. NHE2 is most abundant in the intestinal tract (although it has also been detected in many other tissues), while NHE3 is primarily found in the kidney, stomach and intestine.⁶ NHE4 has been identified

in the stomach, and NHE5 has been discovered in the brain and spleen, with less in the testis and skeletal muscle.⁶ NHE6 has been reported in the brain, skeletal muscle and heart,⁸ while NHE7 is likely expressed ubiquitously, with maximal levels observed in skeletal muscle, secretory tissues and parts of the brain.⁵ Cl-NHE has been detected in the crypt cells of the rat distal colon.⁹ With respect to pharmacology, all NHE family members are inhibited by amiloride and its derivatives, and by benzoyl guanidinium compounds such as HOE694. Typically, NHE1 is significantly more sensitive to these compounds than the others;^{2,5,7,9} however, each isoform has a unique inhibition constant for these drugs.

This thesis focuses on facets of the NHE1 isoform; therefore, information presented in the remainder of this chapter will be restricted to NHE1 unless otherwise indicated.

I-3. Structural Features of the Na⁺/H⁺ Exchanger

The Na⁺/H⁺ exchanger is composed of two structurally distinct domains. Hydropathy profiles identify an N-terminal transmembrane region of approximately 500 amino acids and a C-terminal domain of about 300 residues,¹¹ as depicted in Figure I-1. The N-terminal domain is comprised of 10-12 putative transmembrane segments and is responsible for the translocation of cations across the membrane. Putative membrane-spanning segments 6 and 7 exhibit 95% identity across the isoforms, and have thus been implicated as the actual site of ion exchange.² The N-terminal domain is also glycosylated¹² and contains the

predicted amiloride binding site in putative transmembrane segment 4.¹³ The C-terminal domain is located in the cytosol and is quite divergent amongst the isoforms. This divergence suggests that the C-terminal tail is required for regulation of the exchange activity. Further evidence for the regulatory role of the C-terminal domain comes from the observation that a truncated NHE1 mutant lacking this region is unresponsive to growth factor stimuli.¹¹

Wakabayashi et al.¹⁴ recently published a model for the homology of human NHE1. In their study, a cysteine-less NHE1 protein was generated, and its kinetic and pharmacological properties were confirmed to be similar to wild type. Eighty-three cysteine residues were individually introduced into the mutant NHE1, and biotin-streptavidin chemistry was then used to determine the accessibility of these cysteines in normal and permeabilized cells. In this system, a residue located on the external face of the cell could be detected with biotin and streptavidin in both normal and permeabilized cells; however, if the amino acid was internal, it would only react under permeabilizing conditions. From this exhaustive analysis, the investigators proposed that NHE1 contains twelve transmembrane domains, and that both N- and C-termini are situated in the cytosol.

I-4. Regulation of the NHE1 Protein

A large number of factors have been shown to stimulate the activity of the NHE1 protein including: phorbol esters, hormones, growth factors and chronic acidosis.⁶ The precise molecular mechanisms that stimulate NHE1 activity in response to these agents remain elusive. This section describes the known regulatory mechanisms that act directly on NHE1 (phosphorylation and specific regulatory proteins), and factors that have an indirect effect on NHE1 (acidosis, hormones, growth factors, and ATP).

Phosphorylation

Phosphorylation of NHE1 in response to growth factors is restricted to the distal 178 amino acids of the C-terminal tail (Figure I-1).¹⁵ Protein kinase C (PKC) pathways are important for acute regulatory phosphorylation of NHE1, as demonstrated by several lines of evidence. First, phorbol esters such as phorbol 12-myristate 13-acetate (PMA) activate PKC and stimulate NHE1 activity.⁶ Furthermore, aldosterone activation of NHE1 can be blocked by PKC inhibitors (such as staurosporine and calphostin C) and by the down-regulation of PKC in rat vascular smooth muscle cells.¹⁶ Also, it has been recently reported that PKC-dependent signalling pathways stimulate NHE1 in mouse proximal tubule cells in response to epinephrine.¹⁷

Mitogen-activated protein kinase (MAPK) (classically described as downstream of PKC in signalling cascades¹⁸) has been shown to directly

phosphorylate the C-terminus of NHE1. Wang et al.¹⁹ reported that MAPK-containing fractions from rabbit skeletal muscle and rat smooth muscle could phosphorylate the NHE1 C-terminal domain. Furthermore, MAPK immunodepletion diminished this phosphorylation. Wang et al.¹⁹ also demonstrated that transfection of Chinese hamster ovary cells with an inducible MAPK dominant negative mutant significantly reduced serum-stimulated cytosolic alkalinization. The results of this study clearly emphasize the role of MAPK in agonist-induced NHE1 activation. More recently, studies of isolated cardiomyocytes have confirmed MAPK involvement in mediating NHE1 stimulation.²⁰

Moor et al.²⁰ have identified that the protein kinase, p90^{rsk}, is both a substrate for MAPK, and a kinase of NHE1 in rat myocytes. In these studies, p90^{rsk} from endothelin-stimulated neonatal cardiomyocyte extracts exhibited enhanced phosphorylation of a fusion protein, which contained the carboxy-terminal 178 amino acids from rabbit NHE1. p90^{rsk} has also been shown to phosphorylate NHE1 upon angiotensin II stimulation in vascular smooth muscle cells.²¹

In contrast to PKC, MAPK and p90^{rsk}-mediated NHE1 regulation (which have been demonstrated in a number of cell types), the role of cAMP-dependent protein kinase A (PKA) appears to be cell-specific. For example, Na⁺/H⁺ exchange activity in PS120 fibroblast cells transfected with human or rabbit NHE1 could not be stimulated by cAMP analogues.⁶ However, NHE1 could be

activated by cAMP in murine macrophages, rat osteoblastic cells and rat hepatocytes.⁶ Clearly, the cellular milieu tempers the regulatory effect of PKA on NHE1.

Another kinase, p160ROCK, has recently been added to the list of enzymes that regulate NHE1 by phosphorylation. p160ROCK is involved in organization of the cytoskeleton, particularly the assembly of focal adhesions and actin stress fibres induced by the Rho family of small GTPases.²² It has been shown that treatment of fibroblasts with the NHE1 inhibitor ethylisopropyl amiloride (EIPA) inhibits p160ROCK-induced formation of stress fibres.²² Furthermore, expression of an activated p160ROCK in fibroblasts, stimulated NHE1 activity, and the direct phosphorylation of NHE1 by p160ROCK could be demonstrated *in vitro*.²²

Phosphorylation is an important mode of NHE1 activity modulation, and it is likely that many kinases belonging to NHE1 regulatory pathways remain unknown. Furthermore, roles for specific phosphatases in the control of NHE1 are yet to be defined. Clearly, additional research is required to fully understand the diverse signalling pathways that converge upon NHE1 and modify its activity.

Regulatory Proteins

In addition to regulation of the NHE1 protein by phosphorylation at the distal C-terminus, the proximal portion of this domain binds several proteins that modulate the activity of NHE1. Two sites that bind calmodulin with different

affinities are found within this area (Figure I-1).²³ In the absence of calmodulin, these sites are inhibitory to NHE1. However, upon binding of Ca²⁺-complexed calmodulin to the higher affinity site, inhibition is relieved and NHE1 activity increases.²³ In addition to calmodulin, the related protein, calcineurin homologous protein (CHP), interacts with the proximal C-terminal domain of NHE1 (Figure I-1). In the resting state, CHP is bound to NHE1, however upon activation by growth factors, CHP is released and NHE1 becomes more active.²³ Finally, heat shock protein 70 has also been shown to bind the cytosolic tail of NHE1, but the precise function of this interaction is unknown.²⁴ It is also quite plausible that many other proteins that interact directly with NHE1 await discovery.

Acidosis, Hormones, Growth Factors and ATP

Acidic conditions, hormones, growth factors and ATP have been reported to affect NHE1 activity, and may act through some of the pathways described above. Exposure of cells to chronic acidosis has been shown to alter NHE1 transcription levels in a number of cell types. For example, metabolic acidosis increased NHE1 transcription levels in isolated rabbit renal cortical membrane vesicles, and in whole renal proximal tubule cells exposed to acidic media.¹¹ In contrast, acidic conditions do not activate NHE1 transcription in fibroblasts.¹¹ This implies that the effect of extracellular acidosis on NHE1 transcription levels is a function of cell type.

Several hormones and growth factors can also indirectly regulate NHE1 including: aldosterone,¹⁶ thyroid hormone,²⁵ epidermal growth factor,²⁶ endothelin, thrombin, angiotensin II and epinephrine.²³ Recent studies have demonstrated that some of these hormones (particularly epinephrine) activate NHE1 through pathways involving heterotrimeric GTP-binding proteins.^{27,28}

The apparent ATP-dependence of the antiporter has implied that a hypothetical auxiliary factor may be needed for optimal activity. The energy for NHE1 activity is provided by the inwardly directed Na⁺ gradient; however, ATP is required for maximal activation.² Studies have shown that the rate of exchange is remarkably similar in ATP-depleted canine red blood cells and resealed ghosts (essentially cells with all cytoplasmic factors removed) containing ATP.²⁹ It was proposed that the ATP-dependent NHE ancillary factor was removed when the ghosts were made from the red blood cells. As a result, ATP was not able increase NHE1 activity in the ghosts and the rate of exchange resembled that of ATP-depleted cells. More recently, it was reported that plasmalemmal phosphatidylinositol 4,5-bisphosphate (PIP₂) regulates NHE1 activity, and may account for a considerable portion of NHE1 ATP-dependence.³⁰ In these experiments, it was demonstrated that ATP depletion or plasmalemmal PIP₂ reduction (via hydrolysis or sequestration) inhibit NHE1 activity to a similar extent. Furthermore, a proximal region of the NHE1 C-terminal domain can bind PIP₂, and mutation of these sites significantly reduces [²²Na⁺] uptake by cells. (The two putative PIP₂ binding sites are located at residues 513 to 520 and 556 to

564.) Since metabolic ATP depletion does reduce PIP₂ levels, the dependence of NHE1 on ATP for optimal activity may be due to a requirement for PIP₂. Other ATP-dependent NHE1 regulatory factors remain to be identified, however, because some ATP-sensitive NHE1 activity remained after deletion of the PIP₂ binding sites. Further research is necessary to isolate and characterize these remaining factors.

I-5. NHE1 Expression in Development and Differentiation

NHE1 Expression in Cellular Proliferation and Development

A review published in 1989 lists at least twenty mitogens and co-mitogens that have been demonstrated to activate Na⁺/H⁺ exchange in a variety of cell types,³ and that number has undoubtedly increased since then. In view of this association with growth-promoting factors, the Na⁺/H⁺ exchanger likely plays an important role in cellular proliferation. Numerous findings validate this statement and are discussed in detail below.

In recent studies, NHE1 mRNA levels have been shown to increase in response to proliferative stimuli. For example, when vascular smooth muscle cells (VSMC) were treated with serum, platelet-derived growth factor or fibroblast growth factor for up to 24 hours, steady-state NHE1 mRNA levels were found to increase by approximately 15-fold.¹⁵ However, the V_{max} of NHE1 in these growth factor stimulated cells was only 1.4 times greater than unstimulated

cells. (The lack of correlation between the 15-fold NHE1 mRNA increase and the 1.4-fold rise in NHE1 activity rate implies that post-translational regulatory mechanisms are involved.¹⁵) Also, in primary cultured rat VSMC, an increase in NHE1 mRNA paralleled cell growth. At confluence, NHE1 mRNA decreased to the level measured before the exponential growth period.³¹ In rat hepatocytes, which were chronically stimulated to proliferate, a 2-fold increase in steady-state mRNA levels was observed, and was accompanied by a 1.3-fold rise in pH_i recovery rate following acid loading.³² As well, NHE1 mRNA was found to increase 3-fold by the third day after pressure overload-induced hypertrophy of the rat heart.³¹ The increase in NHE1 mRNA reported in each of the above examples (VSMC and hepatocyte proliferation, cardiac hypertrophy) implies that NHE1 plays a significant role in the process of cell proliferation.

Studies of rat and rabbit development also demonstrate the importance of NHE1 in growth-related processes. Haworth et al.³³ reported a 5-fold decrease in rat ventricular NHE1 mRNA expression over the first 21 days of life. Also, the rate of pH_i recovery following acid-loading was significantly greater in 2 to 4-day-old ventricular myocytes when compared to adult cells. Similar results were obtained with rabbits in two independent studies. Chen et al.³⁴ showed that fetal and neonatal rabbit ventricles had a 1.7 and 1.6-fold more NHE1 mRNA, respectively, than adult ventricles. Takewaki et al.³¹ reported a comparable difference in ventricular NHE1 mRNA in neonatal and adult rabbits. The

elevated quantity of NHE1 mRNA observed in the neonate in each of these examples implies that the NHE1 protein is important in development.

NHE1 Expression in Cellular Differentiation

Differentiation is the process in which cells become more specialized in form or function³⁵. At least three tissue culture models of differentiation have demonstrated the significance of NHE1 in this specialization process.

Human leukemic HL60 cells can be induced to differentiate into granulocytes by treatment with retinoic acid (RA). Rao et al.³⁶ found that NHE1 mRNA was increased 18-fold in HL60 cells subjected to RA for 24 hours when compared to untreated controls. Furthermore, NHE1 protein levels were 7-fold greater in the differentiated cells than HL60 cells not induced with RA.

P19 mouse embryonal carcinoma cells differentiate into a neuronal phenotype upon RA treatment. Dyck et al.³⁷ examined NHE1 transcription in RA-induced differentiation of P19 cells using luciferase reporter gene constructs. The reporter constructs contained the luciferase gene driven by a 125-nucleotide segment from the NHE1 promoter. This particular reporter construct was used because its luciferase activity was equivalent to that of the full (1.1 kb) length NHE1 promoter upon RA-induced differentiation. After RA treatment for 48 hours, cells stably transfected with the reporter construct exhibited a 20-fold increase in NHE1 promoter activity. This heightened NHE1 transcription was correlated with a 3-fold increase in pH recovery rate following acid loading.

Interestingly, β -tubulin, a marker of differentiated neuronal cells, could not be detected in most cells until much later. This implies that activation of NHE1 is an early event in RA-induced differentiation of P19 cells.

Wang et al.³⁸ further investigated the role of NHE1 in RA-induced P19 differentiation by generating and characterizing an NHE1-deficient P19 cell line. The NHE1 null cells grew slowly, and recovered from an acid load at a significantly reduced rate. Most importantly, upon RA treatment, the NHE1-deficient P19 cells did not differentiate into a neuronal phenotype. Also, the NHE1 inhibitor, HOE694, could block RA-induced differentiation of normal P19 cells. These observations indicate that NHE1 is indeed involved in P19 embryonal cell differentiation.

The L6 rat skeletal muscle cell line can be induced to differentiate by reducing the concentration of serum in the media from 20% to 1%.³⁹ This causes the mononucleated myoblast L6 precursor cells to differentiate into elongated multinucleated myotubule cells that express muscle-specific proteins. Using this model of differentiation, Yang et al.³⁹ showed that NHE1 mRNA levels are about 3-fold greater in the differentiated cell type after 6 days of reduced serum conditions, when compared to untreated controls. In contrast to P19 cells where NHE1 message levels peaked early in the RA-induced differentiation, the amount of NHE1 mRNA continued to increase in L6 cells upon cell specialization.

In conclusion, during the induced differentiation of HL60 cells, P19 cells and L6 cells, Na^+/H^+ exchanger mRNA levels have been shown to increase,

suggesting that NHE1 is important during the differentiation process. Furthermore, in at least one cell type (P19 cells), increased NHE1 mRNA is observed ahead of some cell differentiation markers, and therefore implies that NHE1 upregulation may be an early event in differentiation of some cell types. Finally, some cell types (P19 cells) absolutely require NHE1 for differentiation.

I-6. The NHE1 Promoter and Related Transcription Factors

This section begins with a description of the NHE1 promoter and discusses studies that have identified transcription factors important for the NHE1 gene including: C-EBP, AP-2, an HMG-like protein and COUP-TF. Since a portion of this project has examined AP-2 α -null mice and loss-of-function COUP-TFI mice, subsequent sections describe these transcription factors in detail.

The NHE1 Promoter

In 1991, Miller et al.⁴⁰ published the first description of the structure of the human NHE1 gene and 5'-flanking regulatory region. They reported that this gene spans about 70 kilobases and that the coding region of 41.5 kilobases contains 12 exons and 11 introns. Furthermore, these investigators defined the transcription start sites and characterized the NHE1 promoter region up to 1370 bases upstream of the transcription initiation points. Within this promoter

segment, putative binding sites for a number of transcription factors were identified including: four GC boxes to bind the general transcription-enhancing factor Sp-1; three AP-1 sites that can bind the fos/jun dimer in response to PKC activation; a cAMP response element; and four partial glucocorticoid response sites.

Kolyada et al.⁴¹ examined the NHE1 promoter in further detail and identified a specific transcription factor that acts on the NHE1 promoter. These investigators used sequential truncations of the human NHE1 promoter to identify elements essential for driving transcription of the chloramphenicol acetyltransferase reporter gene. Positive regulatory elements acted downstream of nucleotide -252 in human hepatoma cells (HepG2) and rat vascular smooth muscle cells (VSMC) while transcription-suppressing elements acted on a region 5' to nucleotide -252. However, in mouse Balb 3T3 fibroblast cells, negative regulatory activities were observed upstream of nucleotide -654 and transcription enhancing factors acted 3' to -654. Based on these results, the authors suggested that different groups of transcription factors are likely to act on the NHE1 promoter in different cell types. Additionally, elimination of the region between nucleotides -239 to -215 severely disrupted transcription of the reporter gene in both HepG2 cells and rat VSMC. The transcription factor CCAAT/enhancer-binding protein (C/EBP) was discovered to bind this site based on a series of competition assays.

Subsequently, Dyck et al.⁴² demonstrated that a region between nucleotides -106 to -95 of the mouse NHE1 promoter is important for transcriptional activity and contains a putative binding site for the transcription factor AP-2. In these experiments, constructs with truncated versions of the NHE1 promoter were coupled to the luciferase reporter gene and transfected into mouse fibroblast cell lines. It was found that deletion of the promoter upstream of the AP-2 site resulted in a 25% reduction in reporter activity; however, removal of the same upstream region plus the AP-2 site caused an 83% decrease in NHE1 transcription. Similarly, the AP-2 binding site has been shown to be important for NHE1 expression in P19 cells³⁷, and rat neonatal myocytes.⁴³

In addition to C/EBP and AP-2, an HMG (high mobility group)-like protein has been shown to bind the NHE1 promoter. Wang et al.⁴⁴ demonstrated that this HMG-like protein recognized the poly (dA:dT) region between nucleotides -170 to -155 of the mouse NHE1 promoter. This promoter segment is likely quite important to the integrity of NHE1 transcription since its sequence is identical in mice and humans.⁴⁴ Furthermore, the poly (dA:dT) element could be bound by nuclear extracts from a variety of cell types including: mouse renal cortical tubule (MCT) cells, mouse fibroblast NIH 3T3 cells, rat skeletal muscle myoblast (L6) cells, and rat myocardial cells.⁴⁴

Another transcription factor involved in NHE expression is the chicken ovalbumin upstream promoter transcription factor (COUP-TF).⁴⁵ A COUP-TF responsive element is located between nucleotides -841 to -824 in the mouse

NHE1 promoter. COUP-TF can activate tandem copies of this element placed upstream of the minimal NHE1 promoter. Furthermore, NHE1 expression is increased when mouse fibroblast cells are transfected with COUP-TF.⁴⁵ Thus, COUP-TF also plays a role in regulation of NHE1.

In conclusion, the NHE1 promoter is regulated by a number of transcription factors, some of which likely remain unidentified. Also, the activity of certain transcription factors has been suggested to vary with cell type (see the results of Kolyada et al.⁴¹ described above). Taken together, regulation of the Na⁺/H⁺ exchanger at the level of transcription is clearly a complex process and its investigation will provide further insights into the roles of this important protein.

The AP-2 Transcription Factors

Expression of the AP-2 transcription factor is developmentally regulated and can be detected in epidermal and neural crest cell lineages.⁴⁶ The AP-2 transcription factor family currently includes three proteins: AP-2 α , AP-2 β and AP-2 γ . AP-2 α was first isolated from HeLa cells in 1987⁴⁷ and the human AP-2 α cDNA was cloned and characterized in 1988.⁴⁸ Subsequently, AP-2 β was discovered in 1995,⁴⁹ and AP-2 γ was found the following year.⁵⁰

The protein sequence identity is remarkably high between the AP-2 isoforms. AP-2 β and AP-2 γ are 76% and 66% identical to AP-2 α in primary structure, respectively.^{49,51} In fact, a 96 amino acid segment of the DNA binding domain in AP-2 β and AP-2 γ is 96% and 99% identical to AP-2 α , respectively.⁵¹

As a result of the similarities in protein sequence, all of the AP-2 proteins share a common domain structure. The proline and glutamine-rich transcription activation domain is situated near the N-terminus. A basic region and a helix-span-helix motif for DNA binding and dimerization are located in the C-terminal half of the protein.⁵¹

The AP-2 transcription factors are important for vertebrate development and are co-expressed in a significant number of embryonic tissues.^{49,50} Information about the precise roles of AP-2 α and AP-2 β has come from studies of knockout mice. Perinatal lethality occurs in mice nullizygous for AP-2 α . Severe defects were observed in closure of the neural tube and in the development of the ventral body wall, face, eyes, and limbs.^{46,52,53} AP-2 β -null mice die within two days of birth likely resulting from the down-regulation of a subset of antiapoptotic genes, which led to a rapid increase in apoptosis in the medullary region of the kidney, and ultimately complete kidney failure.⁵⁴ Surprisingly, apoptosis is only slightly elevated in AP-2 β -null kidneys at embryonic day 18.5; however, at birth, kidney apoptosis is eight-fold greater in the knockout compared to wild type littermates.⁵⁴ The development of all other organs appeared to be unaffected by the absence of AP-2 β .⁵⁴ AP-2 γ -null mice have not been generated to date.

The Chicken Ovalbumin Upstream Promoter Transcription Factors (COUP-TFs)

The COUP-TFs belong to the steroid/thyroid receptor superfamily of nuclear receptor proteins. The COUP-TFs are defined as orphan nuclear receptors

of this family because their ligand(s) are unknown.⁵⁵ Currently, two COUP-TFs have been identified in humans: COUP-TFI (cloned in 1986) and COUP-TFII (isolated in 1991).⁵⁵ COUP-TFI and COUP-TFII are highly homologous with essentially identical DNA-binding domains and 97% identical putative ligand binding domains. The N-terminal regions are much more divergent, sharing only 45% identity.⁵⁵

The COUP transcription factors regulate transcription of a large number of genes. A current review cites 45 genes negatively regulated by COUP-TFs and 18 genes activated by COUP-TFs.⁵⁵ The expression patterns of COUP-TFI and COUP-TFII in the developing mouse are distinct but overlapping. Both proteins are first detected at embryonic day 7.5, reach maximal levels between E10 to E12 and decrease significantly before birth.⁵⁵

The most insightful evidence for the precise role for each of these transcription factors comes from studies of loss-of-function mutants. Homozygous disruption of COUP-TFI results in perinatal lethality, and is most likely due to malnutrition and dehydration.⁵⁶ COUP-TFI nullizygous neonates have defects in the glossopharyngeal nerve that impair the pharynx and tongue, thereby affecting swallowing mechanisms.⁵⁶ Defects in axon branching and bone formation were also noted in the COUP-TFI knockout animals.⁵⁶ In the COUP-TFII disrupted mice, 100% of homozygotes died at E10 and 66% of heterozygotes expired before three weeks of age.⁵⁷ At E9, COUP-TFII-null homozygotes exhibited: slow growth of head and heart, enlarged blood vessels, malformed

veins, underdevelopment of the atria and sinus venosus, and an overall decrease in blood vessels in the head and spine.⁵⁷ This collection of characteristics suggests that angiogenesis was severely impaired in the COUP-TFII-null animals.⁵⁷

I-7. Phenotype of NHE1 Disrupted Mice

A great deal about the unique function of a protein can be learned from loss-of-function mouse models. Two mouse lines have been reported that completely lack functional NHE1 protein. Cox et al.⁵⁸ described the slow-wave epilepsy (swe) mutant mice. Swe mice arose from a spontaneous point mutation in the NHE1 gene that generated a stop codon between putative transmembrane segments 11 and 12 resulting in a truncated, non-functional protein. Bell et al.⁵⁹ generated the second NHE1-disrupted mouse line by replacing membrane-spanning domains 6 and 7 with a neomycin resistance gene.

Animals homozygous for the swe mutation can be clearly identified at 11 to 14 days of age, as they are smaller in size and move with an ataxic gait.⁵⁸ These mice also experience moments of behavioural arrest that last for several seconds, and are associated with spike-wave absence seizures. Histological analysis of brain sections revealed the degeneration of a small subset of cells in the cerebellum and brainstem of swe mutants. The remainder of the central nervous system appeared normal. Importantly, the cell types affected in the swe mice are more metabolically active than other regions of the brain. Mortality of

the swe mutants differed somewhat with different genetic backgrounds, but only one-half of the mice survived to weaning age (21-days-old) and then died at 35-40 days of age. Post-mortem examination indicated that they had experienced a lethal seizure. The overall phenotype of the swe mutant mice exemplifies the essential traits of human generalized absence epilepsy.

After determining that the swe phenotype arose from a point mutation in the NHE1 gene, Cox et al.⁵⁸ used Northern blot analysis of NHE1 to demonstrate a 90% reduction in NHE1 mRNA transcripts. Furthermore, acid-loaded primary fibroblast cells from swe mutants were incapable of $^{22}\text{Na}^+$ uptake, thereby confirming the absence of NHE1 activity. Remarkably, swe mice had normal levels of serum bicarbonate, Na^+ , K^+ , Cl^- , Ca^{2+} and serum proteins such as albumin and globulin. Also, no histological aberrations were observed in skeletal and cardiac muscle, lung, spleen, liver, kidney, bone or stomach.

The NHE1-null mice created by a targeted disruption of the NHE1 gene by Bell et al.⁵⁹ exhibited four noteworthy similarities to the swe mutants. First, an ataxic gait is apparent in both lines at approximately 2 weeks of age, and the animals are smaller in size compared to wild type littermates. Second, an excitable response followed by total behavioural arrest for a brief period was observed in neonates, and reported to resemble an epileptic-like seizure. Third, the mortality rate was high in both lines prior to weaning. Sixty-eight percent of the *Nhe1*-/- mice died between 16 to 29 days of age while at least 50% of the swe mice expired before reaching 21 days old as noted above. Finally, in both reports,

post-mortem observations suggest that the animals suffered a lethal convulsive seizure.

The two NHE1 loss-of-function mouse models do differ on several points. Bell et al.⁵⁹ observed subtle alterations in the stomach morphology of the *Nhe1*-/- mice (including thinning of the stomach mucosa and increased spacing of the gastric glands) that were not seen in the swe mutants. The specific regions of the central nervous system found to be abnormal in the swe mice were not analyzed in the *Nhe1* -/- line, and thus could not be compared. Also, sixteen hours after death, a waxy material was noted around the ears, eyes, mouth and paws of *Nhe1*-/- mice that was not reported in the swe animals.

In conclusion, the two studies reveal that the absence of the NHE1 protein causes ataxia, growth retardation and epileptic-like seizures. Cox et al.⁵⁸ suggested that other NHE isoforms or Cl⁻/HCO₃⁻ transporters are capable of maintaining homeostasis in the absence of NHE1 in most neurons and nonneuronal tissues. However, since a large number of neuronal signals are pH-dependent (such as transmitter uptake through transporters and gap junction communication between cells⁵⁸), a subset of neurons may not function without the ability to control rapid pH changes via NHE1, which could lead to the epileptic phenotype.

I-8. NHE1 and Disease

This section examines the role of NHE1 in several prevalent pathologies including: heart disease, primary hypertension, diabetes and cancer. Therapies that specifically target the Na^+/H^+ exchanger have been investigated for these diseases. Even so, little is truly known about the precise function of NHE1 in these conditions.

Heart Disease

Heart disease affects a large portion of the North American population. In the United States, 1.5 million Americans experience an acute myocardial infarction each year,⁶⁰ and 400 000 new cases of congestive heart failure are reported annually.⁶¹ In Canada, 26.6% of deaths in 1997 were related to diseases of the heart (www.statcan.ca). These statistics reinforce the importance of research that seeks to define the mechanisms of heart dysfunction, and thereafter create effective therapies.

A myocardial infarction is caused by an occlusion of the coronary artery. This occlusion severely reduces blood flow to the heart, a condition that is known as ischemia. The hypoxic state of ischemia induces acidification of the myocardium due to glycolytic ATP anabolism and accumulation of carbon dioxide.⁶² Consequently, intracellular acidification activates NHE1 (the primary Na^+/H^+ exchanger isoform in the heart⁶³), and the large Na^+ influx activates the $\text{Na}^+/\text{Ca}^{2+}$ exchanger to replace the sodium ions with calcium cations.⁶³ The

subsequent intracellular Ca^{2+} overload is detrimental to contractility and may lead to arrhythmias and other damage.⁶² Calcium overload does not occur during non-ischemic conditions due to the activity of the Na^+-K^+ ATPase that acts in conjunction with the $\text{Na}^+/\text{Ca}^{2+}$ exchanger to expel Na^+ ions. However, in the ATP-scarce environment of ischemia, the Na^+-K^+ ATPase is inhibited and thus the $\text{Na}^+/\text{Ca}^{2+}$ exchanger must act alone to relieve the excessive internal sodium ion concentration.⁶³ Therefore, NHE1 is involved in damage to the myocardium during ischemia by a Ca^{2+} -dependant mechanism.

In instances of ongoing ischemia, eventually the external proton concentration would exceed the internal H^+ activity and thereby inhibit NHE1.⁶² This reverse orientation of the proton gradient has been demonstrated in rabbit papillary muscle after ten minutes of ischemia.⁶² However, upon restoration of blood flow to the heart (known as reperfusion), extracellular protons would be washed out and NHE1 would be activated. This would lead to further internal Ca^{2+} accumulation and subsequent myocardial damage.⁶²

Although less prominent in the literature, at least two Ca^{2+} -independent mechanisms of ischemia/reperfusion-induced heart injury have been hypothesized to involve the Na^+/H^+ exchanger. The first, known as the pH paradox, suggests that ATP depletion during ischemia activates proteases and phospholipases; however, intracellular acidosis inhibits optimal enzyme activity. Upon the restoration of cellular pH by reperfusion, the activated enzymes become functional, and cause damage to the myocardium.⁶³ The second means of Ca^{2+} -

independent ischemia-mediated harm to the heart involves NHE1 and excessive norepinephrine release from sympathetic nerves.⁶⁴ ATP is required for the storage of norepinephrine in the vesicles of sympathetic nerve endings. As a result, the reduction of ATP levels during ischemia cause norepinephrine release into the axoplasm of these neurons. Under physiological conditions, the Na⁺-dependent cotransporter (NET) facilitates norepinephrine uptake in cells. In ischemia, however, the high concentrations of norepinephrine freed from vesicles, coupled with the influx of sodium ions from the NHE1-mediated pH regulatory response, reverses NET activity. Thus a surplus of norepinephrine release occurs, which inappropriately activates neighbouring cells, leading to myocardial dysfunction and arrhythmias.

NHE1 has also been reported to participate in cardiac hypertrophy induced by damage to the heart. For example, one study examined the effect of cariporide (a specific NHE1 inhibitor) on cardiac hypertrophy in rats.⁶⁵ The heart-to-body weight ratio was measured in control and cariporide-treated rats one week after ligation of the left coronary artery to simulate myocardial infarction. The heart-to-body weight ratio increased markedly in control animals; however, no significant change was observed in cariporide-treated rats. This implied that NHE1 was involved in the hypertrophic response of the rat heart to the ligation procedure.

The detrimental effect of NHE1 activity in myocardial infarction and cardiac hypertrophy has inspired many efforts to develop therapeutic inhibitors of

this protein. A current review describes at least ten benefits of NHE1 inhibitor administration in models of myocardial ischemia.⁶³ The list includes improved ventricular recovery during reperfusion, reduction in arrhythmias and decreases in infarct size. Some controversy exists in the literature as to whether administration of inhibitors exclusively during reperfusion is effective. Clearly, inactivating NHE1 in both ischemia and reperfusion would provide maximal cardioprotection; however, this may not be possible in a clinical situation. Currently, the advantages of two NHE1-selective inhibitors, cariporide and eniporide, are being investigated in clinical trials with heart disease patients.⁶³

Primary or Essential Hypertension

Current statistics from the United States indicate that approximately 25% of American adults are afflicted with primary hypertension.⁶⁶ Furthermore, two hypertension-related pathologies, heart disease and stroke, are leading causes of death in the American population.⁶⁶ The principal symptom of hypertension is chronic high blood pressure; however, the etiology of this condition is not understood.

Increased NHE1 activity has been reported in rat models of hypertension and in essential hypertension patients. Specifically, spontaneously hypertensive rats (SHR) exhibit elevated Na^+/H^+ exchange in: kidney epithelial cells, lymphocytes, platelets, neutrophils, erythrocytes, and cultured vascular smooth muscle cells.⁶⁷ Similarly, about 45% of hypertension patients have increased

NHE activity in: lymphocytes, immortalized lymphoblasts, erythrocytes and/or platelets.⁶⁷ In fact, a large body of hypertension research implies that alterations in a number of other monovalent ion transporters (including $\text{Na}^+ \text{-K}^+ \text{-Cl}^-$ cotransporters, amiloride-sensitive Na^+ channels, $\text{Na}^+ \text{-K}^+$ pumps and Ca^{2+} -activated K^+ channels) may also contribute to the disease.⁶⁷

Changes in NHE1 activity appear in almost half of all primary hypertension patients; therefore, NHE1 expression and activity has been investigated to understand the molecular basis of some hypertensive states. Surprisingly, mutations have not been detected in the coding region of NHE1 cDNA in vascular smooth muscle cells (VSMC) from SHR, and NHE1 mRNA is not overexpressed in these cells.⁶⁷ However, the phosphorylation state of NHE1 is altered in SHR. Siczkowski et al.⁶⁸ reported that the level of NHE1 phosphorylation is 2.2-fold greater in SHR myocytes, compared to normal rat myocytes. Furthermore, Phan et al.⁶⁹ discovered that the activity of a 90 kDa NHE1 kinase (later identified as p90^{rsk}²¹) was 1.8-fold higher in SHR VSMC compared to normal rat VSMC. Therefore, alterations in the activity of p90^{rsk} (or proteins that regulate this kinase) may contribute to the pathology of hypertension.

In an effort to isolate the global role of NHE1 in hypertension, Kuro-o et al.⁷⁰ generated transgenic mice that overexpressed NHE1. Immunohistochemistry could only detect the transgene in the cell membranes of renal tubular cells and epithelial cells of the stomach, intestine and glomerulus. (It is not known why

this restricted expression occurred.) The transgenic animals exhibited reduced urinary excretion of water and Na^+ when compared to controls. Systolic blood pressure in the transgenics was only elevated following 4 – 5 weeks of chronic salt loading, and then returned to normal levels after 8 weeks of the high salt diet. The authors concluded that the reduced urinary excretion of Na^+ was due to increased absorption by the renal tubular cells in the NHE1-overexpressing mice, and that the recovery of systolic blood pressure during chronic salt loading indicated the presence of other compensatory mechanisms. No clear conclusions could be made regarding the role of NHE1 in hypertension from these studies.

In summary, primary hypertension is a complex disorder that is not well understood. However, aberrant NHE1 activity clearly participates in some forms of this disease.

Diabetes

The National Institute of Diabetes and Digestive and Kidney Diseases in the United States estimates that approximately 800 000 Americans are diagnosed with diabetes each year (www.niddk.nih.gov/health/diabetes/diabetes.htm). Diabetes is a condition in which abnormalities in glucose metabolism cause systemic hyperglycemia. Type I diabetes is an autoimmune disorder, and patients are dependent on insulin early in life. Type II diabetes results from an insulin-resistant state, and develops at later ages. In both diabetic conditions, the primary pathological effect is vascular disease.⁷¹

The role of the Na^+/H^+ exchanger in diabetes is somewhat controversial. Two biochemical abnormalities prevalent in diabetes are predicted to activate NHE1: hyperglycemia and hyperlipidemia.⁷¹ In hyperglycemia, diacylglycerol (DAG) synthesis increases. One role of DAG is to stimulate PKC, and PKC is known to upregulate NHE1 activity in most cell types.⁷¹ In hyperlipidemia, elevated oxidized low density lipoprotein (LDL) levels stimulate MAPK, which activates NHE1.⁷¹ Also, insulin has been shown to directly increase transcription of the NHE1 promoter.⁷² Activation of NHE1 would exacerbate diabetic macrovascular disease (a condition of rapid arteriosclerosis of coronary and peripheral arteries) by stimulating vascular smooth muscle cell (VSMC) proliferation.³¹ In keeping with these biochemical arguments for activation of NHE1 during diabetes, hyperglycemia has been shown to increase NHE1 activity and mRNA levels in VSMC.⁷³ In contrast however, studies of sarcolemmal vesicles from insulin-dependant diabetic rats have demonstrated a 60% decrease in NHE1 activity⁷⁴ Additionally, the diabetic rat hearts recovered more slowly from an acid-overload, and were significantly resistant to ischemia/reperfusion-induced injury. These observations imply that Na^+/H^+ exchange was reduced; however, there was no difference in NHE1 mRNA in the diabetic rats compared to controls.⁷⁴ In conclusion, NHE1 regulatory mechanisms in diabetic VSMC and in diabetic cardiomyocytes appear very different and the precise role of NHE1 in diabetes remains unknown.

Cancer

In the year 2000, a study conducted by the National Cancer Institute of Canada reported that the lifetime probability of developing cancer for Canadian males and females is 40.4% and 35.3%, respectively (www.statcan.ca). Tumors are caused by a loss of normal growth control and can be initiated by an increasing list of factors.⁷⁵ Furthermore, all tumor cells have a slightly alkaline intracellular pH, even though inadequate vascularization produces an acidic external environment.⁷⁶ As a result, the Na^+/H^+ exchanger and other pH regulatory mechanisms have been implicated in tumorigenicity.

Reshkin et al.⁷⁵ recently examined the role of NHE1 in the malignant transformation induced by the E7 oncoprotein of human papillomavirus type 16 (HPV16). Cellular alkalinization occurred when NIH 3T3 fibroblast cells were infected with recombinant retroviruses expressing the E7 oncoprotein. This alkalinization could be blocked by the NHE1-specific inhibitor 5-(N,N-dimethyl) amiloride (DMA). Also, the pH did not rise in fibroblast cells infected with retroviruses that encoded a transformation-deficient E7 mutant protein. These results suggest that transformation induces NHE1-mediated cellular alkalinization. In addition, the investigators showed that DMA treatment decreased the development of transformation phenotypes (such as serum independence, rapid growth rate and anchorage independence). Most importantly, it was shown that intraperitoneal injections of DMA could retard the growth of HPV16-keratinocyte tumors in nude mice.

Although tumor cell killing *in vitro* with NHE1 inhibitors (often in combination with ionophores and anion exchange inhibitors) has been successfully demonstrated in a number of studies, the *in vivo* results of Reshkin et al.⁷⁵ described above are the exception. Yamagata et al.⁷⁶ reported that a combination of the NHE1 inhibitor 5-(N,N-hexamethylene) amiloride (HMA) with the ionophore nigericin and the Na⁺-dependent HCO₃⁻/Cl⁻ exchanger inhibitor 4,4-diisothiocyanostilbene 2,2-disulfonic acid (DIDS) was extremely toxic to murine tumor cells. However, injection of this cocktail into mouse tumors *in vivo* was significantly less effective in tumor cell killing.

Two probable obstacles to tumor therapies that target NHE1 have been described.⁷⁶ First, the environment of some tumors *in vivo* may not be sufficiently acidic to actually require pH regulation by NHE1. Secondly, the half-life of the inhibitory compounds *in vivo* is much shorter than *in vitro*. Therapy strategies that increase tumor acidity by administration of glucose or hydralazine or that augment NHE1 inhibitor concentrations by continual infusion protocols are currently being investigated.⁷⁶

I-9. Transcription Reporter Genes

To completely understand the purpose and function of a protein, it is imperative to know something about its transcription. Transcription has been extensively examined using reporter genes. Some of the most frequently used

reporter genes include chloramphenicol acetyltransferase (CAT), firefly luciferase, β -Galactosidase (β gal), and the green fluorescent protein (GFP). GFP and β gal reporters were employed in this study to investigate the developmental and tissue-specific regulation of the NHE1 promoter.

The Green Fluorescent Protein

GFP was first isolated from *Aequorea* jellyfish in 1962 by Shimomura et al.⁷⁷ In 1992, the GFP gene was cloned and in 1994, two groups independently showed that expression of the GFP gene in other organisms resulted in fluorescence.⁷⁸ Since that time, GFP has found application in a wide variety of systems including prokaryotes, yeasts, *Caenorhabditis elegans*, *Drosophila*, transgenic plants, mammalian cells, and transgenic vertebrates.

The ability to detect GFP fluorescence in a heterologous system is a result of two important properties of the green fluorescent protein. In jellyfish, bioluminescence is activated by Ca^{2+} , which binds the photoprotein aequorin and causes aequorin to emit blue light. The blue fluorescence transfers energy from aequorin to GFP, resulting in fluorescence of the GFP.⁷⁹ Thus, in order to fluoresce, GFP does not require any additional jellyfish substrates or co-factors, but only needs an exogenous energy source. Also, formation of the chromophore by the post-translational cyclization of Ser, Tyr and Gly at positions 65, 66 and 67, respectively, is an autocatalytic process.⁷⁹ Therefore, since GFP does not

depend on any jellyfish proteins for fluorescence or chromophore formation, the green fluorescent protein is virtually an ideal reporter gene.

The structure of GFP was solved separately by Ormo et al.⁸⁰ and Yang et al.⁸¹ in 1996. GFP consists of an eleven-stranded β -barrel enclosing an α -helix. The chromophore is attached to the α -helix at approximately the middle of the cylinder. As mentioned above, the chromophore is formed from Ser-Tyr-Gly at positions 65-67 by an autocatalytic mechanism.

To date, seven classes of GFP variants are known and are grouped by chromophore properties.⁷⁸ The first two groups are of interest here. Class 1 encompasses the wild type green fluorescent proteins that have two sets of excitation and emission peaks; the major peak excites at 395nm and emits at 508nm, while the minor peak is excited at 475nm and emits at 503nm. Class 2, the phenolate anion family, includes the S65T GFP mutant used throughout this project. The spectrum of S65T GFP has a major excitation peak at 489nm and a corresponding emission peak at 510nm; therefore, it is often referred to as red-shifted GFP. This red shift is particularly advantageous for several technical reasons. First, the major excitation peak is close to the wavelength of light produced by the argon lasers (488nm) found on most confocal microscopes. Second, red-shifted GFP is appropriate for visualization with fluorescein isothiocyanate (FITC) filters. Finally, the fluorescence of S65T GFP is significantly brighter than wild type GFP and remarkably resistant to photobleaching.

Ikawa et al.⁸² were the first to use GFP in transgenic mice. They placed the wild type GFP gene under the control of the chicken β -actin promoter with cytomegalovirus enhancer sequences. This is a very strong promoter, which made fluorescence of the wild type GFP detectable. In fact, green fluorescence could be readily observed in the fingers and tails of live newborn mice using a fluorescent microscope. Since that time, many transgenic mice studies have used GFP variants with enhanced brightness and improved stability.^{83,84,85}

The β -Galactosidase Protein

The second reporter gene used in the present study encodes the bacterial β -galactosidase protein (β gal). Initial studies of β gal explored its inducible formation by *Escherichia coli* in response to certain substances⁸⁶. Discovery of the *E. coli* Lac operon was the end result of further investigation by Jacob and Monod.⁸⁷ As a constituent of the Lac operon, β -galactosidase is encoded by the LacZ gene and catalyzes the hydrolysis of lactose to galactose and glucose. β gal is also able to hydrolyse X-Gal (5-bromo-4-chloro-3-indoyl- β -D-galactopyranoside), a histochemical substrate that produces an insoluble blue precipitate upon hydrolysis. Thus, when tissues are stained with a solution containing X-Gal, a blue colour can be seen in the regions where β gal is present. β gal has been used extensively as a reporter gene in transgenic mice.^{88,89,90,91,92}

I-10. Thesis Objectives

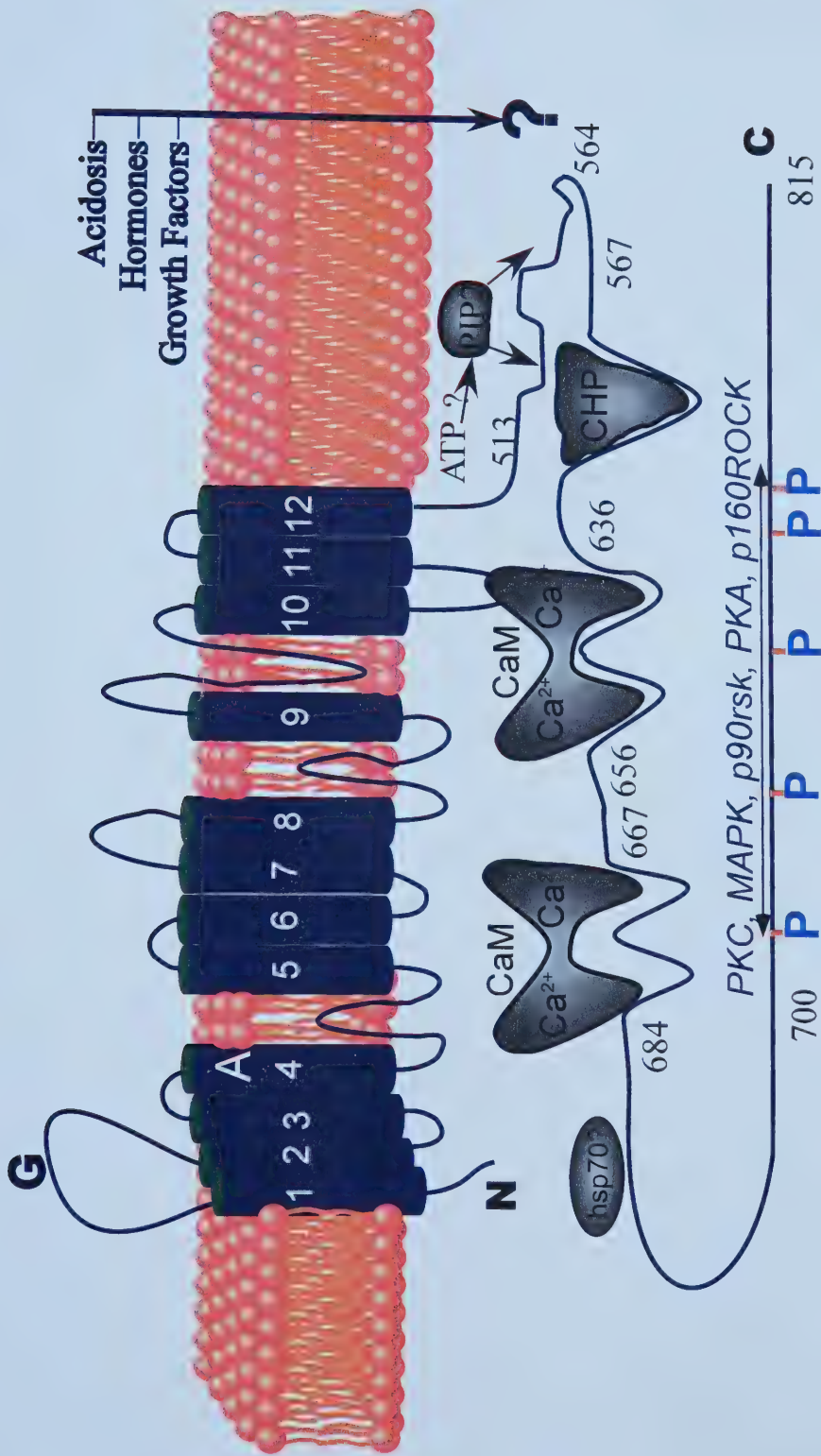
The purpose of this project was two-fold. First, NHE1 expression was investigated using transgenic mice with the GFP or β gal reporter genes under the control of the mouse NHE1 reporter. This system investigated the following questions:

- 1) Is NHE1 transcription elevated in some tissues compared to others at a given age?
- 2) Does the level of NHE1 transcription change in certain organs during murine development?

The second portion of this study examined NHE1 protein levels in the late stage embryo to the adult. This analysis asked:

- 1) Does the amount of NHE1 protein vary in different tissues at a given age?
- 2) Do NHE1 protein levels change in certain organs during postnatal murine development?
- 3) What is the effect of transcription factor disruptions (AP-2 α and COUP-TFI) on NHE1 protein levels in various organs?

Figure I-1. Schematic of the putative topology of NHE1 and the proposed regulatory mechanisms. Structural features of NHE1: black cylinders represent putative membrane-spanning segments 1 to 12; G, glycosylation site; A, putative amiloride binding site; numbers indicate the approximate amino acid position; N, N-terminus; C, C-terminus. Elements proposed to regulate NHE1: PIP2, phosphatidylinositol 4,5-bisphosphate; ATP, adenosine triphosphate; CHP, calcineurin homologous protein; CaM, calmodulin; hsp70, heat shock protein 70; P, phosphorylated region; PKC, protein kinase C; MAPK, mitogen-activated protein kinase; PKA, protein kinase A. External agents that regulate NHE1 are shown in bold in the top right of the figure. The bold question mark indicates that the molecular mechanisms are unknown. See text for details.



Chapter II

Materials and Methods

II-1. Materials

The plasmids used to create the NHE1 promoter-reporter constructs were purchased from: Promega (pSP73), Pharmacia (pTZ18R) or Clontech (pS65T-C1 and p β gal-Basic). Restriction enzymes were obtained from Gibco BRL or New England Biolabs. MWG Biotech, Inc. generated all oligonucleotides for DNA sequencing and PCR primers. NIH 3T3 cells were purchased from the American Type Culture Collection. The Transgenic Facility (University of Alberta Health Sciences Laboratory Animal Services) provided all FVB/n mice. β -Galactosidase activity was detected using the Galacto-Light Plus Chemiluminescent Reporter Assay from Tropix, Inc. Other commercial kits used included the Amersham Enhanced Chemiluminescence Assay for visualization of immunoblot results and the Bio-Rad DC Protein Assay kit for protein quantification. All PCR reagents were obtained from Gibco BRL, including dNTPs, PCR buffer and Taq polymerase. Cryomatrix for freezing embryos and GelTol mounting medium for preparing embryo slides were purchased from Fisher. Reagents for β gal embryo staining (including potassium ferricyanide, potassium ferrocyanide and methyl salicylate) were bought from Fisher, while 5-bromo-4-chloro-3-indoyl- β -D-galactopyranoside (X-Gal) was purchased from Gibco BRL. Antibodies for immunoblotting were obtained from Chemicon (anti-NHE1 monoclonal antibody) and Jackson Immuno Research Labs (goat-anti-mouse antibody). Finally, mice with a disruption of the AP-2 α gene were supplied by Dr. T. Williams (Yale University, New Haven, Connecticut)⁴⁶ and chicken ovalbumin upstream

promoter transcription factor I (COUP TFI) knockout mice were provided by Dr. M.J. Tsai (Dept. Cell Biology, Baylor College of Medicine, Houston, TX).⁵⁶

II-2. Construction of Transgenic Mice with Reporter Genes

Assembly of Reporter Gene Constructs

Two promoter-reporter plasmids were constructed for the purpose of making transgenic mice that expressed NHE1 promoter-controlled reporter genes. Each promoter-reporter construct contains a 3.8 kb fragment of the mouse NHE1 promoter, and a reporter gene, placed after the transcription start site. The two reporter genes used were the green fluorescent protein (GFP) and the β-Galactosidase enzyme (βgal).

The 3.8 kb portion of the mouse NHE1 promoter was obtained from pXP1-5.0.³⁹ pXP1-5.0 contains 5 kb of the mouse NHE1 gene (originally isolated from a mouse lambda Gem-11 genomic DNA library). The pXP1-5.0 plasmid was cut with HindIII and SalI to obtain a 3.8-kb NHE1 promoter fragment, which was cloned into the corresponding sites in the vector, pSP73 (Promega). The resulting plasmid was named pHs-SP (Figure II-1A).

The steps taken to create the GFP reporter plasmid were as follows (Figure II-1B). First, BamHI and BglII digestions eliminated a 51 bp segment of the polylinker from pS65T-C1 (CLONTECH). This was done to remove certain restriction enzyme sites that would have impeded future cloning steps. Next,

NheI and StuI digestions of the "linkerless" pS65T-C1 vector produced a 1.9 kb fragment containing the GFP gene. The GFP gene was then cloned into the XbaI-SmaI sites of pTZ18R (Pharmacia) to create the pTZ(GFP) construct. Next, HindIII and SalI digestions extracted the 3.8 kb mouse NHE1 promoter fragment from pHSG-SP (Figure II-1C). The NHE1 promoter segment was then placed upstream of the GFP gene to create the final plasmid, pHSG-TZ(GFP). Restriction mapping and DNA sequencing confirmed that pHSG-TZ(GFP) was correctly constructed.

The β gal reporter construct was generated as follows (Figure II-1D). XhoI and SalI digestions removed a 4.6 kb fragment containing the β gal gene from pGal-Basic (CLONTECH). Next, the β gal gene was ligated into pHSG-SP at the SalI site to produce the desired plasmid, pHSG-SP(β gal) (Figure II-1E). Restriction mapping and DNA sequencing confirmed that pHSG-SP(β gal) was correctly constructed.

The DNA Sequencing Laboratory (Department of Biochemistry, University of Alberta, Edmonton, Alberta, Canada) sequenced the 3.8-kb mouse NHE1 promoter fragment using a CEQ2000 Beckmann capillary sequencer. MWG Biotech, Inc. made the necessary synthetic oligonucleotides. The sequences of these oligonucleotides were:

T7 primer: 5'-AAT ACG ACT CAC TAT AG-3'

Primer 1b: 5'-GGT TCT TCT CCG ATC TGC-3'

Primer 1c: 5'-CAC TAC TGC ATC CTG ATT C-3'

Primer 1d: 5'-CCA TCC ATG TGG TTG CTG GG-3'
Primer 1e: 5'-AAA GTG TTG GGG ATC GAA CC-3'
Primer 1f: 5'-GTC TCC ATT CTC CAA GGT AC-3'
Primer 2a: 5'-GTC TGT CTG TCT GTC TGG-3'
Primer 2b: 5'-CAC AGA ACC GTG TGC GTC C-3'
Primer 2c: 5'-GGG TGG TCC ATA CCC AGT T-3'

Construction of Transgenic Mice

Before the transgenic mice construction, restriction enzyme digests extracted the NHE1 promoter and reporter gene from each plasmid (HindIII and EcoRI cut pHs-TZ(GFP) creating an 5572-bp piece; XhoI and SalI cut pHs-SP(β gal) yielding an 8221-bp fragment). The linearized DNA fragments were injected into the pronucleus of preimplantation embryos (obtained from the oviducts of pregnant FVB/N females less than 20 hours after fertilization).⁹³ Once injected, fertilized eggs were transferred into the oviduct of a 0.5-day-postcoitum pseudopregnant FVB/N female. Mating with vasectomized males generated the pseudopregnant females. (Dr. Peter Dickie of the Transgenic Facility, University of Alberta Health Sciences Laboratory Animal Services, Edmonton, Alberta, Canada, performed all transgenic procedures.)

II-3. Assay of Reporter Gene Activity in Mammalian Cells

Transfection of NIH 3T3 Cells

To ascertain that the reporter constructs had activity, a CaPO₄ precipitation protocol was used to transiently transfect NIH 3T3 cells with the βgal (pHS-SP(βgal)) or the GFP (pHS-TZ(GFP)) reporter plasmid.⁹⁴ First, cells were plated in 35 mm dishes and allowed to grow to approximately 60% confluence in RPMI media (Gibco) supplemented with 10% fetal bovine serum. In some dishes, cells were grown on coverslips for transfection with the GFP reporter and subsequent microscopy. Prior to transfection, each dish of cells was given 4 ml of fresh medium. For each plate to be transfected, 4-24 µg DNA was added to 100 µl 250 mM Ca₂Cl and the final volume was adjusted to 200 µl with ddH₂O. This solution was mixed and added drop wise to a tube containing 200 µl 2x HEPES buffered saline (280 mM NaCl, 10 mM KCl, 1.5 mM Na₂HPO₄•2H₂O, 12 mM dextrose and 50 mM HEPES). The resulting mixture was left for 20 min to facilitate precipitate formation. Next, the DNA precipitate solution was added drop wise to the cells while the plate was gently swirled. Plates were incubated at 37°C overnight in a humidified, 5% CO₂ atmosphere. On the following day, GFP reporter-transfected cells were used for microscopy and cell extracts were prepared from βgal reporter-transfected cells.

Microscopy of GFP-transfected NIH 3T3 Cells

Coverslips containing GFP reporter-transfected NIH 3T3 cells were washed five times with PBS, and then fixed with 4% paraformaldehyde for 15 min. After rinsing twice with PBS, coverslips were mounted on glass slides using 5 μ l of 50% glycerol/PBS. Slides were viewed with an Olympus BX50 fluorescent microscope (Olympus, Japan) and photographed using a SPOT digital camera (Diagnostic Instruments, Inc.).

Luminometer Assay for β gal Activity

β gal activity in the β gal reporter-transfected NIH 3T3 cells was detected using the Galacto-Light Plus Chemiluminescent Reporter Assay (Tropix). Extracts were prepared from the β gal reporter-transfected NIH 3T3 cells by washing the cells twice with PBS, and then adding 250 μ l Lysis Solution (Tropix) with 1 mM dithiothreitol to each dish. Cells were scraped from the plates, transferred to tubes, and centrifuged for 2 min to pellet any debris. The supernatant was retained for the β gal detection assay.

To quantify the β gal activity in the cells, 20 μ l of cell extract was added to 100 μ l Reaction buffer (Tropix) and the mixture was incubated for 1 hour at room temperature. An LKB luminometer was used to measure the amount of β gal activity in each sample.

II-4. Genotyping by Step-down PCR

Polymerase chain reaction (PCR) was used to identify mice harboring the reporter genes. The genomic DNA used for PCR was obtained from the tail biopsies of embryos or the ear notches of neonates and adults. To extract genomic DNA, tails or ear notches were placed in 40 µl of a buffer containing 50 mM KCl, 10 mM Tris Cl (pH 8.3), 2.5 mM MgCl₂, 0.45% wt/vol Nonidet P-40, and 0.45% wt/vol Tween 20.⁹⁵ Each sample was digested with 20 µg Proteinase K (Gibco) from a 10 mg/ml stock dissolved in 10 mM Tris HCl pH7.5, 20 mM CaCl₂ and 50% glycerol. Digestion proceeded at 60°C for 3-4 hours with periodic vortexing. These crude DNA preparations were used for PCR.

The 50 µl PCR reaction contained: 5 µl 2 mM dNTPs, 5 µl 10x PCR buffer (Gibco), 5 µl 15 mM MgCl₂, 5 µl 4 µM forward primer, 5 µl 4 µM reverse primer, 19.5 µl ddH₂O and 5 µl crude genomic DNA (prepared from tails or ear notches). The forward and reverse primers used are complementary to the reporter coding region (GFP or βgal gene) and the sequence of each is listed below.

GFP Forward #1: 5'-TGG TGA TGT TAA TGG GCA CAA-3'

GFP Reverse #2: 5'-CAG CAC GTG TCT TGT AGT TCC CG-3'

βgal Forward #1: 5'-CCA TGT CGT TTA CTT TGA CCA ACA A-3'

βgal Reverse #6: 5'-CGG CCT CAG GAA GAT CGC ACT CC-3'

Next, a step-down PCR protocol was used.⁹⁶ The cycling steps were as follows:

1. 94°C for 10 min, after which 0.5 µl Taq polymerase (Gibco) was added (This step must be done for at least 10 min to destroy any residual Proteinase K activity in the crude DNA preparations before adding Taq polymerase.)
2. Three cycles of 94°C for 1', 69°C for 2' and 72°C for 1.5'
3. Three cycles of 94°C for 1'; 66°C for 2' and 72°C for 1.5'
4. Three cycles of 94°C for 1'; 63°C for 2' and 72°C for 1.5'
5. Three cycles of 94°C for 1'; 60°C for 2' and 72°C for 1.5'
6. Three cycles of 94°C for 1'; 57°C for 2' and 72°C for 1.5'
7. Three cycles of 94°C for 1'; 55°C for 2' and 72°C for 1.5'
8. Ten cycles of 94°C for 1'; 55°C for 2' and 72°C for 1.5'
9. 72°C for 7'

The PCR products were run in a 7% polyacrylamide gel for analysis. PCR of the genomic DNA from mice carrying the GFP gene produced a band of approximately 400 base pairs, as did the βgal-positive product.

II-5. Preparation and Microscopy of GFP-positive Embryos

Mouse embryos were dissected from the uterus at different ages, and immediately placed in an ice-cold phosphate buffer (P-buffer), containing 13.8 g/l NaH₂PO₄ and 14.2 g/l Na₂HPO₄. Next, embryos were transferred to individual wells of a 12-well plate, fixed in 2% paraformaldehyde/P-buffer for 1 h at room temperature, and then embedded in 30% sucrose/P-buffer at 4°C overnight. The next day, embryos were washed with P-buffer for 1 h, incubated in 50% Cryomatrix (Shandon)/P-buffer for 8 h at room temperature, and then incubated at 4°C overnight in 100% Cryomatrix. (All fixations, washing and incubation steps were done with agitation.) On the third day after harvest, the embryos were mounted on styrofoam supports with Cryomatrix, and then frozen by immersion in 2-methylbutane cooled by liquid nitrogen. Frozen embryos were stored at -80°C prior to sectioning and microscopy.

All slides were coated with poly-L-lysine prior to mounting embryo sections. Seven microliters of 1 mg/ml poly-L-lysine (Sigma) in ddH₂O was used to coat a pair of slides by dropping the solution on one, and spreading it with the face of the second slide. This coating facilitated adherence of the embryo sections to the slides.

Sagittal cryostat sections were cut to a thickness of 10 µm and mounted in GelTol mounting medium (Shandon). Images were obtained using a 10x Plan-Apochromat objective on a Zeiss LSM 510 confocal microscope. The samples

were excited at 488 nm with an argon laser. Using a long pass filter, all emissions with wavelengths greater than 505 nm were taken as the GFP signal. Embryos were too large for a single microscope field therefore a series of photomicrographs were collected and reassembled in Adobe Photoshop to illustrate the entire specimen.

High magnification images of embryonic day 12 hearts were obtained using a 100x Plan-Apochromat objective on the Zeiss LSM 510 confocal microscope. Excitation was at 488 nm and emissions above 505 nm were collected. A series of photomicrographs was reassembled in Adobe Photoshop to illustrate a larger area of the heart.

II-6. Quantification of GFP Fluorescence

Fluorescence intensity was quantified using the public domain NIH Image program (developed at the U.S. National Institutes of Health and available on the Internet at <http://rsb.info.nih.gov/nih-image>). Briefly, the organ of interest was selected using the polygon tool, and a histogram of fluorescence intensity was generated. The fluorescence intensity of the organ was taken as the sum of all counts with a pixel intensity greater than 240 (on a scale of 0 to 255 pixel intensities). Quantification was repeated for at least three similar sections from the same embryo to account for any differences in section depth. Statistical analysis was done using Statview software and all results are expressed relative to control.

II-7. X-Gal Staining of β -Galactosidase Reporter Embryos

Mouse embryos were dissected from the uterus at different ages, and immediately placed in an ice-cold phosphate buffer (P-buffer), containing 13.8 g/l NaH₂PO₄ and 14.2 g/l Na₂HPO₄. Next, embryos were transferred to individual wells of a 12-well plate and fixed. Fixation was done for 1 hour, at room temperature, with agitation, in Fix buffer (0.2% gluteraldehyde, 5 mM EGTA pH 7.3, and 20 mM MgCl₂ in P-buffer). Next, embryos were rinsed three times, for 30 min each, in Wash buffer (100 mM sodium phosphate pH7.3, 2 mM MgCl₂, 0.01% sodium deoxycholate, 0.02% NP-40). Embryos were stained for 36-48 hours at 37°C in Staining solution (5 mM potassium ferricyanide, 5 mM potassium ferrocyanide, 1 mg/ml X-gal in Wash buffer). Once sufficient staining was evident, embryos were post-fixed overnight in 10% formalin, at 4°C with agitation. At this point, embryos were washed twice with ddH₂O for 30 min each, and then placed in 70% ethanol for storage at 4°C.

Prior to photographing stained whole embryos, tissues were cleared with methyl salicylate (protocol from: www.muridae.com/wmc/docs/lac_zbible.html). First, embryos were dehydrated by replacing the 70% ethanol storage solution with 95% ethanol, and incubating for 30 min, at room temperature, with agitation. Embryos were then washed twice, for 30 min each, with 100% ethanol. Finally, embryos were transferred to 100% methyl salicylate in glass tubes, and incubated at room temperature, with agitation, for 10-15 min until the tissue cleared sufficiently. (It is essential to use glass containers at this point because methyl

salicylate dissolves polystyrene.) Embryos were photographed using a Leica MonoZoom 7 light microscope equipped with a Sanyo Hi-Resolution Color CCD camera.

To see the staining of internal organs more clearly, whole stained embryos were cut in half using a cryostat. The embryos were frozen in cryomatrix as described for the GFP-positive embryos above. Sections of 20 µm thickness were cut and discarded until about half of the embryo remained. The embryos were washed with ddH₂O to remove any residual cryomatrix material, dehydrated with ethanol, and then cleared with methyl salicylate as described above. The bisected embryos were photographed using a Leica MonoZoom 7 light microscope equipped with a Sanyo Hi-Resolution Color CCD camera.

II-8. NHE1 Immunoblot Analysis

Preparation of Crude Microsomes from Mouse Organs

To prepare the mice for dissection of the required organs, adults were euthanized with CO₂, and neonates were first anesthetized with CO₂ than decapitated. (The Health Sciences Animal Policy and Welfare Committee approved all animal protocols in accordance with the Canadian Council of Animal Care.) The organs were removed, and immediately frozen in liquid nitrogen. Next, tissues were placed in homogenization buffer which contains 1 M NaCl, 100 mM Tris pH7.4, 0.1 mM PMSF, 0.1 mM Benzamidine, 37.5 µM ALLN

(calpain I inhibitor) and 1:2000 proteinase inhibitor cocktail (0.02 µM Aprotinin, 1.4 µM E-64, 1 µM Leupeptin, 1 µM Pepstatin, 100 µM Phosphoramidon, 100 µM TLCK, 200 µM TPCK and 10 µM APMSF). Samples were homogenized at 4°C for 30 sec, incubated on ice for 30 sec, and then homogenized again for 30 sec using an Omni International 2000 electric homogenizer. To obtain crude microsomes, homogenates were subjected to a series of centrifugation steps. First, homogenates were centrifuged for 10 min at 3000 RPM. The resulting supernatant was then centrifuged at 10000 RPM for 15 min. The supernatant was again retained, and was centrifuged at 30000 RPM for 1 h to obtain a fraction enriched in crude microsomes. Finally, the crude membrane pellet was resuspended in homogenization buffer with 1% SDS to aid in solubilization. (An immunoblot of supernatant and pellet from adult heart and kidney samples showed that the crude membrane pellet contained a large majority of the total NHE1.) Total protein was quantified using the Bio-Rad DC Protein Assay kit.

NHE1 Immunoblots

For the NHE1 immunoblots, crude membrane fractions (containing 60-100 µg total protein) were aliquotted, heated at 37°C for 5 min and placed on ice. These samples were then run on 9% polyacrylamide gels, followed by transfer to nitrocellulose membranes. To confirm that equal amounts of sample were loaded into each lane, blots were stained with Ponceau S (3-hydroxy-4-[2-sulfo-4-(sulfo-phenylazo)phenylazo]-2,7-naphthalene disulfonic acid). To do this, the Ponceau

S stock (2% Ponceau S, 30% trichloroacetic acid, 30% sulfosalicylic acid) was diluted 1:10 with ddH₂O, and the membrane was incubated in this solution for 10 min, at room temperature, with agitation. Next, the membrane was washed for 1-2 min in PBS. To record the staining pattern on the blot, the blot was scanned with an Agfa ArcusII scanner and the electronic image was saved on disk. To remove the Ponceau S stain, the membrane was washed for 10-20 min in PBS with frequent solution changes.

For the immunological reaction, membranes were incubated overnight at 4°C in 10% milk/TBS, and then washed three times for 5 min each in TBS at room temperature. Membranes were probed at 4°C overnight with anti-NHE1 monoclonal antibody, at a concentration of 1:2000 in TBS. Following three 5 min washes with TBS, membranes were incubated with 1:5000 goat-anti-mouse antibody in TBS at room temperature for 45 min. After three 5 min washes in TBS, the Amersham Enhanced Chemiluminescence reaction was used to visualize immunoreactivity. Blots were scanned and quantified with Image Gauge (Bio-Rad) software.

Immunoprecipitation of NHE1

Andrea Moor performed the immunoprecipitation of NHE1 as described previously.²⁰

II-9. Rat Heart Metabolic Experiments

Preparation of Rat Neonatal Myocyte Primary Cultures

Rat neonatal myocyte primary cultures were prepared by Andrea Moor, as previously described.²⁰ Following euthanasia by decapitation, hearts were removed from 5-6 day old rats, and placed in 5 ml of Solution I. (The recipes for Solutions I-V are given in Table II-1.) Hearts were rinsed twice with Solution I. Next, the ventricles were separated from atria, blood vessels and connective tissue using a knife. The ventricles were then transferred to a new dish, washed once with Solution I, and then minced with a scalpel. Next, the tissue was transferred to a flask containing 15 ml of Solution II, and incubated at 37°C with stirring for 20 min. After allowing the tissue fragments to settle to the bottom of the flask, the liquid portion was removed, and placed in a tube containing 15 ml Solution III. Fifteen millilitres of fresh Solution II was added to the remaining tissue fragments, and a second 20 min incubation at 37°C was followed by removal of the liquid portion. This procedure was repeated three more times. Next, each of the four tubes (containing 15 ml Solution II, 15 ml Solution III and the myocytes) was vortexed, and then filtered using a Falcon cell strainer (#352350). The filtrate was centrifuged at 2000 RPM for 5 min, and the supernatant was discarded. The remaining pellet was resuspended in 15 ml Solution IV. At this point, the myocytes were placed in a T-75 Corning flask and incubated at 37°C for 20 min. During this period, fibroblasts, endothelial cells and smooth muscle

cells attached to the flask while myocytes remain in solution. Next, the media (containing myocytes) was transferred to a new T-75 flask. Fresh Solution IV was added to the former flask to repeat the 20 min incubation period and the media was again retained. The two 25 ml volumes containing the myocytes were pooled into one flask, and left overnight at 37°C in a humidified, 5% CO₂ atmosphere. By the following day, the myocytes were attached to the flask and the media was replaced with Solution V. Myocytes were aliquotted to 35 mm dishes, and maintained with daily media replacement for 3-5 days prior to beginning the metabolic experiments.

Treatment of Primary Myocyte Cultures with Different Metabolic Conditions

After washing once with PBS, cells were treated with control (5 mM glucose, no fat), high glucose (20 mM glucose, no fat) or high fat (5 mM glucose, with palmitate) media for 24 hours at 37°C. Other studies have used a concentration of 1% BSA-complexed palmitate in high fat media recipes⁹⁷; therefore, this amount was included in the present experiments. Recipes for the various media are tabulated (Table II-2).

Preparation of Microsomes from Myocyte Cultures

Dishes (35 mm size) with 4-5 day old primary rat cardiomyocyte cultures were washed twice with ice-cold PBS and then scraped into tubes containing 2 ml PBS with 5 mM EDTA. Next, the tubes were centrifuged at 2000 RPM for 5 min, and the supernatant was discarded. The cell pellet was then resuspended in 10 ml PBS, centrifuged at 2000 RPM for 5 min, and the supernatant was again discarded. Cells were resuspended in 5 ml Lysis buffer (10 mM Tris pH8.0, 25 mM KCl, 2 mM MgCl₂, 2 mM EGTA, 2 mM EDTA), and incubated on ice for 15 min. At this point, protease inhibitors were added including: 1 mM PMSF, 1 mM benzamidine and 1:2000 protease inhibitor cocktail (0.02 µM Aprotinin, 1.4 µM E-64, 1 µM Leupeptin, 1 µM Pepstatin, 100 µM Phosphoramidon, 100 µM TLCK, 200 µM TPCK and 10 µM APMSF). The mixture was homogenized using a glass homogenizer for 40 strokes. Five milliliters of Lysis buffer with 250 mM sucrose and 6 mM β-mercaptoethanol was added, and the homogenization was repeated. Next, the mixture was centrifuged at 8000 RPM for 20 min at 4°C. The supernatant was retained and centrifuged at 36500 RPM for 75 min at 4°C. The resulting pellet was resuspend in 45 µl resuspension buffer (1 M NaCl, 100 mM Tris pH7.4, 0.1 mM PMSF, 0.1 mM Benzamidine, 37.5 µM ALLN (calpain I inhibitor), 1% SDS and 1:2000 proteinase inhibitor cocktail. Total protein was quantified using the Bio-Rad DC Protein Assay kit.

NHE1 Immunoblots of Myocyte Microsomes After Different Metabolic Treatment

Crude microsome fractions containing 5-10 µg total protein were run on 9% polyacrylamide gels followed by transfer to nitrocellulose membranes. The immunological reactions and quantification were done as described above.

II-10. Genotyping of AP-2 α Knock-out Mice

Crude genomic DNA preparations were made from tails or ear notches as described above (*Genotyping by Step-down PCR* section). The 50 µl PCR reaction contained: 5 µl 2 mM dNTPs, 5 µl 10x PCR buffer (Gibco), 5 µl 15 mM MgCl₂, 5 µl 4 µM Alpha KO primer, 5 µl 4 µM Neo KO primer, 19.5 µl ddH₂O and 5 µl crude DNA prepared from the tails or ear notches. The sequences of the Alpha KO and Neo KO primers are listed below.

Alpha KO primer:

5'-CGT GTG GCT GTT GGG GTT GTT GCT GAG GTA C-3'

Neo KO primer:

5'-AAC GCA CGG GTG TTG GGT CGT TTG TTC G-3'

The PCR cycling steps were as follows:

1. 94°C for 10 min after which 0.5 µl Taq polymerase (Gibco) was added (This step must be done for at least 10 min to destroy any residual Proteinase K activity in the crude DNA preparations before adding Taq polymerase.)
2. Thirty cycles of 95°C for 40 sec and 72°C for 2 min
3. 72°C for 10 min

PCR products were run in a 7% polyacrylamide gel for analysis. PCR of genomic DNA from mice carrying the AP-2 α gene disruption produced a band of approximately 300 base pairs.

Figure II-1. Construction of NHE1 Promoter-Reporter Gene Plasmids.
(continued pages 62-69) A: Steps to obtain the NHE1 promoter. Cloning steps are described in bold italics in boxes. Selected restriction enzyme sites are indicated. GFP, green fluorescent protein gene; Bgal, β -Galactosidase gene; NHE1P, NHE1 promoter; P_{CMV IE}, cytomegalovirus immediate early promoter; MCS, multiple cloning site; SV40 poly A, SV40 early mRNA polyadenylation signal; f1 ori, f1 single strand DNA origin; P_{amp}, *E. coli* promoter; SV40 ori, SV40 origin for replication; P_{SV40}, SV40 early promoter; Kan^r, kanamycin resistance gene; Neo^r, neomycin resistance gene; HSV TK poly A, Herpes simplex virus thymidine kinase polyadenylation signal; pUC ori, pUC plasmid replication origin; P_{T7}, T7 promoter; lac Z, β -Galactosidase gene; Amp, ampicillin resistance gene; Luc, luciferase gene.

A

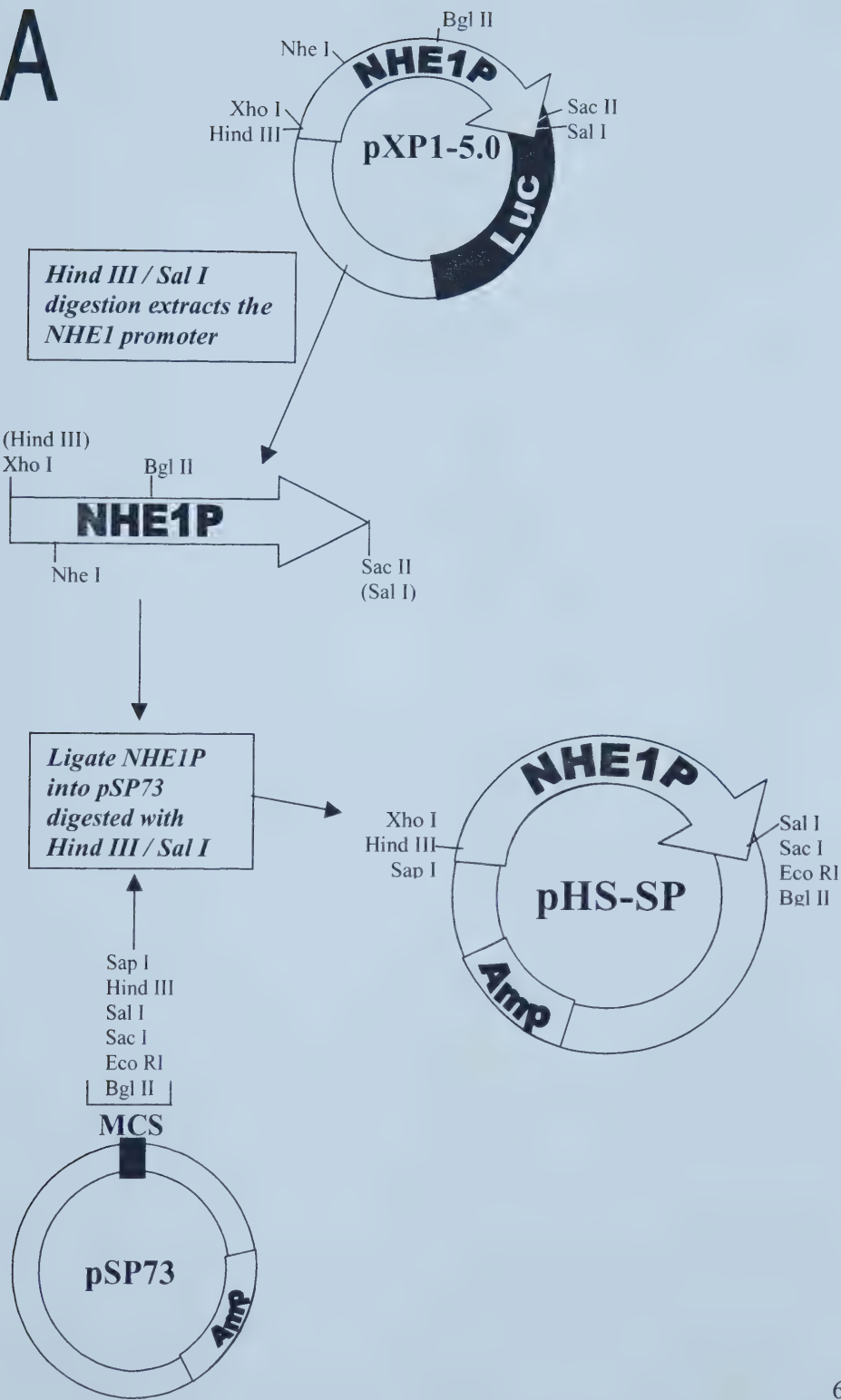


Figure II-1. Construction of NHE1 Promoter-Reporter Gene Plasmids. (continued from page 60) B: Steps to obtain the GFP gene. Cloning steps are described in bold italics in boxes. Selected restriction enzyme sites are indicated. GFP, green fluorescent protein gene; Bgal, β -Galactosidase gene; NHE1P, NHE1 promoter; P_{CMV IE}, cytomegalovirus immediate early promoter; MCS, multiple cloning site; SV40 poly A, SV40 early mRNA polyadenylation signal; f1 ori, f1 single strand DNA origin; P_{amp}, *E. coli* promoter; SV40 ori, SV40 origin for replication; P_{SV40}, SV40 early promoter; Kan^r, kanamycin resistance gene; Neo^r, neomycin resistance gene; HSV TK poly A, Herpes simplex virus thymidine kinase polyadenylation signal; pUC ori, pUC plasmid replication origin; P_{T7}, T7 promoter; lac Z, β -Galactosidase gene; Amp, ampicillin resistance gene; Luc, luciferase gene.

B

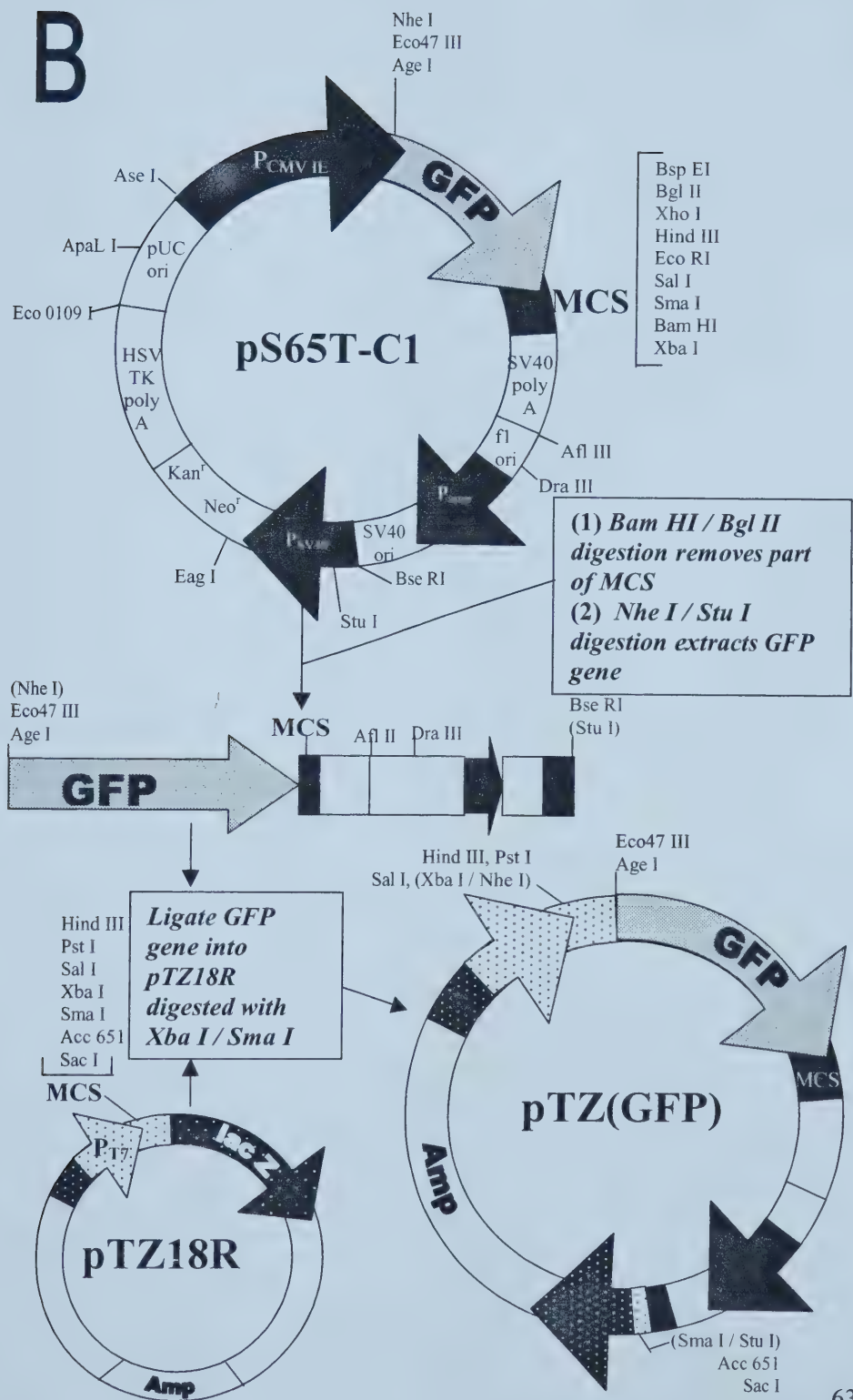


Figure II-1. Construction of NHE1 Promoter-Reporter Gene Plasmids.
(continued from page 60) C: Creation of the pHS-TZ(GFP) plasmid. Cloning steps are described in bold italics in boxes. Selected restriction enzyme sites are indicated. GFP, green fluorescent protein gene; Bgal, β -Galactosidase gene; NHE1P, NHE1 promoter; P_{CMV IE}, cytomegalovirus immediate early promoter; MCS, multiple cloning site; SV40 poly A, SV40 early mRNA polyadenylation signal; f1 ori, f1 single strand DNA origin; P_{amp}, *E. coli* promoter; SV40 ori, SV40 origin for replication; P_{SV40}, SV40 early promoter; Kan^r, kanamycin resistance gene; Neo^r, neomycin resistance gene; HSV TK poly A, Herpes simplex virus thymidine kinase polyadenylation signal; pUC ori, pUC plasmid replication origin; P_{T7}, T7 promoter; lac Z, β -Galactosidase gene; Amp, ampicillin resistance gene; Luc, luciferase gene.

C

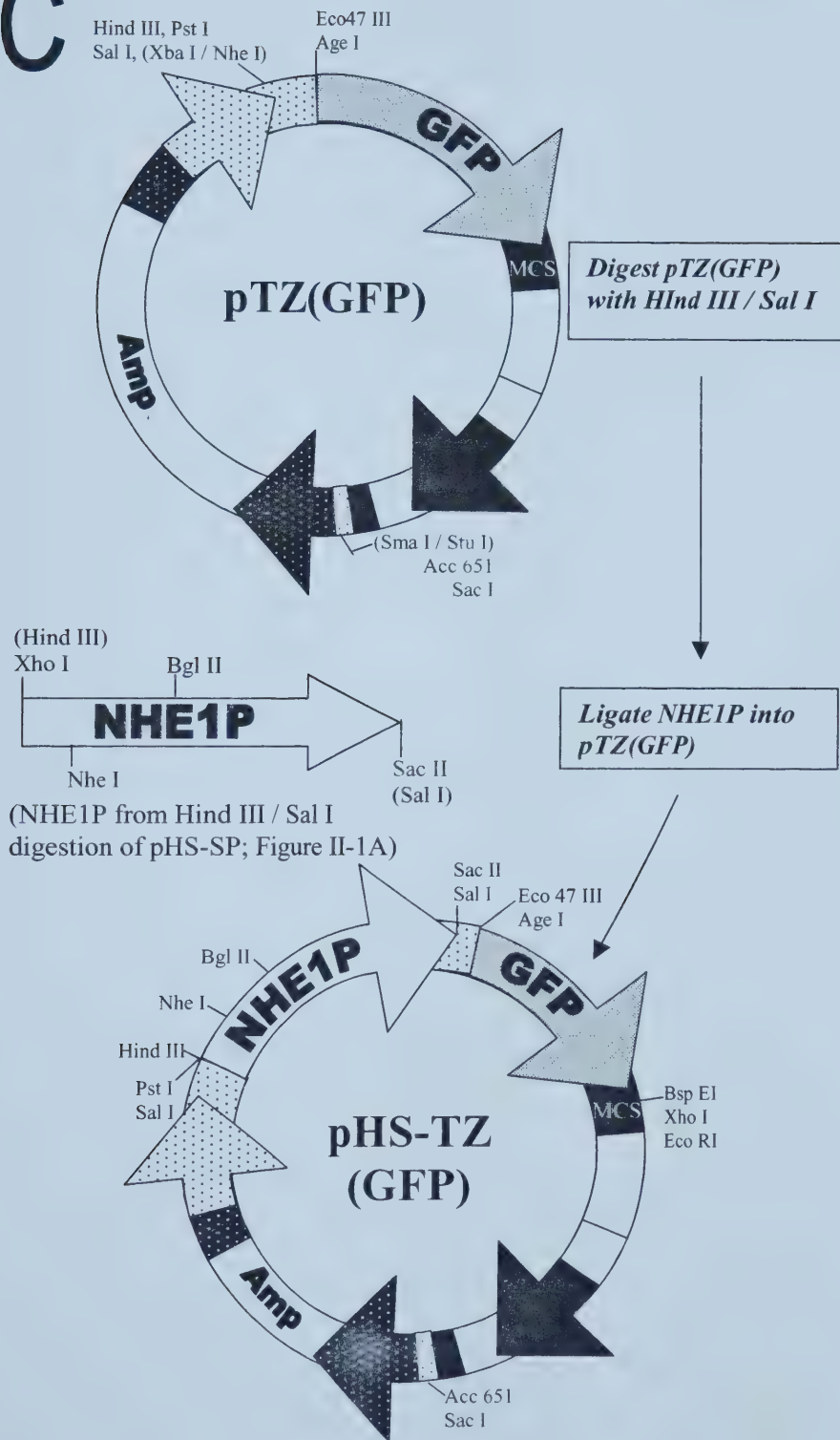
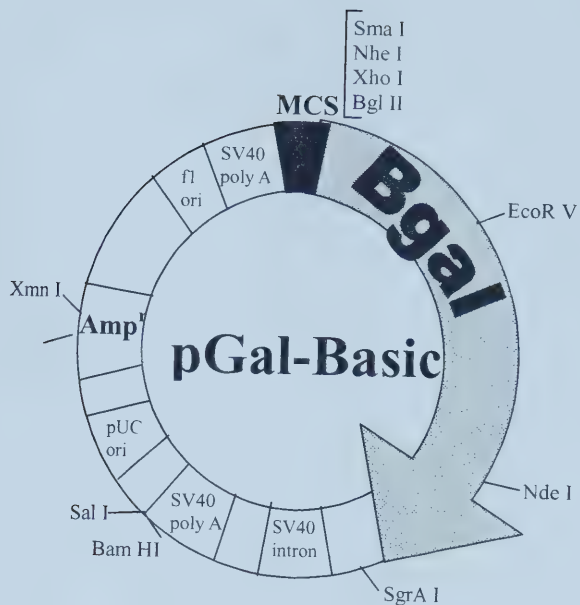


Figure II-1. Construction of NHE1 Promoter-Reporter Gene Plasmids.
(continued from page 60) D: Steps to obtain the β -Galactosidase gene. Cloning steps are described in bold italics in boxes. Selected restriction enzyme sites are indicated. GFP, green fluorescent protein gene; Bgal, β -Galactosidase gene; NHE1P, NHE1 promoter; P_{CMV IE}, cytomegalovirus immediate early promoter; MCS, multiple cloning site; SV40 poly A, SV40 early mRNA polyadenylation signal; f1 ori, f1 single strand DNA origin; P_{amp}, *E. coli* promoter; SV40 ori, SV40 origin for replication; P_{SV40}, SV40 early promoter; Kan^r, kanamycin resistance gene; Neo^r, neomycin resistance gene; HSV TK poly A, Herpes simplex virus thymidine kinase polyadenylation signal; pUC ori, pUC plasmid replication origin; P_{T7}, T7 promoter; lac Z, β -Galactosidase gene; Amp, ampicillin resistance gene; Luc, luciferase gene.

D



*Xho I / Sal I
digestion extracts
the β gal gene*

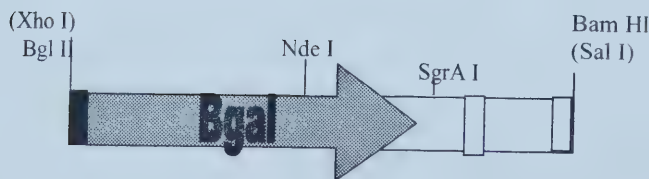


Figure II-1. Construction of NHE1 Promoter-Reporter Gene Plasmids.
(continued from page 60) E: Creation of the pHS-SP(β gal) plasmid. Cloning steps are described in bold italics in boxes. Selected restriction enzyme sites are indicated. GFP, green fluorescent protein gene; Bgal, β -Galactosidase gene; NHE1P, NHE1 promoter; P_{CMV IE}, cytomegalovirus immediate early promoter; MCS, multiple cloning site; SV40 poly A, SV40 early mRNA polyadenylation signal; f1 ori, f1 single strand DNA origin; P_{amp}, *E. coli* promoter; SV40 ori, SV40 origin for replication; P_{SV40}, SV40 early promoter; Kan^r, kanamycin resistance gene; Neo^r, neomycin resistance gene; HSV TK poly A, Herpes simplex virus thymidine kinase polyadenylation signal; pUC ori, pUC plasmid replication origin; P_{T7}, T7 promoter; lac Z, β -Galactosidase gene; Amp, ampicillin resistance gene; Luc, luciferase gene.

E

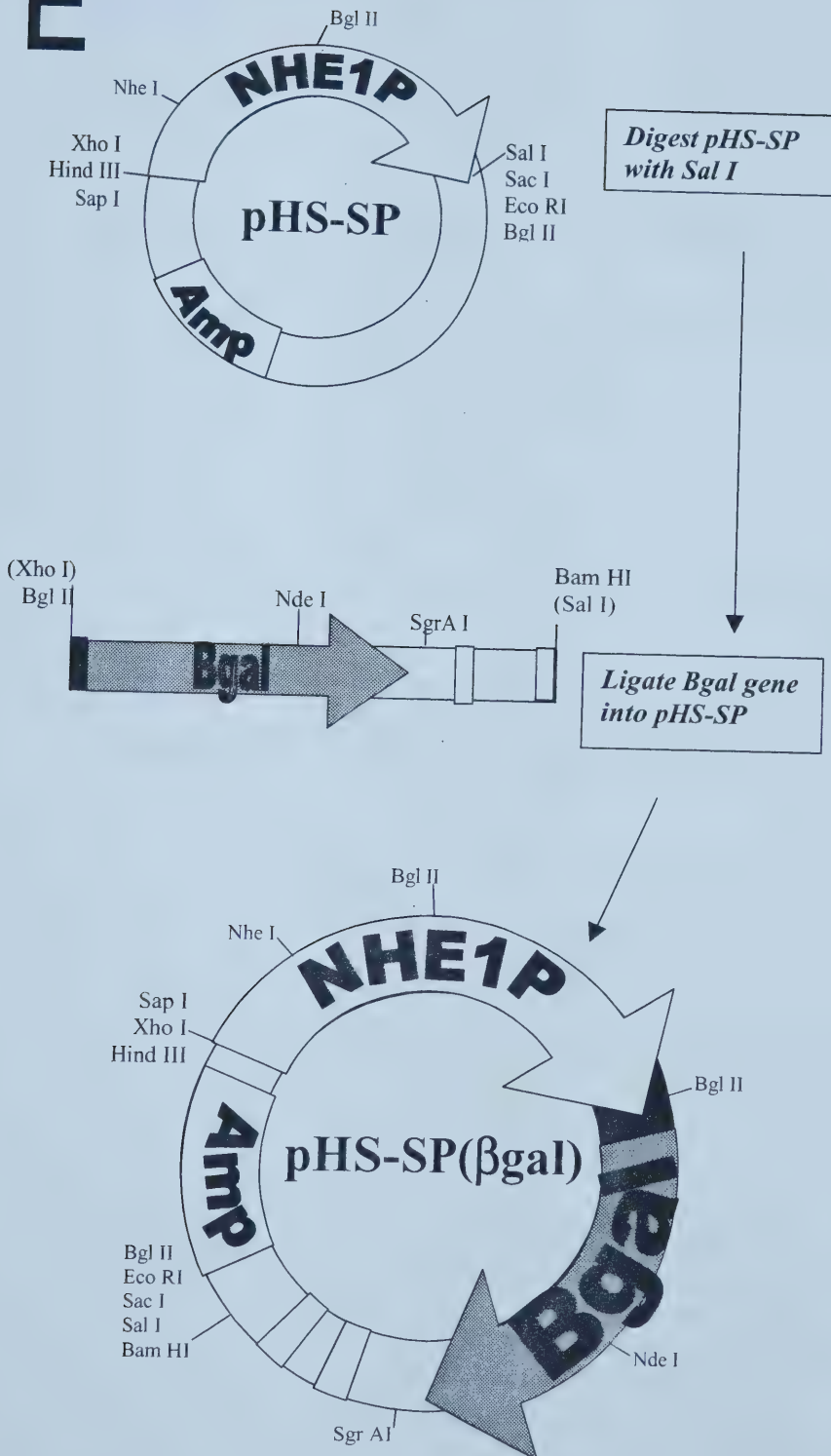


Table II-1: Recipes for Rat Neonatal Myocyte Culture Solutions

Solution	Contents
Solution I	20 mM HEPES and 1% penicillin/streptomycin in 1x HBSS (Hanks Buffered Salt Solution)
Solution II	0.1% collagenase, 1% penicillin/streptomycin, and 20 mM HEPES in 1x HBSS
Solution III	20% fetal bovine serum and 1% penicillin/streptomycin in 1x HBSS
Solution IV	DMEM F12 media pH7.3 (Gibco) plus: 15% fetal bovine serum 10 g/l BSA 0.25 g/l fetuin (Sigma, F-2379) 2.5 mg/l transferrine 1% penicillin/streptomycin 5 µg/l insulin 5 µg/l transferrin 10 ng/ml selenium 80 µg/l CaCl ₂ 20 µg/l L-ascorbic acid 1x MEM-Nonessential amino acids (Sigma A-4403) 1x Vitamin 100x (Gibco) 2 ml BSA-palmitate (see below) per litre Solution IV
Solution V	DMEM F12 media pH7.3 (Gibco) plus: 10% fetal bovine serum 30 mM HEPES 10 µg/ml transferrin 10 µg/ml insulin 1% penicillin/streptomycin 0.1 mM bromodeoxyuridine 5 µg/ml linoleic acid 2 mg/ml BSA 1x MEM nonessential amino acids (Sigma A-4403) 1x Vitamin (Gibco) 10 ng/ml selenium 3 mM pyruvic acid 100 µM ascorbic acid
BSA-palmitate	1.2 g BSA was added to 20 ml ddH ₂ O (therefore, final solution is approximately 6% BSA) and placed in a dialysis bag. The bag was dialyzed in PBS supplemented with 1.4 g palmitate in 10 ml 95% ethanol and 10 mM EDTA.

Table II-2: Media Recipes for Rat Myocyte Metabolism Experiments

Media	Contents
4x Common Mix	40 µg/ml transferrin 40 µg/ml insulin 0.1 mM bromodeoxyuridine 40 ng/ml selenium 0.1 mM ascorbic acid 1x MEM nonessential amino acids (Gibco) 1x Vitamin 100x (Gibco)
Control	1x Common Mix 0.15 mM BSA 15 mM L-Glucose 1% penicillin/streptomycin 1x MEM (Gibco; contains 5 mM D-Glucose)
High Glucose	1x Common Mix 0.15 mM BSA 15 mM D-Glucose 1% penicillin/streptomycin 1x MEM (Gibco; contains 5 mM D-Glucose)
High Fat	1x Common Mix 1% BSA-palmitate (see Table II-1) per ml media 15 mM L-Glucose 1% penicillin/streptomycin 0.25 mM carnitine 1x MEM (Gibco; contains 5 mM D-Glucose)

Chapter III

NHE1 Promoter Activity During Mouse Development

III-1. Introduction

This chapter examines the developmental and tissue specific regulation of Na⁺/H⁺ exchanger isoform 1 expression in the mouse embryo, neonate and adult. Consequently, two questions were pursued. First, is NHE1 transcription elevated in some tissues compared to others at a given age? Secondly, does the level of NHE1 transcription change in certain organs during murine development? To answer these questions, transgenic mice were generated which expressed the GFP or βgal reporter gene under the control of the mouse NHE1 promoter. The 3.8 kb NHE1 promoter fragment used contains all the crucial upstream components for gene expression in mammalian cells.⁴³

Transgenic mice and reporter gene technology were used in this analysis of NHE 1 transcriptional regulation for two reasons. First, only a relatively small amount of NHE1 protein is expressed in cells⁹⁸ thereby making detection problematic. The use of reporter genes facilitates this examination by providing an enhanced, visual signal of NHE1 transcriptional activity. Second, the presence of the reporters in transgenic mice allows analysis of NHE1 expression in the context of a whole, intact organism.

III-2. Results

Development of NHE1 Promoter-Reporter Constructs and Creation of Transgenic Mice

Two promoter-reporter DNA constructs were created for the purpose of making transgenic mice that expressed NHE1 promoter-controlled reporter genes. Each promoter-reporter construct contains a 3.8 kb fragment of the mouse NHE1 promoter, and a reporter gene, placed after the transcription start site. The linear DNA fragments used to generate the transgenic mice are depicted in Figure III-1. The construct used to make the GFP mouse lines contains the S65T-GFP gene under the control of the NHE1 promoter (Figure III-1A). The DNA fragment expressed by the β gal mouse lines has the bacterial LacZ gene that encodes β -galactosidase in this position (Figure III-1B).

In conjunction with the promoter-reporter fragment construction, the 3.8 kb mouse NHE1 promoter used in the constructs was sequenced. The last 1.1 kb leading to the transcription start site had been previously sequenced.⁴² The complete 3.8 kb primary structure is shown in Figure III-2.

To confirm that the plasmids were constructed correctly and could express the respective reporter genes, each construct was transiently transfected into NIH 3T3 fibroblasts. The GFP reporter-transfected cells were examined using fluorescent microscopy. Figure III-3A shows that the GFP-positive cells had significantly more green fluorescence than mock-transfected controls. A

chemiluminescence assay was used to detect β -galactosidase activity in the β gal reporter transfectants, and the results are illustrated in Figure III-3B. The NHE1-promoter β gal-reporter plasmid showed ten-fold more β gal activity than mock-transfected controls. NIH 3T3 cells were also transfected with an SV-40- β gal reporter plasmid, as a positive control. The β gal activity of cells transfected with this plasmid was much greater than the cells transfected with the NHE1 promoter- β gal reporter. Clearly, the NHE1 promoter is much weaker than the SV-40 promoter.

Polymerase chain reaction (PCR) was used to identify mice harboring the reporter genes. The genomic DNA used for PCR was obtained from the tail biopsies of embryos or the ear notches of neonates and adults. Representative examples of the PCR products are shown in Figure III-4. Lane C shows the absence of products from the negative control PCR reaction, which lacked any template DNA (Figure III-4A&B). Lane P illustrates the 400 base pair product of the positive control reaction, containing the NHE1 promoter-GFP reporter gene plasmid template and the GFP primers (Figure III-4A). PCR of the genomic DNA from mice carrying the GFP gene also produced a band of approximately 400 base pairs (Figure III-4A, lanes 1, 4, 8 & 9). Figure III-4B depicts the 400 base pair PCR reaction product using the β gal primers. Here, lane P shows the positive control product from the NHE1 promoter- β gal reporter gene template. From this litter, only mouse 3 is positive for the β gal gene (lane 3, Figure III-4B).

Five founder animals were selected and used to establish five separate lines: three GFP-reporter lines (denoted G16, G31 and G34) and two β gal-reporter lines (named β 2 and β 3).

Analysis of the NHE1-promoter GFP-reporter transgenic mice

To determine the extent of NHE1 transcriptional activation during embryonic development, embryos were examined at 12, 15 and 18 days after conception. Figure III-5 illustrates the GFP fluorescence of sagittal, whole embryo sections at these ages. (Minor variations in size between embryos of the same age are due to small differences in the section depths of the illustrated embryos.) Figure III-5A shows 12-day-old embryos (E12) from control, G16 and G34 mouse lines. The third GFP line, G31, did not strongly express GFP (not shown), and was therefore not analyzed further. A qualitative comparison of the GFP positive pictures to that of the control reveals significant fluorescence in the heart and liver, indicating an activation of NHE1 transcription in these tissues at E12. Similarly, fluorescence of the heart and liver in 15-day-old embryos (E15) appears to be greater in G16 and G34 animals compared to control, though to a lesser extent than E12s (Figure III-5B). Finally, Figure III-5C illustrates that the GFP reporter does not give an obvious fluorescent signal in any tissues of 18-day-old embryos (E18). E18 results were similar for the G34 line (not shown).

The quantitative analysis of GFP fluorescence in various organs at E12 is shown in Figure III-6. Representative heart and liver sections from control, G16

and G34 lines are depicted in Figure III-6A. Fluorescence was quantified using NIH Image software as described in *Material and Methods* (Chapter II), and results from the heart, liver and lung are depicted in Figures III-6B, III-6C and III-6D, respectively. GFP fluorescence was found to be more than 5-fold greater in the GFP-positive heart compared to control animals (Figure III-6B) while the liver exhibited a 12-fold increase in reporter expression (Figure III-6C). The fluorescence of the lung was quantified as a negative control and does not show significant fluorescence over background in either GFP line (Figure III-6D). Thus, it appears that NHE1 transcription is activated in both the heart and liver at embryonic day 12, while it remains below the level of detection in the lung and other tissues.

The E12 hearts were also examined at 100 times magnification (Figure III-7). The microscope was focussed on the centre of the heart wall (the myocardium) because this region was noted to fluoresce brightly at lower magnification (Figure III-6A). The photomicrographs (Figure III-7) illustrate that GFP is expressed in the cytoplasm, and that a subset of cells have a higher level of transgene expression. The GFP-expressing cells are most likely myocytes based on their numbers, morphology and location.⁹⁹

Figure III-8 shows the quantification of fluorescence in 15-day-old embryos. Representative sections of heart and liver regions are given in Figure III-8A. GFP fluorescence was found to be about 2- to 3-fold greater in the E15 reporter-bearing hearts compared to control (Figure III-8B). In the liver, the

reporter signal was approximately 2.8-fold higher in the GFP lines than background (Figure III-8C). The lung did not show significant fluorescence at E15 (Figure III-8D). Although NHE1 transcriptional activation can be detected in both the heart and liver of 15-day-old embryos, compared to E12s, this activation was 2-fold less in the heart and was reduced by 6-fold in the liver.

The subsequent quantitative analyses were performed exclusively on the heart. Hearts from 18-day-old embryos, 1-day-old neonates, 14-day-old neonates and adults are illustrated in Figure III-9A. For quantification, controls were assigned a value of 1.0. The quantity of GFP expressed at each age was then normalized to the respective, equal aged controls. Figure III-9B shows that none of the GFP positive hearts had significantly greater fluorescence than controls at these ages. Therefore, the level of cardiac NHE1 transcription is below the level of detection in the 18-day-old embryo, neonate and adult.

Analysis of the NHE1-promoter β gal-reporter transgenic mice

Figure III-10 shows 12-day-old embryos stained with X-Gal to visualize the β gal reporter. Although these results are less conclusive than that of the GFP-reporter embryos, they confirm the GFP-reporter findings. First, the β gal transgenics clearly express the reporter (Figure III-10A). More importantly, in a cross-sectional view of stained β gal-positive and age-matched control embryos, there appears to be significant blue staining in the heart and liver of the β gal-positive animal compared to the control (Figure III-10B).

Since both the β gal and GFP transgenics strongly express the respective reporters in the heart and liver, reporter expression is a function of the NHE1 promoter and not the reporter gene. Staining of other tissues is also observed in both the control and β gal-positive embryos and is likely due to endogenous β gal activity.⁹³

III-3. Discussion

This study examined the regulation of NHE1 transcription during development in the intact mouse. Transgenic mouse embryos with the NHE1 promoter coupled to a GFP or β gal reporter were analyzed. Two important observations were made by qualitative and quantitative analysis of the GFP-reporter transgenic mice. First, NHE1 transcription is highest in the heart (specifically, cardiomyocytes (Figure III-7)) and liver relative to other tissues, at the earliest two embryo stages examined. Second, NHE1 transcription in these tissues decreases from E12 to E18, and plateaus at the lower level thereafter.

It must be noted that the level of GFP can be influenced by mRNA stability, protein translation and protein stability. However, since the level of GFP expression in this study was low, it is likely that it was within a linear range, whereby GFP levels faithfully represent transcription. It is unlikely that higher expression levels of GFP caused a non-linear relationship between transcription and GFP levels.

Studies of cardiac hypertrophy in adult rabbit hearts have demonstrated the importance of NHE1 in heart growth. Takewaki et al.¹⁰⁰ showed that cardiac hypertrophy (induced by pressure-overloading) resulted in a three-fold increase in NHE1 mRNA, three days following the pressure-overloading procedure. Heart enlargement was not apparent until the seventh day. This suggests that NHE1 expression precedes growth of the cardiac tissue. Furthermore, Yoshida et al.¹⁰¹ demonstrated that cardiac hypertrophy could be attenuated by the specific NHE1 inhibitor cariporide. Cariporide was included in rat diets for one week prior to ligation of the left coronary artery to induce myocardial infarction. One week following the surgery, it was found that the heart mass to body mass ratio was increased by 12% in control animals but only 3% in animals treated with cariporide. Thus, NHE1 appears to play a significant role in cardiac hypertrophy.

A number of proteins have been reported to revert to fetal expression patterns during cardiac hypertrophy including: β -myosin heavy chain, skeletal α -actin and Na^+/K^+ ATPase $\alpha 3$ subunit.¹⁰⁰ This suggests that certain proteins are important for growth of the fetal heart during development and enlargement of the adult heart in cardiac hypertrophy. NHE1 likely also belongs to this group because NHE1 expression levels were elevated in the embryonic heart in the present study and are increased during adult cardiac hypertrophy as discussed above.

Given that NHE1 is important for growth in the heart, why would NHE1 transcription decrease from E12 to E18? Although the absolute answer is

unknown, it is insightful to consider the development of the heart during murine embryogenesis. The heart is the first organ to differentiate and function.¹⁰² Formation of the heart begins at E8 and by E9 the heart beats in a strong, regular rhythm. Growth and differentiation of the heart and vascular system proceeds throughout the period from E9 to E12. By E13, inter-atrial and inter-ventricular septation has occurred and cardiac valves can be observed. Development of the heart and vascular system is essentially complete by E15. In the present study, NHE1 transcription in the heart was observed to decrease from E12 to E18. In light of the timeline for mouse heart development, it appears that NHE1 is important during heart differentiation, and the need for NHE1 is dramatically reduced once formation of the heart is completed. In fact, a role for NHE1 in differentiation has been previously described in several tissue culture models of differentiation including: human leukemic HL-60 cells,³⁶ mouse P19 embryonal cells³⁷ and rat L6 skeletal muscle cells.³⁹ (Chapter I-5 describes these reports in detail.) Further studies are required to elucidate the precise molecular function of NHE1 in the differentiation process *in vivo*.

NHE1 expression was also found to be high in the liver at the earliest embryo stage examined. Previous reports have shown that NHE1 is important for hepatocyte proliferation. For example, when the rat liver was constantly stimulated to proliferate (using a bile duct ligation procedure), steady-state NHE1 mRNA increased two-fold.³² Also, treatment of Hep G2 hepatoma cells with epidermal growth factor and transforming growth factor-alpha can stimulate

NHE1 activity.¹⁰³ Furthermore, addition of the NHE1 inhibitor hexamethylene amiloride decreases hepatocyte viability.¹⁰⁴ It is therefore clear that NHE1 is important in hepatocyte proliferation, and that the results of the present work likely reflect a role for NHE1 in embryonic liver cell growth.

To explain the decrease in NHE1 transcription that was observed in the liver in the later stages of embryogenesis, the development of this organ must be considered. At embryonic day 10.5, the liver is small and its boundaries are not well defined.¹⁰² However, at E11 the liver enlarges rapidly such that it is very well differentiated by E12. Also, at E11 the liver takes over the majority of hematopoiesis from the yolk sac. In fact, one of the major functions of the liver in the later stages of embryogenesis is hematopoiesis (the process whereby red and white blood cells are formed from stem cells). Hematopoiesis continues in the liver through E15 and E16, however by E18, the spleen and bone marrow replace the liver in this process. The liver is thereby free to assume its postnatal role in detoxification. Thus, in a simplified view, two processes are occurring in the embryonic liver between E11 and E18: differentiation and hematopoiesis. The significance of NHE1 to both of these processes has been reported. As noted above, NHE1 has been shown to be important for proliferation of hepatocytes.^{32,105,104} A role for NHE1 in hematopoiesis has also been suggested since hematopoietic differentiation of mouse bone marrow cells could be inhibited by the NHE1-specific drug hexamethylene amiloride.¹⁰⁶ In the present study of the GFP-reporter transgenic embryos, NHE1 promoter activity in the liver was

highest at E12, the earliest age examined. Thus, it appears that NHE1 expression is activated in parallel with differentiation and hematopoiesis in the E12 liver. NHE1 transcription decreased substantially by E15, and by E18 the promoter activity in the liver was not detectable above background levels. It is plausible to conclude that NHE1 transcription is less at E15 than E12 because liver differentiation is essentially complete at this point; however, the potential hematopoietic need for NHE1 persists. Finally by E18, the liver is absolved of hematopoiesis and NHE1 transcription levels fall accordingly. It is important to stress that although these correlations can be suggested, the exact molecular role of NHE1 in the process of hepatocyte differentiation or hematopoiesis is not known, and further research in this area is required.

The results showing developmental regulation of NHE1 transcription lead to a limited investigation of transcription factors that are expressed in the E12 mouse heart and liver (when NHE1 promoter activity was greatest), and that have putative binding sites within the NHE1 promoter. To accomplish this, two database searches were performed and compared. The first analysis identified proteins expressed in the E12 mouse heart and liver (www.informatics.jax.org/searches/anatdict_form.shtml). The second search listed putative transcription factor binding sites located in the NHE1 promoter (<http://molsun1.cbrc.aist.go.jp>). Three transcription factors were common to both searches: GATA-1, SCL/Tal-1, and Myb. All of these proteins are important for development of the murine hematopoietic system¹⁰⁷, and therefore may account

for the augmented NHE1 promoter activity at E12 and E15 in the liver. No heart-specific NHE1-binding transcription factors were identified.

In this study, NHE1 transcription was also examined using β gal-reporter transgenics. Reporter activity was difficult to detect in these embryos likely owing to the low level of NHE1 normally expressed,⁹⁸ the weakness of the NHE1 promoter (Figure III-3B), and the reduced sensitivity of the β gal reporter compared to the GFP reporter. Chiocchetti et al.¹⁰⁸ analyzed the sensitivities of these two reporters. Their study compared transgenic mice expressing either reporter gene under the control of the human hemopexin promoter, which drives expression of hemopexin in the liver and to a lesser extent, in the brain. The pattern of GFP expression matched *in situ* hybridization results more closely than the β gal reporter sections (with respect to the number of cells expressing the transgene and the intensity of expression). Also, in liver sections, eight-fold more GFP fluorescent cells were detected than β gal stained cells while in brain sections, seventy times more GFP fluorescent cells were counted compared to β gal stained cells. Thus, the minimal success with the NHE1-promoter β gal-reporter transgenic embryos in the present report is quite possibly due to the lower sensitivity of this reporter gene.

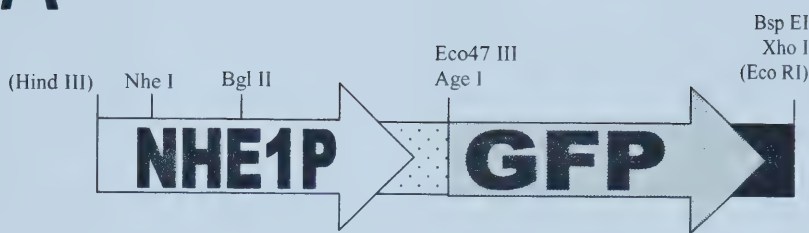
This chapter has examined the transcriptional activity of the NHE1 promoter during mouse development. It was found that NHE1 expression was greatest in the heart and liver at the earliest embryonic age examined. The transcription reporter signal decreased markedly thereafter, and NHE1

Chapter III

transcription could no longer be detected in embryos just before birth. Taken together, these findings imply that NHE1 has a very significant role in early development and differentiation of the heart and liver. Once morphogenesis of these organs is completed, the need for NHE1 diminishes.

Figure III-1. Schematic diagram of the NHE1 promoter-reporter gene DNA constructs used to generate the transgenic mice. A: NHE1 promoter (NHE1P) – green fluorescent protein (GFP) reporter gene construct. This fragment was excised from the pHS-TZ(GFP) plasmid (Figure II-1C) by digestion with Hind III and Eco RI, and was then used to create the transgenic mice. B: NHE1 promoter (NHE1P) - β -Galactosidase (BGAL) reporter gene construct. This fragment was excised from the pHS-SP(β gal) plasmid (Figure II-1E) by digestion with Xho I and Sal I, and was then used to create the transgenic mice.

A



B

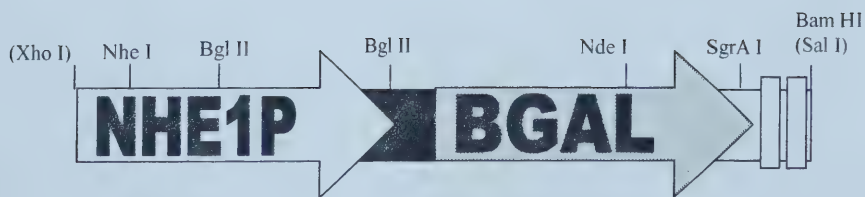


Figure III-2. Nucleotide sequence of the 3.8-kb NHE1 promoter region. (continued on page 91) Sequencing primer sites are indicated above the sequence. Arrows denote the transcription start site. Nucleotides previously sequenced are indicated in italics.³⁹

	10	20	30	40	50
-3536	AGGCCTCGAG	CAGCTGAAGC	TTTATTTATG	TACATTCCCT	AATATTCTGA
-3486	CTACAGCACCC	ACAAGGTTGG	CCCTGTGCT	TTATGGTGGAA	AGAACTTGGAA
-3436	ACAGAGACTG	ATTACTCCAG	GTCTCACGCC	TGTGGTGGTG	CTGGGACAGG
-3386	GTCTAGACAG	TGGCCATCTG	TGTTAGGCAG	CCCTGAAGCC	TCCTGGGACT
-3336	GTGCCCTAGC	TACAAGCTAG	GATTATTTC	TGATACTGTT	AAGTTTTAT
-3286	<u>AACCTCTCC</u> Primer 1b → <u>TCTTCTCGA</u>	ATGCTCTGTA	GGACCTCCAC	CAGGGGTGGT	ATTTCT <u>GGT</u>
-3236		<u>TCTGCTCT</u>	CTTGAGCTGG	CACCAAAGAC	TTACTGAGGG
-3186	CTGGAGGGGG	TGGGGTGGGG	GTGGGGAAACA	CCAGTGACTG	CCAGTGGCCT
-3136	CAAGGCTTGG	GAGTAAAGTG	CCTACACTAG	CCCTGCCCTT	CCTCTCCCTT
-3086	TAGTAATCCG	TACTGAGTCT	GCAGTGTAA	TAACGCTGG	CTTTAAATGT
-3036	TAGCACTGCT	TCCCCACAGC	TATGTGATCT	TAGGCAAACA	GCTTCAAAAT
-2986	<u>CCAACCTTG</u> Primer 1c → <u>GCATCCTGAT</u>	GTGCTTATC	TGTCAAGTGA	GAATGGGAAT	AAT <u>CACTACT</u>
-2936		<u>TCTCTGTTAT</u>	ACGGCATAGC	AGTTGGTTT	CAGTTCTCAG
-2886	TGACTCCACA	AGGCATTGTT	GATTCTGATC	CTCTGGGGTT	TTAGTTATTG
-2836	AGAATGGAAC	ACAGTGCATT	TTATATGCTA	GGCAAGCACT	CCAGTGCTGA
-2786	GCTATGTTCC	CACCACCTTA	TTTTATTATC	ATTATTATTA	ATATTATAGA
-2736	TTTATGTATT	TATTTATGT	ATATGAGTAC	ACTGTCGCTG	TCTT ^{TT} AGACT
-2686	<u>CACCAAGAAGA</u> Primer 1d → <u>GTGGTTGCTG</u>	GGGCATCAGA	TCCCATTACA	GATGGTTGTG	<u>AGCCATCCAT</u>
-2636		<u>GGAATTGAAC</u>	TCAGGACCTC	TGGAAGAGCA	GTCAGTGCTC
-2586	TTAACCTCTG	AACCCAGTCC	TGCATTATCT	TTTATATCAT	TTTATTGAA
-2536	AGCAAGCTCT	CCAAAGTTGA	TCATGCTAGC	TTTGAGCTCA	CTCTGTAGAC
-2486	CTTGAGGGT	TTGAACTTTC	CATCCTCTG	ACTCAGTCTC	CTGAGAAGTC
-2436	TCATCTCAAT	GCCAGATGGC	AAGCCTGGCT	TGTTCTGATC	TGTGACCTAG
-2386	AAGTCATTCC	CTTTCTCAC	<u>CTCCATTGGA</u> Primer 1e → <u>AGTGTGGGG</u>	GCTACTGTTT	GTCTTTCATC
-2336	TGTTCTCAGT	ATTGTCTAA	<u>ATCGAACCGG</u>	GGTGTGCTC	
-2286	ATGCTAGGAC	AGCTGCTCCA	TGATAGTCTC	CGAACCCAT	AACACACCCC
-2236	TCATGTGTGT	ATGGGTATGG	TATATGCATA	GTGTGTTGTG	TTGTGTGCAA
-2186	GTGCATCAGC	CTTGTACAGG	CAGACGCCA	ACTAGGAATC	<u>ACCTGGAGCC</u> Primer 1f → <u>CATTCTCCAA</u>
-2136	AGGCTGGTGG	GCAGCAAGCC	CTAGCAATCT	<u>TTTTGTCTC</u>	
-2086	<u>GGTACGAGGG</u>	TTAAAGGTGT	GTGGGCATAC	TGGCTTTCTT	GTTCCTTCT
-2036	TTTAACCTCTG	AGAGCTGGGG	ATTATTGTA	ATGATGGTCC	TTAGCCACTA
-1986	AAGCATTTT	CCAGGTCTGT	TTCTGAATCT	TCTCTTTCTT	TCTTCTTTC
-1936	TTCTTCTTCT	TCTTCTTCTC	TTCTTTCTT	TCTTCTTCTT	TCTTCTTCT
-1886	TTCTTCTTCTT	CTTCTTCTCT	TTCTTTCTT	TTTCTTTTT	TTTTTTTTT
-1836	CCGGTCACCT	CCCAGTGTCC	GAATCTATT	CTGGAAAAAC	GTGGCAAGGT
-1786	TCAGAAAAGT	CAGAAATGTT	TTACACTTGG	TTGTCAATAC	ACACTCTTGT

Figure III-2. Nucleotide sequence of the 3.8-kb NHE1 promoter region.
(continued from page 89)

	10	20	30	40	50
-1736	TACTTGAAAA	CACCTTTTTC	CAGATGGAAA	GTACACAAAC	TCTGAAGGCA
-1686	TGGTGAACTC	CCACAACATA	ACTGCTTCTG	GAGTA <u>ACTGG</u>	Primer 2c <u>GTATGGACCA</u>
-1636	<u>CC</u> CAGTGAAG	GAACAGGACG	CTCCCAGAGC	TGGGAAGCTC	ACCTTGAGCT
-1586	CTGGAGCTGA	CCCTAATCAC	CATTACAGT	CCCACCTCCAC	GCCTCATGCC
-1536	TATGTCCCTA	GCTCAGCAGA	AATCCTTGTC	AAGAAAGTTC	TGAAGAGATT
-1486	TGTCAACAGA	AAACAAACCC	CTCTAACAGC	CCCTTGAACA	AATCACCTG
-1436	GATTTTCGG	CTTTAATTAA	CCTTCCATG	AAACAGGATG	GCATTGAAA
-1386	TGATTTAAA	ACTTCTCAGT	CTGGGCTCAG	CGGTGGTGTG	CTTACT <u>AGGA</u>
-1336	<u>CG</u> CAGACGGT	<u>TCTGTGTTCA</u>	GATCTACTTC	TGAGGGGGGG	CACAATGTCT
-1286	CGACCTTTCT	GAACTCTAAT	CAATATCATT	CATTCAAATT	CCAGTTCCGG
-1236	CTGTGTGTGG	TGGTGCATAC	CAGTAATCCC	ACTTGAGAGG	GAGAGGCAGG
-1186	AGGATTGCCA	AAAATTAGAA	GCCAGCTGGG	CTACATTGTA	AGAATGTAGC
-1136	CTTTCGCACA	AAACAGAACAA	TGCCCTTCT	GGAAGCTGTT	TTCTGTCG Primer 2a <u>CAGACAGACAA</u>
-1086	AGATAATAAA	AATCCTTCTT	TTCTCTTAA	<u>ACCAGACAGA</u>	
-1036	GATAGACAGA	CAGACAAAAAA	CAATACCCAG	CCTCTTACTT	TTTGGTTGTT
-986	TCACTACTGT	TATGAGTTGA	AACACGCCCT	TTCAAAAGAA	GCTGAAGTCC
-936	TACCCCTGCC	CACCCCTCAG	TGCCCGAGAA	TGTGGCTTTA	TTTAGATGAG
-886	GGGTTTTGTT	GTTGTTGTTG	TTGTTTAAA	TCTCTTGTAG	ACAGGGTCTC
-836	CCTACTGACC	TCAGCCTGGT	CTAGAACTCA	CTTTGTACAA	CAAGCTGACG
-786	TTGAGTTAAA	AATTCCCTCTT	TCTTTAGTTT	CCCAAATGCT	GGAATTACAG
-736	TTTCCCACCG	TTCGTGGCTC	AGATTGGGTT	TTTGAAGTTG	ATCAAGGTAA
-686	GGTACGCCAT	TAGGGCCAAT	TCCTAAATTCA	ATTTGCTTGG	AGTCCTTTA
-636	AAGGGGGAAA	TTTGGACCTA	AAGACGGATA	CAGGGAGGCT	GGGGTTATGC
-586	CGCCACAGTC	AAGGGAGGCC	AATACATTGC	CATCAAAGCA	CCTGTGGCTG
-536	GGATGCAGGA	ACGGATTTC	GCTCACACGG	TCCTCAGCAC	AGGTCAATGC
-486	TTGGGAACAT	ACAGAGTGC	GATTCTAGC	CCATTTCATT	CATTCAATTAA
-436	ACTTTATTTT	GTGACACTGG	GCATAGGAAC	CAATGGTAGA	CAAGCACTCT
-386	ACCTCTGAAC	CACGATCCC	TCCCTTTCAT	TCTAAACATT	TCTCATAGAT
-336	CACCTCATTT	AACCATCTT	TTATCCTTTT	GTATAGCTA	TCCATCTCCA
-286	CCTTACAGTT	GAGAAAGCTG	TGAAACAGAG	AGGCTAAATA	ACTTGTTCCA
-236	AAGTCACATG	CTAACAAAGAA	AAACACTTGT	AGATAGTACA	GTATGTCACT
-186	CGTGTAGAT	TGTACTTTTT	TTTTTTTTT	CCAATTAGG	TCTCGCTTC
-136	CTCTCTTAC	GTGACACTTC	CTTCCCTGGG	CGACAGGGGC	CGCTGCACCG
-86	CGCGGGCGCT	GACAGGTCTC	TCTAGCTTGC	TGCGCC <u>TGCT</u>	ACTCGTTGGT
-36	GCCTATAAAT	GGCTGCGCTG	TGCTCAGCGA	GGCATCAGTC	CGCTACCGCG
16	GGACCC				

Figure III-3. Expression of the NHE1 promoter-reporter gene constructs in transiently transfected NIH 3T3 cells. A: Expression of the GFP-reporter in NIH 3T3 cells. Cells were transiently transfected with 4 µg GFP-reporter (+GFP) or no DNA for controls (-GFP), and grown on coverslips as described in *Materials and Methods* (Chapter II). The coverslips were washed with PBS, fixed with 4% paraformaldehyde and photomicrographs were taken using an Olympus BX50 fluorescent microscope (Olympus, Japan), equipped with a SPOT digital camera (Diagnostic Instruments, Inc.). B: Expression of the β gal-reporter in NIH 3T3 cells. Cells were transiently transfected with 24 µg NHE1- β gal reporter, 14 µg SV-40- β gal reporter (positive control) or no DNA (negative control) as described in *Materials and Methods* (Chapter II). β gal activity in cell extracts from transfectants was quantified using the Galacto-Light Plus Chemiluminescent Reporter Assay (Tropix). The β gal activity measured in the control was set to one and the other values are given relative to the control.

A



B

**Relative β -Galactosidase Activity of
NIH 3T3 Transfectants**

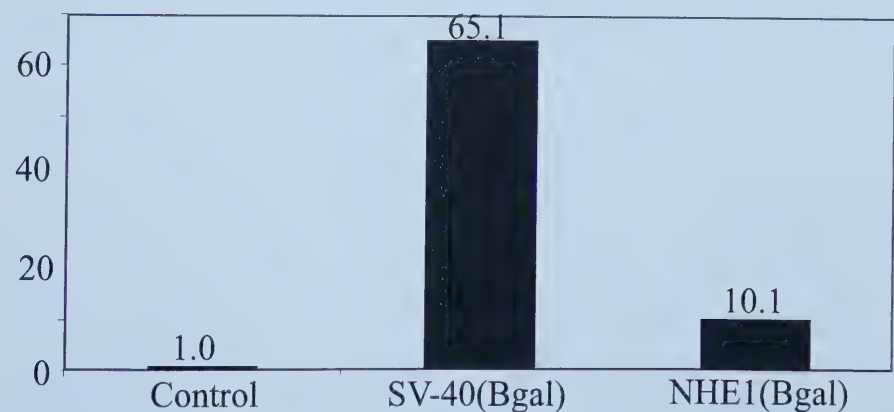
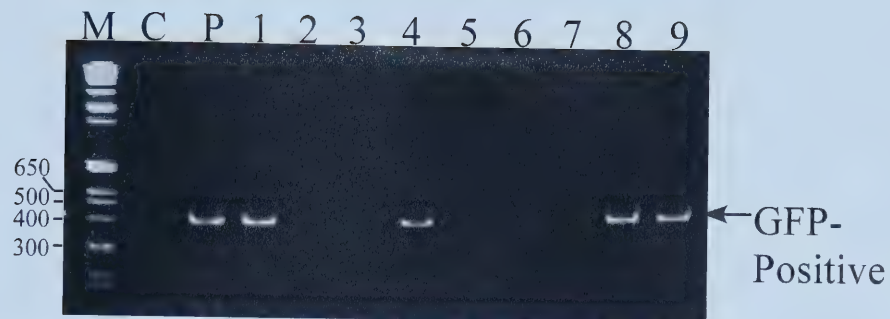


Figure III-4. Genotyping Mice by Step-down PCR. A: Analysis of nine ear notch DNA samples from a G16 litter. B: Analysis of six ear notch DNA samples from a β 3 litter. M, 1 Kb DNA ladder (Gibco); C, control (no template DNA); P, positive control (GFP- or β gal-reporter plasmids, respectively, as templates). Select marker band sizes are given in base pairs and arrows indicate the positions of PCR products from reporter-positive animals.

A



B

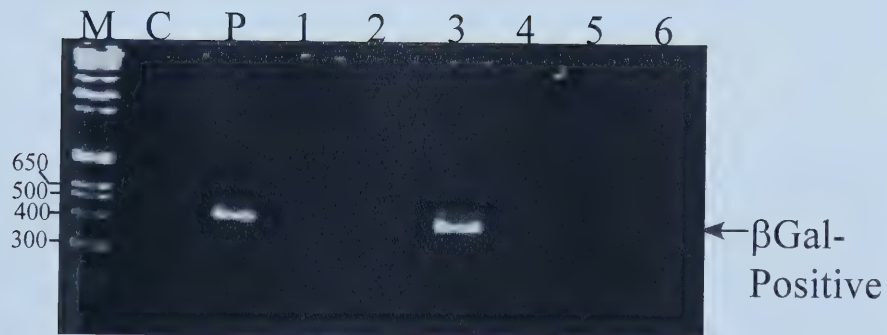


Figure III-5. Activation of the NHE1 promoter in GFP-positive embryos at 12-, 15- and 18-days-old. Sagital sections from control, G16 and G34 transgenic mouse lines were prepared at a thickness of 10 μ m as described in Chapter II. Images were collected using a Zeiss confocal microscope to visualize GFP fluorescence. Since the embryos were too large for the microscope field, photomicrographs were taken in parts and reconstructed in Adobe Photoshop. A: 12-day-old embryos. B: 15-day-old embryos. C: 18-day-old embryos.

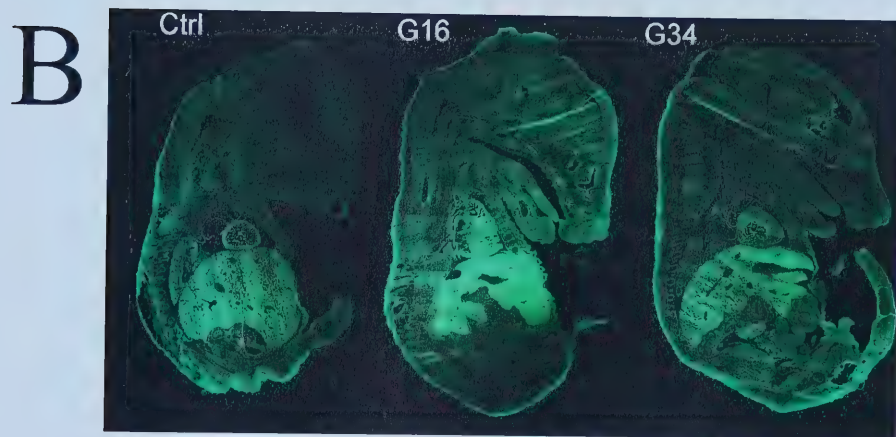


Figure III-6. Quantification of NHE1 promoter activity in the heart, liver and lung of 12-day-old embryos. A: Representative heart and liver sections of 12-day-old embryos from control, G16 and G34 lines. B, C, & D: relative GFP fluorescence in the heart, liver and lung, respectively. Fluorescence intensity was quantified using NIH Image software as described in Chapter II. Results are expressed relative to control fluorescent intensities and are mean +/- SE of three to four sections for each sample represented.

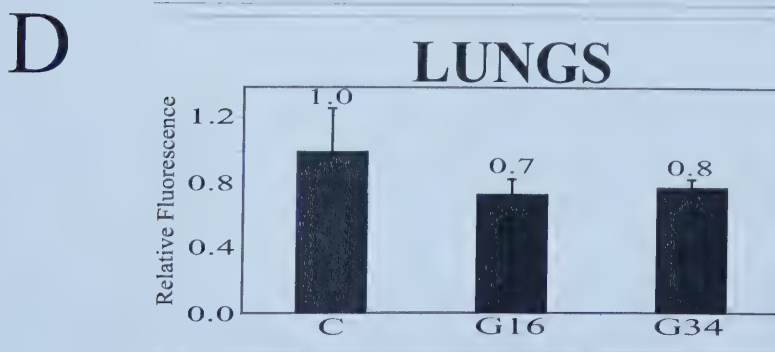
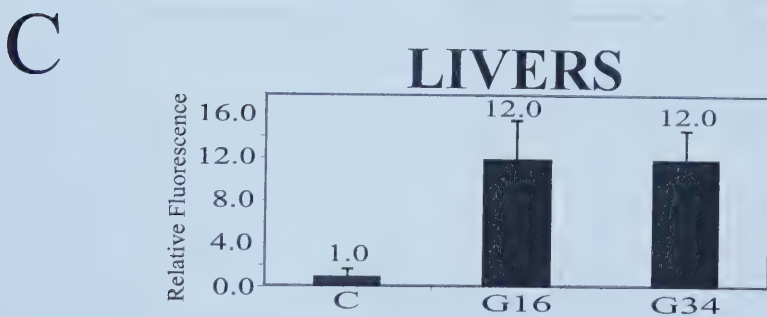
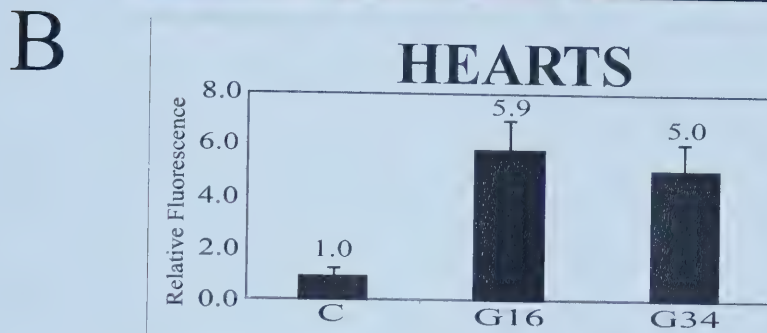


Figure III-7. Activation of the NHE1 promoter in 12-day-old embryo hearts visualized at high magnification. Images were obtained using a 100x Plan-Apochromat objective on the Zeiss LSM 510 confocal microscope. A series of photomicrographs was reassembled in Adobe Photoshop to illustrate a larger area of the heart. Control sections were from a wild type 12-day-old embryo. GFP sections were from a G34 12-day-old embryo.

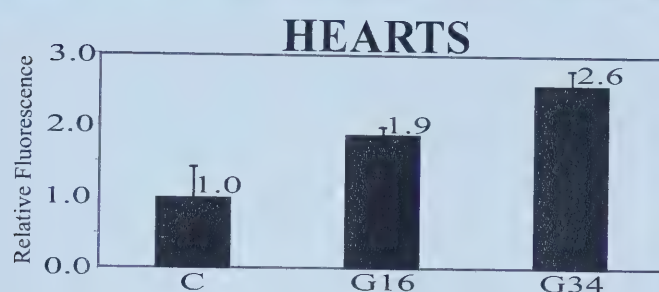


Figure III-8. Quantification of NHE1 promoter activity in the heart, liver and lung of 15-day-old embryos. A: Representative heart and liver sections of 15-day-old embryos from control, G16 and G34 lines. B, C, & D: Relative GFP fluorescence in the heart, liver and lung, respectively. Fluorescence intensity was quantified using NIH Image software as described in Chapter II. Results are expressed relative to control fluorescent intensities and are mean +/- SE of three to four sections for each sample represented.

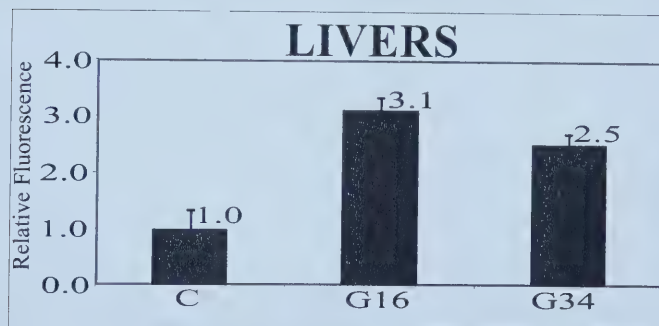
A



B



C



D

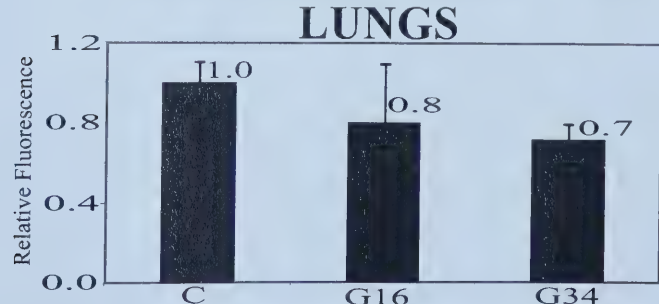
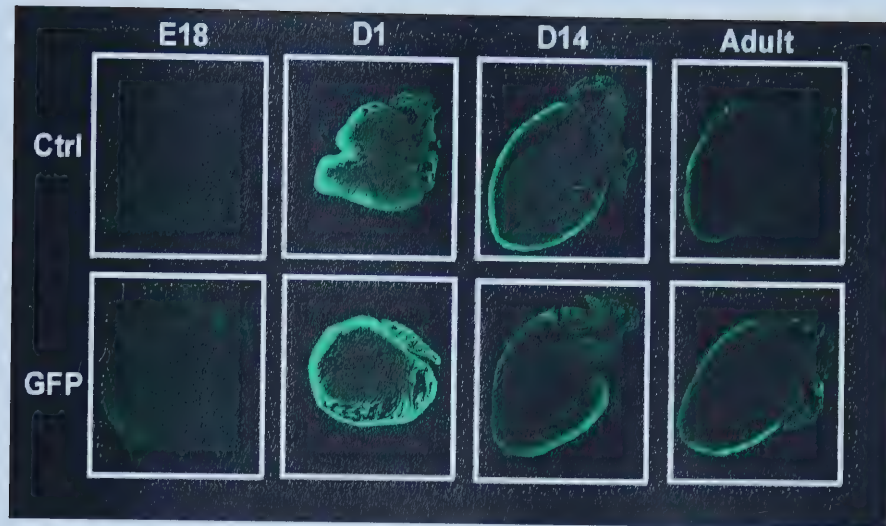


Figure III-9. Quantification of NHE1 promoter activity in hearts of: 18-day-old embryos, 1-day-old neonates, 14-day-old neonates and adults. A: Representative heart sections from control, G16 and G34 lines at the indicated ages. All ages are shown on a scale relative to the respective controls. E18, 18-day-old embryo heart; D1, 1-day-old neonate heart; D14, 14-day-old neonate heart. B: Relative GFP fluorescence in the heart. Fluorescence intensity was quantified using NIH Image software as described in Chapter II. Results are expressed relative to the fluorescent intensities of the controls. Three to four sections were quantified for each sample represented. Fluorescence was not significantly greater than controls in any of the GFP positive hearts at these ages ($P < 0.05$). E18, 18-day-old embryo hearts; D1, 1-day-old neonate hearts; D14, 14-day-old neonate hearts; Ad, adult hearts.

A



B

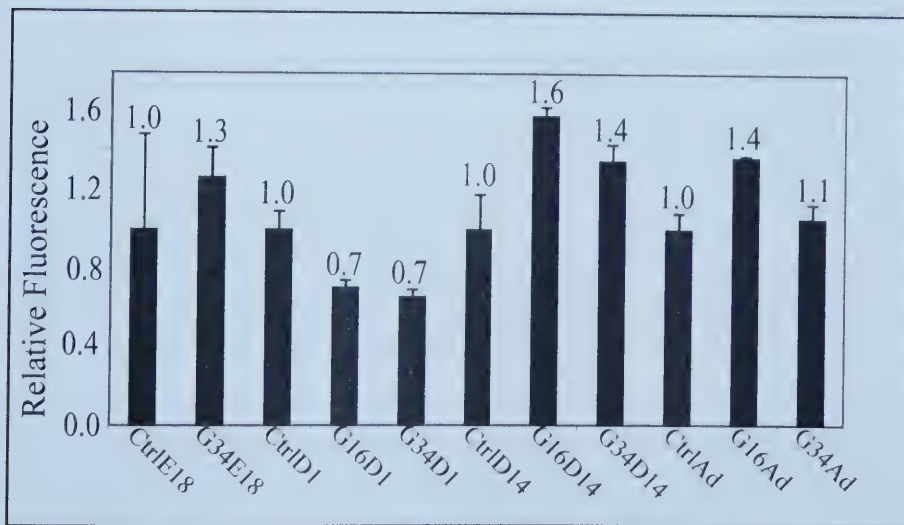
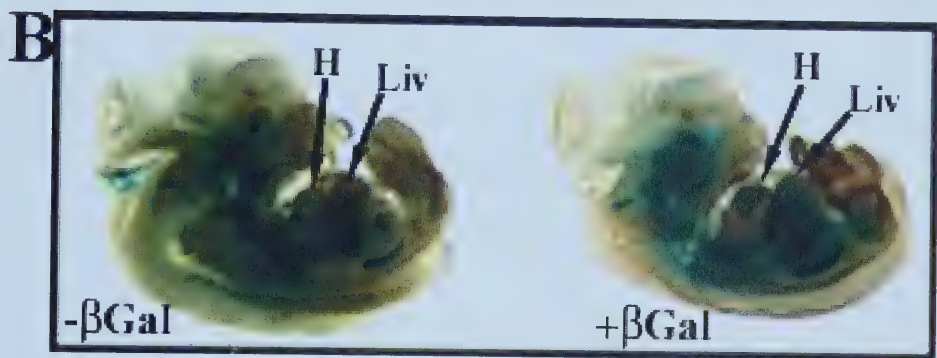


Figure III-10. Activation of the NHE1 promoter in β gal-positive embryos at 12-days-old. A: Whole X-gal stained embryos. Embryos were harvest, stained and cleared with methyl salicylate as described in Chapter II. Photomicrographs were obtained using a Leica MonoZoom 7 light microscope equipped with a Sanyo Hi-Resolution Color CCD camera. B: Cross-section of X-gal stained embryos. Whole X-gal stained embryos were frozen in cryomatrix, cut in half using a cryostat (see ChapterII) and cleared with methyl salicylate. Photomicrographs were taken as in A.



Chapter IV

NHE1 Protein Expression in Late Mouse Embryogenesis to Adulthood

IV-1. Introduction

A number of reports have indicated that the Na^+/H^+ exchanger is important in early postnatal development. For example, Haworth et al.³³ reported a 5-fold decrease in rat ventricular NHE1 mRNA expression over the first 21 days of life. Also, the rate of pH_i recovery following acid-loading was significantly greater in 2 to 4-day-old rat ventricular myocytes when compared to adult cells. Similarly, Chen et al.³⁴ showed that fetal and neonatal rabbit ventricles had a 1.7 and 1.6-fold more NHE1 mRNA, respectively, than adult ventricles. Furthermore, characterization of the mouse NHE1 promoter has unveiled binding sites for two developmentally relevant transcription factors: activating protein 2 (AP-2)⁴² and the chicken ovalbumin upstream promoter transcription factor (COUP-TF).⁴⁵ The presence of these transcription factor binding sites suggests that AP-2 and COUP-TF may be responsible for alterations in NHE1 protein expression during development.

In this chapter, expression of the NHE1 protein was investigated throughout the development process, beginning with the late stage mouse embryo and concluding with the adult. Immunoblotting with an anti-NHE1 monoclonal antibody was used to measure NHE1 protein levels in 18-day-old embryos, neonates and adults. To investigate the importance of the transcription factors AP-2 α and COUP-TFI, NHE1 protein was quantified in mice with disruptions in these genes. These results represent the first systematic study of the level of

NHE1 protein during postnatal development, and the first examination of the role of transcription factors in NHE1 expression in the intact animal.

IV-2. Results

NHE1 Protein Expression in the Late Embryo to the Adult

Immunoblotting was used to examine the level of NHE1 protein in the mouse tissues. The first step in this analysis was to optimize the immunoblotting protocol (Figure IV-1). Crude membrane preparations from adult heart and kidney were subjected to a five-minute incubation at different temperatures, prior to loading the SDS-polyacrylamide gel (Figure IV-1A). After probing the blots with a commercial monoclonal antibody (raised against the cytoplasmic domain of NHE1), preincubation at 37°C was observed to give the most abundant 100-105 kDa band, with the least amount of apparent degradation. Conversely, incubation of the samples at higher temperatures (60°C or 100°C) resulted in a loss of the 100 kDa NHE1 signal. Therefore, for all subsequent immunoblotting experiments, samples were incubated at 37°C for 5 minutes, prior to loading the SDS-polyacrylamide gel.

A second experiment to ensure optimal NHE1 immunoblotting confirmed the ability of the commercial anti-NHE1 monoclonal antibody to detect the NHE1 protein (Figure IV-1B). First, a polyclonal antibody (raised against the C-

terminal 178 amino acids) immunoprecipitated NHE1 from a rat heart extract. The immunoprecipitate was run on SDS-PAGE, and probed with the anti-NHE1 monoclonal antibody used in Figure IV-1A. This anti-NHE1 monoclonal antibody recognized a band of approximately 100 kDa; therefore, confirming that it does indeed recognize the Na^+/H^+ exchanger.

Next, the optimized immunoblotting protocol was used to determine the relative amounts of NHE1 protein in various tissues from 18-day-old embryos, 1-day-old neonates, 2-day-old neonates, 14-day-old neonates and adults. Five organs were examined: heart, lung, liver, kidney and brain. These organs were selected based on microscopic data from the GFP transgenics (Chapter III), and because enough of these tissues could be obtained from embryos and neonates, for analysis. Representative immunoblots are shown in Figure IV-2, adjacent to the quantified results. In all tissues studied, the amount of NHE1 protein appears to peak in the 14-day-old neonates. Specifically, in comparison to the 18-day-old embryo, the NHE1 protein is 3.5, 3.6, 2.8 and 3.0-fold more abundant in the 14-day-old neonates in the heart, lung, liver and kidney respectively. There was only a small increase (1.7-fold) in the level of NHE1 protein in the brain of 14-day-old neonates compared to the 18-day-old embryos.

Immunoblotting was also used to compare the relative amount of NHE1 protein present in the heart, lung, liver, kidney and brain at each age. Figure IV-3 shows representative immunoblots for tissues from 18-day-old embryos, 1-day-old neonates, 14-day-old neonates and adults. Quantified values are

expressed relative to the amount of NHE1 measured in the brain at each age. At embryonic day 18 and postnatal day 1, NHE1 protein is 2 to 3-fold higher in the heart, lung, liver and kidney compared to the brain. By 14 days of age however, there is a change in relative NHE1 protein levels such that it is 5.3, 4.1, 3.9, and 2.2-fold greater than the brain in the heart, lung, liver and kidney, respectively. In the adult, the brain also expressed the least amount of NHE1 compared to other tissues. The adult heart, lung, liver and kidney had 5.8, 8.7, 7.3 and 7.0-fold more NHE1 protein than the adult brain, respectively.

The finding that NHE1 protein is most abundant in all tissues at 2 weeks of age compared to younger and older mice (Figure IV-2) lead to a closer examination of postnatal development at this stage. Prior to 14 days of age, mice and rats consume only maternal milk; however, between the second to third week of life, pups commence weaning. During weaning, a transition is made from a high fat, low carbohydrate milk diet to the low fat, high carbohydrate sustenance of rodent chow.¹⁰⁹ Since this dietary change occurs at the same age that NHE1 protein levels were observed to peak, the effect of high glucose or high fat media on NHE1 expression in neonatal rat cardiomyocytes was examined. (High glucose media contained 20 mM glucose, high fat media contained 1% palmitate-complexed BSA, and control media contained 5 mM glucose and no fat.) Both metabolic treatments caused a 4-fold increase in NHE1 protein levels in the isolated cardiomyocytes (Figure IV-4).

NHE1 Protein Expression in Mice Lacking the Transcription Factors AP-2 α or COUP-TFI

Next, NHE1 protein levels were quantified in tissues of 4-week-old mice with a disruption in one allele of the AP-2 transcription factor gene. The NHE1 promoter contains a binding site for the AP-2 transcription factor, which is important for NHE1 transcription in cultured cells.^{42,43} Figure IV-5A shows a photograph of the female littermates used in this analysis. The mouse heterozygous for the AP-2 gene disruption (Figure IV-5A, lower panel) was considerably smaller than its wild type littermate (Figure IV-5A, upper panel). This size difference was extremely rare and only observed in two cases over the 13 months these animals were maintained. The genotypes of the mice were determined using PCR. The PCR amplified a portion of the neomycin gene that was introduced into the AP-2 locus to facilitating the disruption. Therefore, genomic DNA from AP-2 knock-out heterozygotes or homozygotes yielded a band of approximately 300 bp after PCR, while no PCR products were generated from wild type genomic DNA. The results are given in Figure IV-5B. The PCR products in lanes "wt" and "+/-" are from the genomic DNA of the wild type and heterozygous mice shown in Figure IV-5A. The lane marked "m" is the PCR result from the heterozygous mother of these animals. A immunoblot of heart, lung, liver, kidney and brain from the 1-month-old heterozygote and wild type mouse showed no dramatic changes in NHE1 expression in the organs examined (Figures IV-5C & IV-5D).

The expression of NHE1 was also examined in 18-day-old embryos from wild type and AP-2 disrupted lines. The genotype of each embryo was determined by PCR (Figure IV-6A). It was not necessary to PCR the one embryo homozygous for the AP-2 disruption in these litters, because it was severely deformed in accordance with the previously described phenotype.⁴⁶ Crude membrane fractions from each of the AP-2 heterozygotes and wild type embryos were separately pooled for each organ examined. NHE1 protein in the heart, lung, liver, kidney and brain was quantified by immunoblotting (Figures IV-6B & 6C). Like the 4-week-old mice, there were no major changes in the NHE1 protein abundance in 18-day-old embryos with the gene disruption of one AP-2 allele. In contrast, brain tissue from the 18-day-old embryo homozygous for the AP-2 knockout shows a surprisingly large increase in Na⁺/H⁺ exchanger expression. The homozygous AP-2 knockout embryo is severely deformed⁴⁶ and only the brain could be readily identified for analysis.

In a similar experiment, NHE1 protein levels were quantified in 18-day-old embryonic tissues from a COUP-TFI loss-of-function mutant mouse line. Figure IV-7 examines the amount of NHE1 protein in the heart, lung, liver, kidney and brain of wild type and COUP-TF1 knock out mice at embryonic day 18. No outstanding differences in NHE1 protein levels were evident between the wild type and COUP-TF1-null embryos. The degradation products present in these blots are likely due to the freezing and shipping of the samples from the laboratory of Dr. M.J. Tsai in Houston, TX.

IV-3. Discussion

Immunoblotting with a monoclonal antibody against the cytoplasmic domain of NHE1 was used to detect NHE1 protein levels in murine tissues. Heating the crude membrane samples at temperatures above 60°C prior to loading the SDS-PAGE severely reduced the amount of NHE1 immunoreactive protein detected on the blot. As a result, in all subsequent immunoblots, samples were only heated to 37°C before loading the SDS-PAGE.

NHE1 protein levels were examined in the heart, lung, liver, kidney and brain of 18-day-old embryos, neonates and adults by immunoblotting. NHE1 protein levels were found to peak at 14 days of age in all tissues assessed (Figure IV-2). The quantity of NHE1 protein remained high in the adult lung, liver and kidney but decreased in the adult heart to essentially the same amount found in the 18-day old embryos. The reduction of cardiac Na⁺/H⁺ exchanger protein is consistent with an earlier study that showed that sarcolemma NHE1 activity was reduced by 2 to 3-fold in adult rats compared to 6-day-old neonatal rats.³³ Also, a 1.6-fold decrease has been reported for similar ages in rabbit myocardium.³⁴

NHE1 protein levels were also compared in the heart, lung, liver, kidney and brain from mice of the same age. The brain expressed the least amount of NHE1 protein at all ages examined. Interestingly, the pattern of relative NHE1 expression changed significantly between neonatal days 1 and 14. More specifically, NHE1 was only two-fold more abundant in the heart, lung, liver and kidney compared to the brain at E18 and 1 day of age. However, NHE1 protein

was 4 to 5-fold greater than brain in the heart, lung and liver of 14-day-old animals (Figure IV-3). This increase further emphasizes the importance of NHE1 in certain tissues at 2 weeks of age. Also, NHE1 expression in the heart, lung, liver, kidney and brain increased from 2 to 5-fold greater than brain at 2 weeks old, to 6 to 9-fold more than brain in the adult (Figure IV-3). This suggests that the heightened demand for NHE1 in certain tissues persists from the 14-day-old neonate stage through to adulthood.

The reason for the rise in NHE1 protein at 2 weeks of age is uncertain. At this age, mice begin the process of weaning. During weaning, the high fat and low carbohydrate diet of the mother's milk is gradually replaced with the low fat and high carbohydrate content of rodent chow.¹⁰⁹ A large number of changes also occur in the animal at this time including: opening of eyes and ears, autonomous control of thermal homeostasis, maturation of hunger mechanisms and modifications in metabolism to coincide with the change in diet.¹⁰⁹ Since NHE1 protein levels are elevated during the weaning period, the effect of high fat and high glucose treatments on NHE1 expression in primary rat cardiomyocyte cultures was examined. Both high fat (1% palmitate-complexed BSA) and high glucose (20 mM glucose) growth media resulted in a four-fold elevation in NHE1 protein levels compared to control (no fat, 5 mM glucose) (Figure IV-4). Thus, using primary cardiomyocytes, the increase in NHE1 protein expression in 2-week-old neonates cannot be directly correlated to the change in diet at this age.

Two separate studies of NHE1-null mice have emphasized the importance of NHE1 at the 2-week-old stage. Bell et al.⁵⁹ generated NHE1 knock-out mice that exhibited a normal phenotype at birth, but by 14 days of age, mutants were significantly smaller than controls. Also, the 14-day-old NHE1-null animals displayed an ataxic gait, and 68% of the mutants died between 16 to 29 days old. Cox et al.⁵⁸ examined a mouse line bearing a spontaneous point mutation in the NHE1 gene that resulted in a truncated, non-functional protein. The development of an ataxic gait and a smaller size in mutants 11 to 14 days of age was also reported in this study. In both NHE1 null lines, at least 50% of the mice did not live to weaning age (21-days-old); however, the exact number of surviving animals depended on the genetic background. Furthermore, the appearance of the mutants after death suggested that a convulsive seizure had caused the lethality. Surprisingly, the only two histological abnormalities observed in these studies were subtle alterations in the stomach morphology including: thinning of the stomach mucosa, increased spacing of the gastric glands,⁵⁹ and a degeneration of a small subset of neurons in the central nervous system.⁵⁸ It is apparent from the lack of aberrant histology in most tissues from the NHE1-null animals, and the dependence of neonatal lethality on genetic background, that the precise role of NHE1 at this stage is complex. Even so, the importance of NHE1 to the 14-day-old mouse is emphasized in these published reports, and is thereby consistent with the present study.

Previous studies have characterized the NHE1 promoter in detail and have identified binding sites for the AP-2 transcription factors.⁴² Furthermore, in mouse fibroblast cells, deletion of the promoter upstream of the AP-2 site resulted in a 25% reduction in NHE1 promoter activity; however, removal of the same upstream region plus the AP-2 site caused an 83% decrease in NHE1 transcription.⁴² As a result of the apparent importance of this transcription factor in intact cells, NHE1 protein levels were measured in mice with an AP-2 α gene deletion. At 4 weeks of age and at embryonic day 18, there were no major alterations in Na⁺/H⁺ exchanger protein expression in heart, lung, liver, kidney and brain from animals heterozygous for the AP-2 α deletion compared to wild type controls (Figures IV-5 & IV-6). In contrast, a remarkable increase in NHE1 protein expression was demonstrated in the brain of an 18-day-old embryo homozygous for the AP-2 α disruption (Figures IV-6B & IV-6C). Perinatal lethality occurs in mice nullizygous for AP-2 α . Severe defects have been described in closure of the neural tube, and in the development of the ventral body wall, face, eyes, and limbs.^{46,52,53} It is possible that with such an extensive array of deformities, some cell types may be altered. Although speculative, this may have occurred in the brain and could account for the elevated NHE1 protein levels observed. Due to the extreme deformity of the homozygous AP-2 α knockouts, no other organs could be clearly distinguished, and the death of these animals at birth made it impossible to obtain tissues from older animals for analysis.

One allele of the AP-2 α gene was disrupted in the heterozygous AP-2 α -null mice, yet NHE1 protein levels were the same in wild type and heterozygote animals at the two ages investigated. One explanation for this apparent discrepancy may be that the AP-2 α transcription factor activates transcription of the NHE1 gene much earlier in embryonic development. In fact, expression of AP-2 α is first detected at E8.75, peaks at E11.5, and decreases from this point,¹¹⁰ such that AP-2 α is barely detectable in adult tissues.⁴⁹ Coincidentally, NHE1 transcription levels were high at E12 and diminished from E12 to birth (Chapter III). Therefore, given the essential role for AP-2 α in vertebrate embryogenesis, and its decrease thereafter, it is likely that any effect of the AP-2 α -null mutation on NHE1 protein levels must be observed in mid-gestation, when AP-2 α is most abundant.

An alternative explanation for the lack of change in NHE1 protein levels in the AP-2 α heterozygote mice is that another member of the AP-2 transcription factor family may be responsible for activation of the NHE1 gene. To date, three proteins have been placed in this family: AP-2 α , AP-2 β , and AP-2 γ . Although they recognize a common DNA binding sequence, members differ somewhat in their expression patterns.¹¹¹ Theoretically, when one member is knocked-out, other proteins from that family may be overexpressed as a compensatory mechanism. This could explain the abundance of Na⁺/H⁺ exchanger protein observed in the brain of the 18-day-old homozygote knockout mouse (Figure IV-

6B). It is of interest that in gel mobility shift assays, purified commercial AP-2 α protein produces a smaller shift than that seen with proteins derived from nuclear extracts.⁴³ Taken together, it is plausible that a different member of the AP-2 transcription factor family may regulate NHE1 expression.

NHE1 protein levels were also examined in various organs from 18-day-old COUP-TFI-null embryos. The COUP transcription factors have been shown to be important in Na⁺/H⁺ exchanger expression.⁴⁵ Figure IV-7 shows that there are no major differences in the quantity of NHE1 protein in organs from animals lacking COUP-TFI compared to wild type embryos. Similar to AP-2 α , COUP-TFI is first detected at E7.5, reaches a maximum between E10 to E12, and decreases significantly before birth.⁵⁵ Analogous to the discussion of NHE1 expression in the AP-2 α -null mice above, it may be that COUP-TFI acts on the NHE1 promoter at a different stage of development. Alternatively, another member of the chicken ovalbumin upstream promoter family of transcription factors may be responsible for activation of the NHE1 promoter. It has been previously demonstrated that COUP-TFII is more effective in enhancing Na⁺/H⁺ exchanger expression than COUP-TFI.⁴⁵ Thus, COUP-TFII may have a greater role in regulating Na⁺/H⁺ exchanger transcription in intact animals than COUP-TFI.

This chapter has investigated the levels of NHE1 protein in the mouse embryo, neonate and adult. The NHE1 protein was maximally expressed at 14 days of age in the heart, lung, liver, kidney and brain. Also, at one age, the NHE1

protein was of lowest abundance in the brain and present at 2 to 9-fold higher levels in other tissues depending on the age of the mice. Animals lacking at least one allele of the transcription factors AP-2 α (at E18 and 4-weeks-old) and COUP-TFI (at E18) do not exhibit diminished NHE1 protein levels. This suggests that AP-2 α and COUP-TFI are not likely involved in NHE1 regulation at E18 or older. In conclusion, the variance of NHE1 protein levels with age indicates that NHE expression is developmentally regulated. Furthermore, NHE1 protein levels differ between tissues at one age, suggesting that NHE1 expression is subject to tissue-specific control.

Figure IV-1. Optimization of Western blot analysis for the Na^+/H^+ exchanger protein from mammalian heart and kidney. A: Western blot of adult heart (H) and kidney (K) crude membrane preparations. Samples were heated for five minutes at 25°C, 37°C, 60°C or 100°C prior to loading the SDS-polyacrylamide gel. After transfer, samples were immunoblotted with anti-NHE1 monoclonal antibody. Molecular weight markers are indicated in kDa. B: Western blot of NHE1 protein immunoprecipitated from rat heart extracts with an antibody against the C-terminal 178 amino acids of the protein. The immunoprecipitate was then probed with the anti-NHE1 monoclonal antibody.

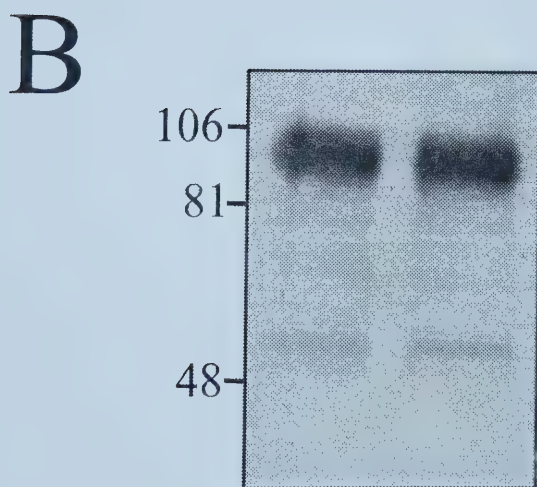


Figure IV-2. Comparison of NHE1 protein expression levels in various organs from 18-day-old embryos, 1-day-old neonates, 2-day-old neonates, 14-day-old neonates and adults. (continued on page 127) Left panel: Representative Western blots of heart, lung, and liver collected at the ages indicated and probed with anti-NHE1 monoclonal antibody. Molecular weight markers are indicated in kDa. Right panel: Amounts of NHE1 protein are expressed relative to the amount of protein in 18-day-old embryo tissues. Blots were scanned and quantified using Image Gauge (Bio-Rad) software. Results are mean +/- SE for 3-5 different protein samples. E18, 18-day-old embryos; D1, 1-day-old neonates; D2, 2-day-old neonates; W2, 2-week-old neonates; A, adult.

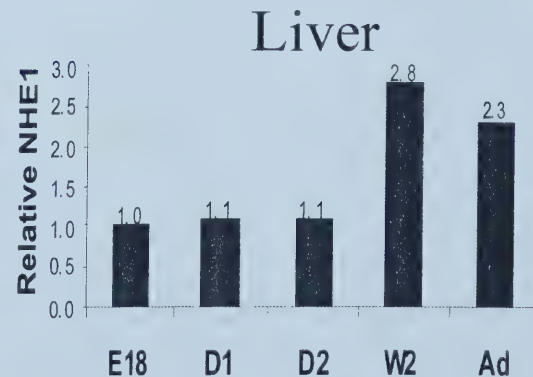
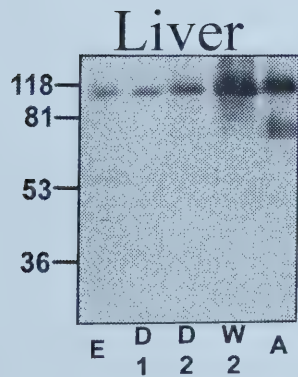
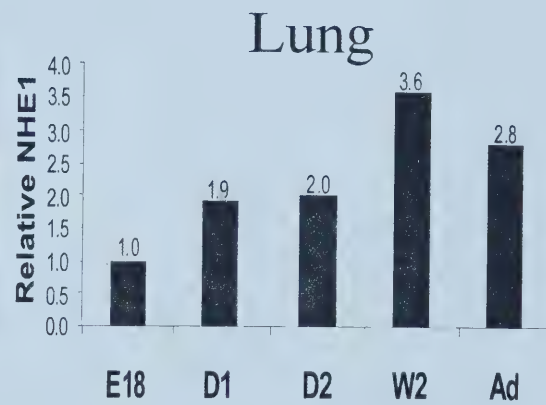
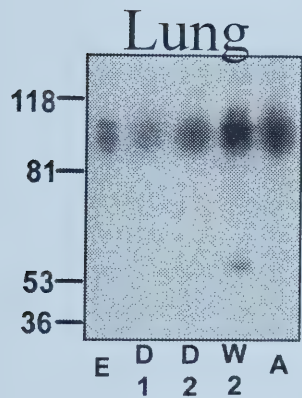
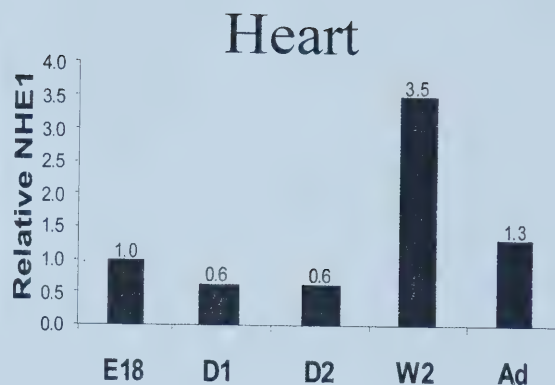
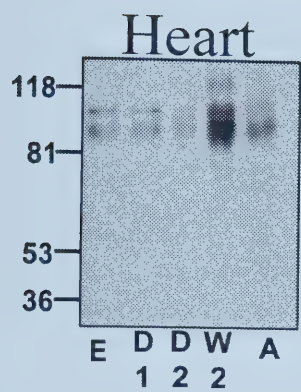


Figure IV-2 Continued. **Comparison of NHE1 protein expression levels in various organs from 18-day-old embryos, 1-day-old neonates, 2-day-old neonates, 14-day-old neonates and adults.** (continued from page 125) Left panel: Representative Western blots of kidney and brain collected at the ages indicated and probed with anti-NHE1 monoclonal antibody. Molecular weight markers are indicated in kDa. Right panel: Amounts of NHE1 protein are expressed relative to the amount of protein in 18-day-old embryo tissues. Blots were scanned and quantified using Image Gauge (Bio-Rad) software. Results are mean +/- SE for 3-5 different protein samples. E18, 18-day-old embryos; D1, 1-day-old neonates; D2, 2-day-old neonates; W2, 2-week-old neonates; A, adult.

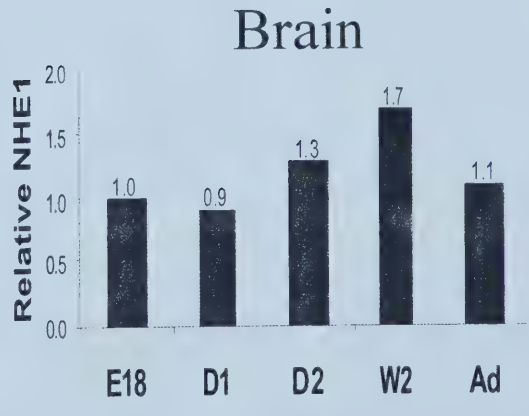
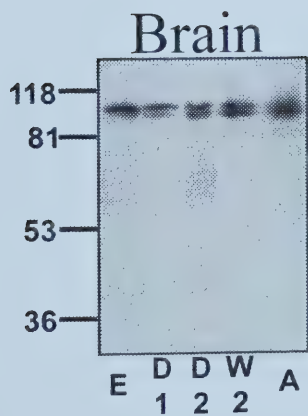
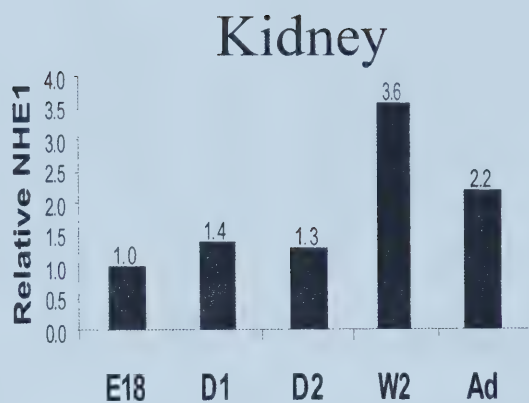
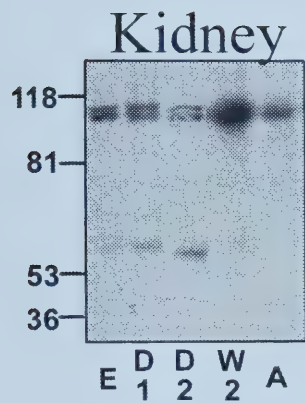
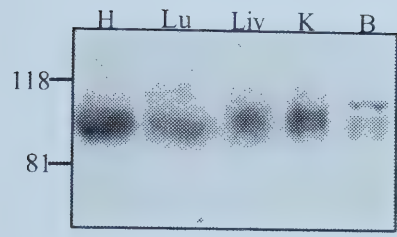
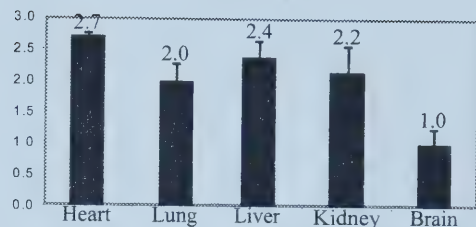


Figure IV-3. Comparison of NHE1 protein expression levels in the heart, lung, liver, kidney and brain at various ages. (continued on page 131) Left panel: Representative Western blots of heart, lung, liver, kidney and brain collected at the ages indicated and probed with anti-NHE1 monoclonal antibody. Molecular weight markers are given in kDa. Right panel: Amounts of NHE1 protein are expressed relative to the amount of protein in the brain. Blots were scanned and quantified using Image Gauge (Bio-Rad) software. Results are mean +/- SE for 3-5 different protein samples. E18, 18-day-old embryos; D1, 1-day-old neonates; H, heart; Lu, lung; Liv, liver, K, kidney, B, brain.

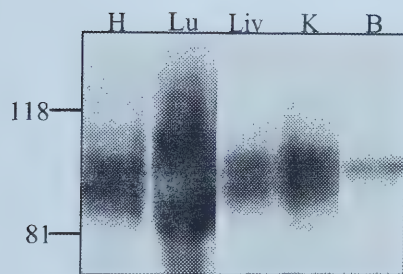
E18



E18



D1



D1

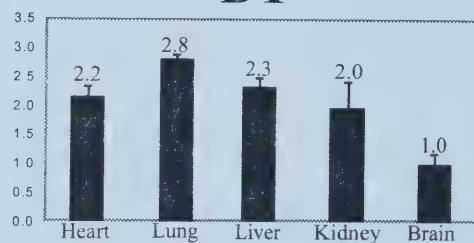


Figure IV-3 Continued. **Comparison of NHE1 protein expression levels in the heart, lung, liver, kidney and brain at various ages.** (continued from page 129) Left panel: Representative Western blots of heart, lung, liver, kidney and brain collected at the ages indicated and probed with anti-NHE1 monoclonal antibody. Molecular weight markers are given in kDa. Right panel: Amounts of NHE1 protein are expressed relative to the amount of protein in the brain. Blots were scanned and quantified using Image Gauge (Bio-Rad) software. Results are mean +/- SE for 3-5 different protein samples. D14, 14-day-old neonates; A, adult; H, heart; Lu, lung; Liv, liver, K, kidney, B, brain.

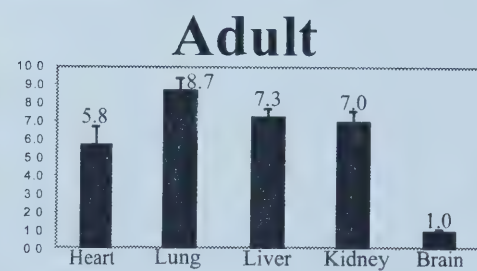
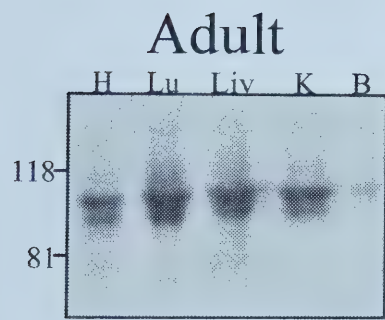
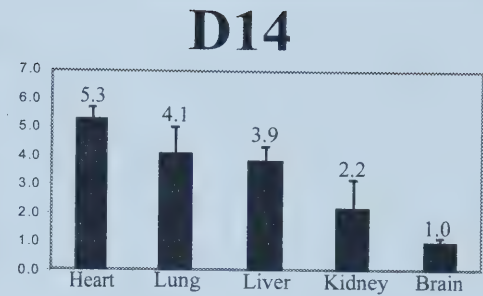
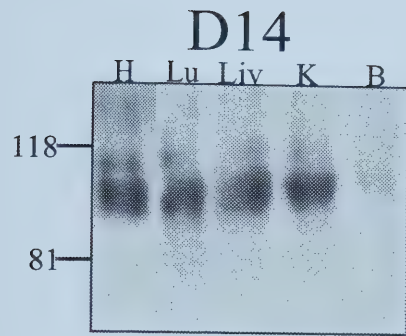
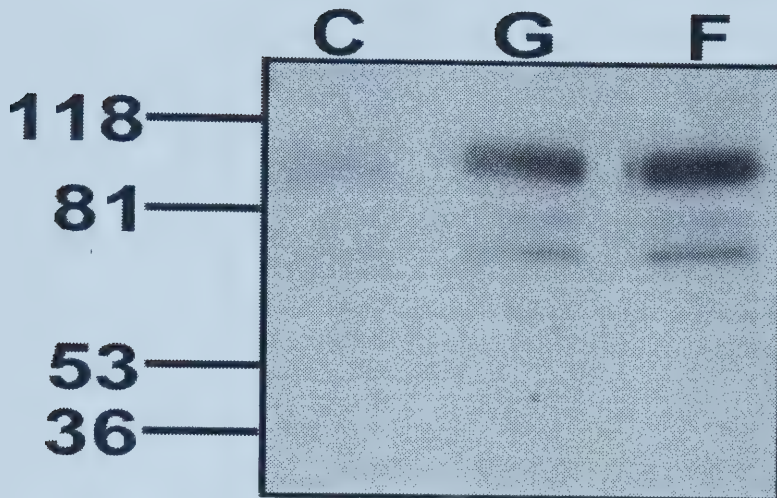


Figure IV-4. Comparison of NHE1 protein expression levels in rat cardiomyocytes treated with control, high glucose or high fat media. A: Representative Western blot of rat cardiomyocytes treated with control (C; 5 mM glucose, no fat), high glucose (G; 20 mM glucose) or high fat (F; 1% palmitate-complexed BSA) media for 24 h prior to preparation of crude microsomes for Western blotting. Molecular weight markers are indicated in kDa. B: Amounts of NHE1 protein are expressed relative to the amount of protein in control-treated cells. Blots were scanned and quantified using Image Gauge (Bio-Rad) software.

A



B

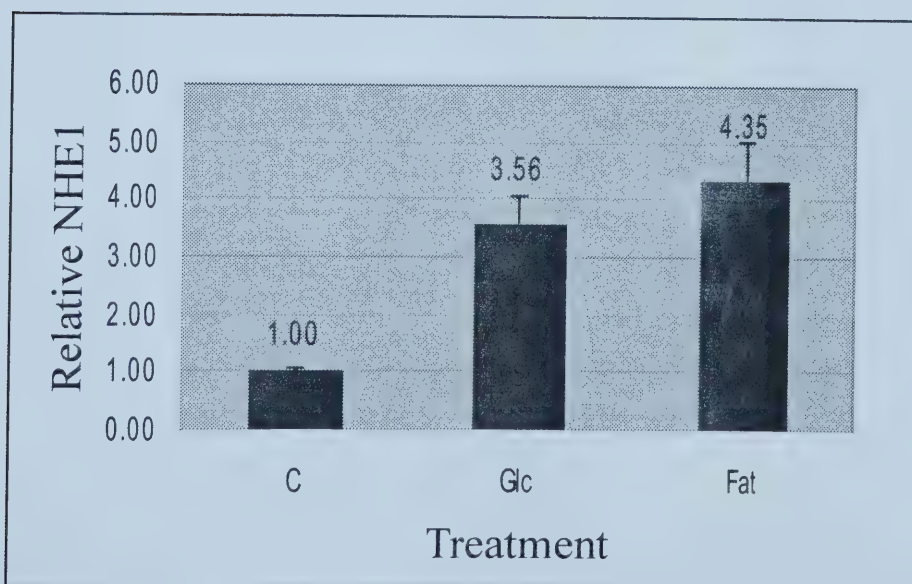
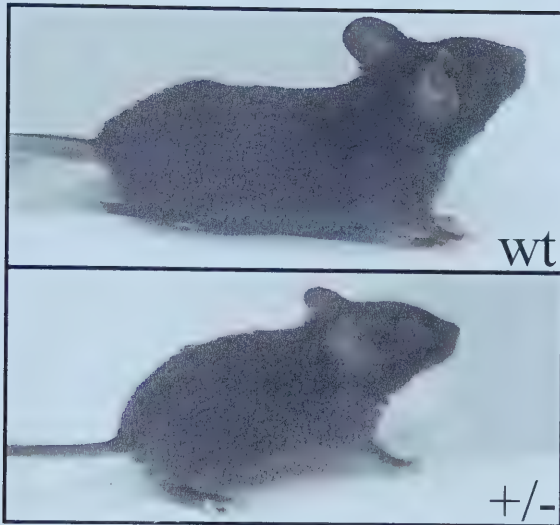


Figure IV-5. Analysis of NHE1 protein expression in 1-month-old mice lacking the AP-2 α transcription factor. (continued on page 137) A: Wild type (wt) and AP-2 α heterozygous mutant (+/-) mice used in the analysis. B: PCR was used to amplify a 300 bp fragment that was introduced into the AP-2 α knockout mice. The presence of a band indicates that at least one AP-2 allele has been disrupted. M, 1-kb DNA ladder (Gibco); C, control PCR reaction lacking template; m, PCR of mother of littermates shown in A; wt, wild type PCR; +/-, AP-2 α heterozygous disruption PCR.

A

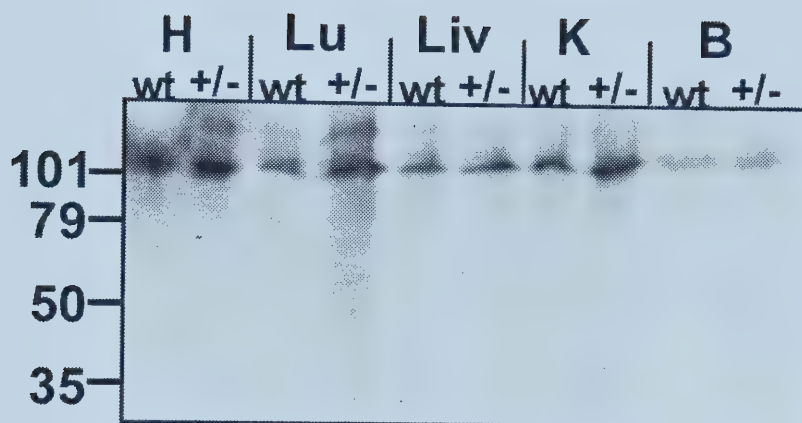


B



Figure IV-5 Continued. **Analysis of NHE1 protein expression in 1-month-old mice lacking the AP-2 α transcription factor.** (continued from page 135) C: Western blot for NHE1 protein in the heart (H), lung (Lu), liver (Liv), kidney (K) and brain (B) of wild type (wt) and AP-2 α heterozygous disruption (+/-) mice shown in A. Molecular weight markers are indicated in kDa. D: Amounts of NHE1 protein are expressed relative to the amount of protein in wild type tissues. Blots were scanned and quantified using Image Gauge (Bio-Rad) software.

C



D

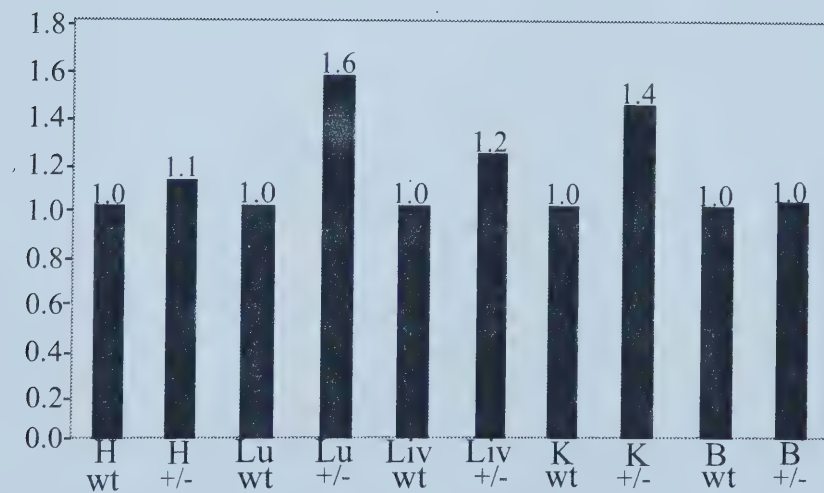


Figure IV-6. Analysis of NHE1 protein expression in 18-day-old embryos lacking the AP-2 α transcription factor. (continued on page 141) A: PCR was used to amplify a 300 bp fragment that was introduced into the AP-2 α knockout mice. The presence of a band indicates that at least one AP-2 allele has been disrupted. Lanes 1-6 in the left panel represent six heterozygous embryos from the same litter. Lanes 1-7 in the right panel represent seven wild type embryos from the same litter. M, 1-kb DNA ladder (Gibco); C, control PCR reaction lacking template.

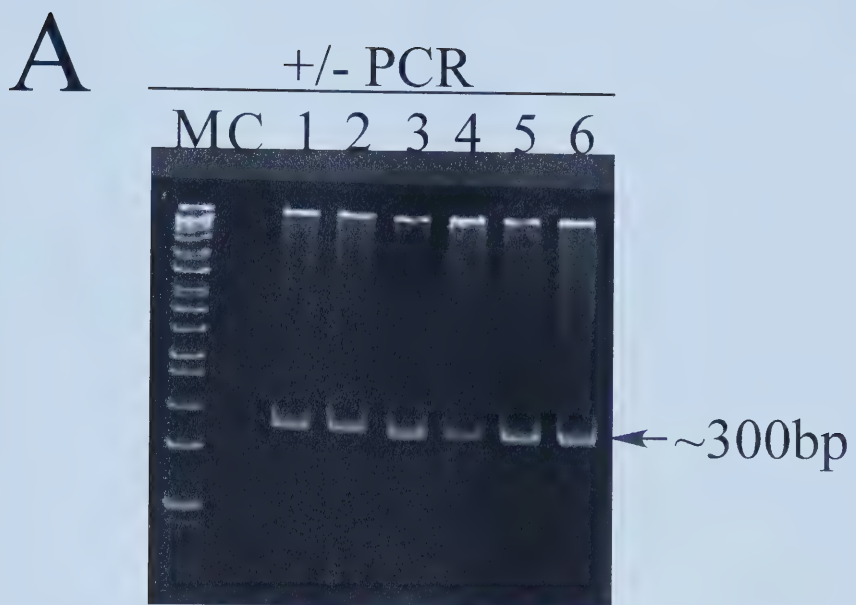
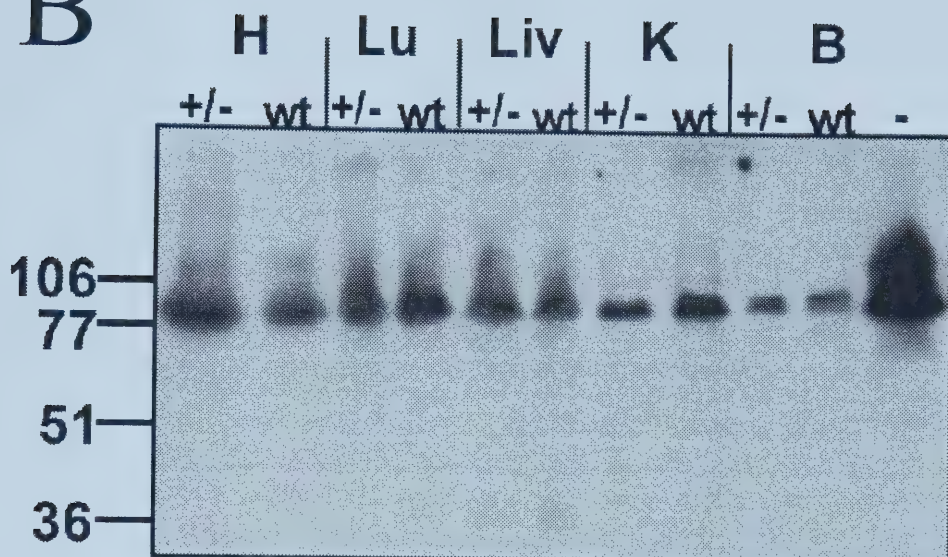


Figure IV-6 Continued. **Analysis of NHE1 protein expression in 18-day-old embryos lacking the AP-2 α transcription factor.** (continued from page 139)
B: Western blot for NHE1 protein in the heart (H), lung (Lu), liver (Liv), kidney (K) and brain (B) of wild type (wt), heterozygous-for-AP-2 α -disruption (+/-) and homozygous AP-2 α -null (-) embryos. Molecular weight markers are indicated in kDa. C: Relative amount of NHE1 protein. Blots were scanned and quantified using Image Gauge (Bio-Rad) software. Results are expressed relative to the amount of protein in wild type tissues.

B



C

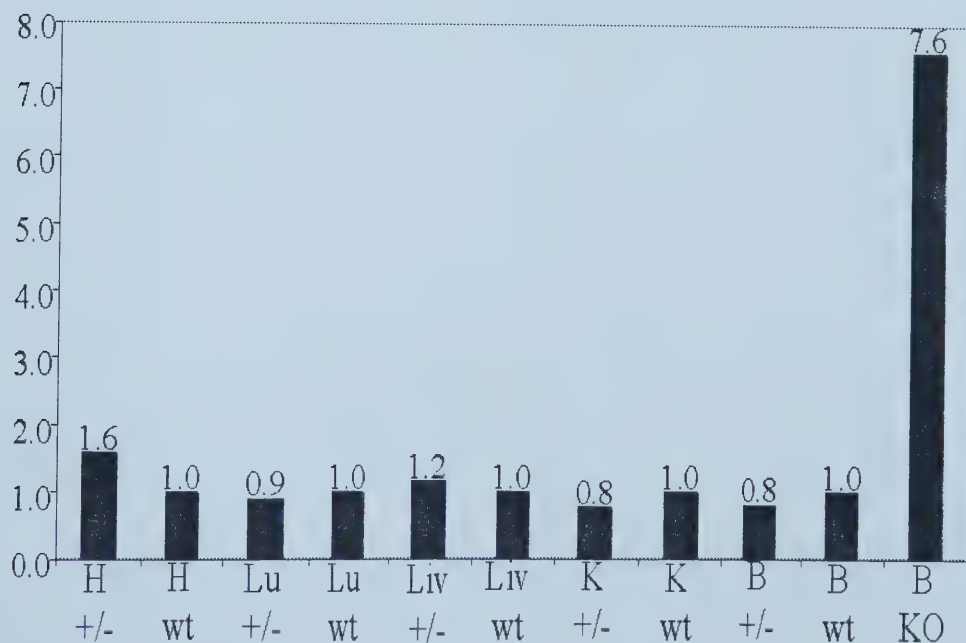
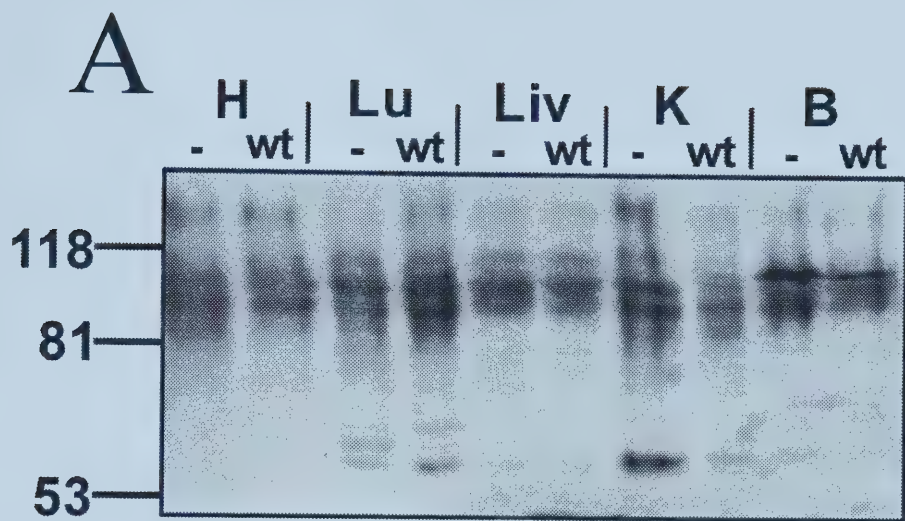
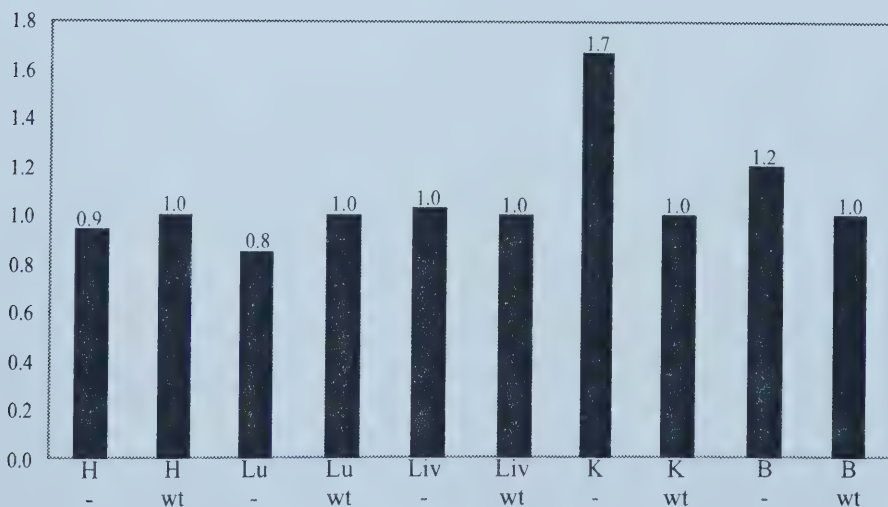


Figure IV-7. Analysis of NHE1 protein expression in 18-day-old embryos lacking the COUP-TFI transcription factor. A: Western blot analysis of NHE1 protein in the heart (H), lung (Lu), liver (Liv), kidney (K) and brain (B) of homozygous COUP-TFI-null (-) and wild type (wt) mouse embryos. Molecular weight markers are indicated in kDa. B: Relative amount of NHE1 protein. Blots were scanned and quantified using Image Gauge (Bio-Rad) software. Results are expressed relative to the amount of protein in wild type tissues.



B



Chapter V

Summary and General Conclusions

V-1 Summary and General Conclusions

The developmental regulation of NHE1 transcription and protein levels has been investigated in this thesis. NHE1 transcription was examined in GFP-reporter transgenic mouse embryos at E12, E15 and E18. From these studies, two primary observations were made:

- 1) NHE1 transcription is highest in the heart and liver of the youngest embryos examined (E12 and E15).
- 2) NHE1 transcription decreases in both the heart and liver from E12 to E18 and remains at the lower level thereafter.

It can be concluded from these observations that NHE1 is likely to play a significant role in early heart and liver development.

A developmental role for NHE1 is supported by a number of published studies. First, in cardiac hypertrophy, NHE1 expression and activity increases.³¹ Furthermore, cardiac hypertrophy can be attenuated by the specific NHE1 inhibitor cariporide.⁶⁵ Both of these results suggest that NHE1 is important for heart growth. Second, in hepatocyte proliferation, NHE1 steady-state mRNA is increased,³² NHE1 activity is stimulated by growth factors,²⁶ and an NHE1 inhibitor decreases hepatocyte viability.¹⁰⁴ These observations imply that NHE1 is important in growth of the liver. Third, a role for NHE1 in differentiation has

been described in several tissue culture models including: human leukemic HL-60 cells,³⁶ mouse P19 embryonal cells³⁷ and rat L6 skeletal muscle cells.³⁹ Finally, increased NHE1 transcription can be correlated with stages of significant growth and differentiation in murine heart and liver development (see Discussion, Chapter III).

In the second half of this project, NHE1 protein levels were investigated throughout the development process, beginning with the late stage mouse embryo and concluding with the adult. Immunoblotting with an anti-NHE1 monoclonal antibody was used to measure NHE1 protein levels in 18-day-old embryos, neonates and adults. The expression of NHE1 protein was also examined in AP-2 α and COUP-TFI gene disruption mice. From these experiments it was found that:

- 1) The NHE1 protein is maximally expressed at 14 days of age in the heart, lung, liver, kidney and brain.
- 2) For a given age, the NHE1 protein is of lowest abundance in the brain. Other tissues express 2- to 9-fold higher NHE1 protein levels (relative to brain), depending on the age of the mice.
- 3) Animals lacking at least one allele of the transcription factors AP-2 α (at E18 and 4-weeks-old) and COUP-TFI (at E18) do not exhibit diminished NHE1 protein levels.

Therefore, it can be concluded from this analysis of NHE1 protein levels in 18-day-old embryos, neonates and adults that:

- 1) NHE1 expression is developmentally regulated since NHE1 protein levels vary with age.
- 2) NHE1 expression is subject to tissue-specific control since NHE1 protein levels were found to differ between tissues at one age.
- 3) AP-2 α is not likely involved in NHE1 expression at E18 or older.
- 4) COUP-TFI is not essential for NHE1 expression in 18-day-old mouse embryos.

These conclusions are in agreement with several previous reports. First, developmental regulation of NHE1 expression has been described in the heart. For example, one study showed that sarcolemma NHE1 activity was reduced by 2 to 3-fold in adult rats, compared to 6-day-old neonatal rats.³³ Also, a 1.6-fold decrease in NHE1 transcription has been reported for similar ages in rabbit myocardium.³⁴ Second, the 14-day-old stage (where maximal NHE1 protein was observed in the present study) has been emphasized in other reports. For example, NHE1-null mice exhibited a normal phenotype at birth, but by 14 days of age, mutants were significantly smaller than controls.⁵⁹ The onset of an ataxic gait was also observed between 11 to 14 days of age in the NHE1-null mice.^{58,59} Furthermore, rodents begin the process of weaning at this age, and undergo a large number of metabolic changes.¹⁰⁹ Third, expression of both AP-2 α and

COUP-TFI transcription factors has been reported to peak between E7.5-E8.5^{55,110} and decrease significantly by birth.^{49,55} Therefore, these transcription factors could act on the NHE1 promoter at earlier development stages than those examined in the present study. Furthermore, alternate isoforms of the AP-2 and COUP-TF families may be responsible for activation of the NHE1 gene.^{55,111}

V-2 Future Experiments

As with many research efforts, the findings of this study are accompanied by a new list of questions, and the potential for new approaches to answer these questions. Some of these questions and possible experiments are listed below:

- At what stage of cellular differentiation is the greatest fluorescence produced from the NHE1 promoter-GFP reporter transgenic mice?
 - Flow cytometry of E7.5 to E11 heart or liver whole cell extracts immunostained for differentiation markers may provide some insights regarding this question.
- Is the increase in NHE1 protein expression observed at 2 weeks of age actually related to weaning of the mice?
 - Immunoblotting of tissues from fasted mice and mice prevented from weaning may be useful to examine this question.

- How is NHE1 expression affected in AP-2 α and COUP-TFI null mice between E7.5 to E12? (These transcription factors are normally most abundant between E7.5 to E12.^{55,110})
 - Although it is very difficult to obtain enough protein to immunoblot at these ages, perhaps *in situ* PCR could be used to investigate this question.
- Is NHE1 protein expression altered in mice lacking other isoforms of AP-2 (AP-2 β or AP-2 γ) or COUP-TF (COUP-TFII)?
 - Immunoblotting could be used to measure NHE1 protein levels in AP-2 β null animals up to two days of age. (AP-2 β -null mice die within two days of birth.⁵⁴) AP-2 γ null mice have not been generated to date but a similar immunoblotting approach may be useful if these animals become available. Finally, an *in situ* PCR strategy could be used to determine NHE1 expression in COUP-TFII disrupted mice younger than E10. (All COUP-TFII null mice die at E10.⁵⁷)

Chapter VI

References

VI. References

- ¹ Moe, OW, Alpern RJ (1996) Regulation of Cell pH. In Molecular Biology of Membrane Transport Disorders. SG Schultz et al, Eds., Plenum Press, New York, pp 407-425
- ² Orlowski J, Grinstein S (1997) Na^+/H^+ Exchangers of Mammalian Cells. *J Biol Chem* 272: 22373-22376
- ³ Grinstein S, Rotin D, Mason MJ (1989) Na^+/H^+ exchange and growth factor-induced cytosolic pH changes. Role in cellular proliferation. *Biochim Biophys Acta* 988: 73-97
- ⁴ Sardet C, Franchi A, Pouyssegur J (1989) Molecular cloning, primary structure, and expression of the human growth factor-activatable Na/H antiporter. *Cell* 56: 271-280
- ⁵ Numata M, Orlowski J (2001) Molecular Cloning and Characterization of a Novel $(\text{Na}^+, \text{K}^+)/\text{H}^+$ Exchanger Localized to the *trans*-Golgi Network. *J Biol Chem* 276: 17387-17394
- ⁶ Orlowski J, Shull G (1996) Characteristics of the Plasma Membrane Na^+/H^+ Exchanger Gene Family. In *The Na^+/H^+ Exchanger*. Fliegel L, Ed., RG Landes Company, Texas, pp 123-148
- ⁷ Attaphitaya S, Park K, Melvin JE (1999) Molecular cloning and Functional Expression of a Rat Na^+/H^+ Exchanger (NHE5) Highly Expressed in Brain. *J Biol Chem* 274: 4383-4388
- ⁸ Numata M, Petrecca K, Lake N, Orlowski J (1998) Identification of a Mitochondrial Na^+/H^+ Exchanger. *J Biol Chem* 273: 6951-6959
- ⁹ Rajendran VM, Geibel J, Binder HJ (2001) Characterization of apical membrane Cl^- -dependent Na/H exchange in crypt cells of rat distal colon. *Am J Physiol* 280: G400-G405
- ¹⁰ Fliegel L, Murtazina R, Dibrov P, Harris C, Moor A, Fernandez-Rachubinski FA (1998) Regulation and characterization of the Na^+/H^+ exchanger. *Biochem Cell Biol* 76: 1-7
- ¹¹ Fliegel L, Frohlich O (1993) The Na^+/H^+ exchanger: an update on structure, regulation and cardiac physiology. *Biochem J* 296: 273-285

¹² Haworth RS, Frohlich O, Fliegel L (1993) Multiple carbohydrate moieties on the Na^+/H^+ exchanger. Biochem J 289: 637-640

¹³ Harris CV, Fliegel L (1999) Amiloride and the Na^+/H^+ exchanger protein: Mechanism and significance of the inhibition of the Na^+/H^+ exchanger. Int J Mol Med 3: 315-321

¹⁴ Wakabayashi S, Pang T, Su X, Shigekawa M (2000) A Novel Topology Model of the Human Na^+/H^+ Exchanger Isoform 1. J Biol Chem 275(11): 7942-7949

¹⁵ Berk BC (1996) Regulation of the Na^+/H^+ Exchanger in Vascular Smooth Muscle. In The Na^+/H^+ Exchanger. Fliegel L, Ed., RG Landes Company, Texas, pp 47-67

¹⁶ Ebata S, Muto S, Okada K, Nemoto J, Amemiya M, Saito T, Asano Y (1999) Aldosterone activates Na^+/H^+ exchange in vascular smooth muscle cells by nongenomic and genomic mechanisms. Kidney Int 56: 1400-1412

¹⁷ Liu F, Gesek FA (2001) α_1 -Adrenergic receptors activate NHE1 and NHE3 through distinct signalling pathways in epithelial cells. Am J Physiol 280: F415-F425

¹⁸ Alberts B, Bray D, Lewis J, Raff M, Roberts K, Watson JD (1994) Diacylglycerol Activates Protein Kinase C. In Molecular Biology of the Cell. Garland Publishing, Inc., New York, pp 747-748

¹⁹ Wang H, Silva NLCL, Lucchesi PA, Haworth R, Wang K, Michalak M, Pelech S, Fliegel L (1997) Phosphorylation and Regulation of the Na^+/H^+ Exchanger through Mitogen-Activated Protein Kinase. Biochemistry 36: 9151-9158

²⁰ Moor AN, Fliegel L (1999) Protein Kinase-mediated Regulation of the Na^+/H^+ Exchanger in the Rat Myocardium by Mitogen-activated Protein Kinase-dependent Pathways. J Biol Chem 274(33): 22985-22992

²¹ Takahashi E, Abe J, Berk, BC (1997) Angiotensin II Stimulates p90^{rsk} in Vascular Smooth Muscle Cells. Circ Res 81: 268-273

²² Tominaga T, Ishizaki T, Narumiya S, Barber DL (1998) p160ROCK mediates RhoS activation of Na-H exchange. EMBO J 17: 4712-4722

²³ Fliegel L (1999) Functional and Cellular Regulation of the Myocardial Na^+/H^+ Exchanger. J Thromb Thrombolysis 8: 9-13

²⁴ Silva NLCL, Haworth RS, Singh D, Fliegel L (1995) The Carboxyl-Terminal Region of the Na⁺/H⁺ Exchanger Interacts with Mammalian Heat Shock Protein. *Biochemistry* 34: 10412-10420

²⁵ Wolska BM, Averyheart-Fullard V, Omachi A, Stojanovic MO, Kallen RG, and Solaro RJ (1997) Changes in Thyroid State Affect pH_i and Na_i⁺ Homeostasis in Rat Ventricular Myocytes. *J Mol Cell Cardiol* 29: 2653-2663

²⁶ Strazzabosco M, Poci C, Spirli C, Zsembery A, Granato A, Massimino ML Crepaldi G (1995) Intracellular pH regulation in Hep G2 cells: effects of epidermal growth factor, transforming growth factor-alpha and insulin-like growth factor-II on Na⁺/H⁺ exchange activity. *Hepatology* 22:588-97

²⁷ van Willigen G, Nieuwland R, Nurnberg B, Gorter G, Akkerman JN (2000) Negative regulation of the platelet Na⁺/H⁺ exchanger by trimeric G-proteins. *Eur J Biochem* 267: 7102-7108

²⁸ Garnovskaya MN, Gettys TW, van Biesen T, Prpic V, Chuprun JK, Raymond JR (1997) 5-HT_{1A} Receptor Activates Na⁺/H⁺ Exchange in CHO-K1 Cells through G_{iα2} and G_{iα3}. *J Biol Chem* 272: 7770-7776

²⁹ Aharonovitz O, Demaurex N, Woodside M, Grinstein S (1999) ATP dependence is not an intrinsic property of Na⁺/H⁺ exchanger NHE1: requirement for an ancillary factor. *Am J Physiol* 276:C1303-C1311

³⁰ Aharonovitz O, Zaun HC, Balla T, York JD, Orlowski J, Grinstein S (2000) Intracellular pH Regulation by Na⁺/H⁺ Exchange Requires Phosphatidylinositol 4,5-Bisphosphate. *J Cell Biol* 150: 213-224

³¹ Takewaki S, Kuro-o M, Hiroi Y, Yamazaki T, Noguchi T, Miyagishi A, Nakahara K, Aikawa M, Manabe I, Yazaki Y, Nagai R (1995) Activation of Na⁺-H⁺ Antipporter (NHE1) Gene Expression during Growth, Hypertrophy and Proliferation of the Rabbit Cardiovascular System. *J Mol Cell Cardiol* 27: 729-742

³² Elsing C, Reichen J, Marti U, Renner EL (1994) Hepatocellular Na⁺/H⁺ Exchange Is Activated at Transcriptional and Posttranscriptional Levels in Rat Biliary Cirrhosis. *Gastroenterology* 107: 468-78

³³ Haworth RS, Yasutake M, Brooks G, Avkiran M (1997) Cardiac Na⁺-H⁺ Exchanger During Postnatal Development in the Rat: Changes in mRNA Expression and Sarcolemmal Activity. *J Mol Cell Cardiol* 29: 321-332

³⁴ Chen F, Jarmakani JM, Van Dop C (1995) Developmental Changes in mRNA Encoding Cardiac Na⁺/H⁺ Exchanger (NHE1) in Rabbit. Biochem Biophys Res Commun 212: 960-967

³⁵ Canadian Dictionary of the English Language (1988) International Thomson Publishing, Ontario, Canada

³⁶ Rao GN, Sardet C, Pouyssegur J, Berk BC (1992) Na⁺/H⁺ Antiporter Gene Expression Increases During Retinoic Acid-Induced Granulocytic Differentiation of HL60 Cells. J Cell Physiol 151: 361-366

³⁷ Dyck JRB, Fliegel L (1995) Specific Activation of the Na⁺/H⁺ Exchanger Gene during Neuronal Differentiation of Embryonal Carcinoma Cells. J Biol Chem 270: 10420-10427

³⁸ Wang H, Singh D, Fliegel L (1997) The Na⁺/H⁺ Antiporter Potentiates Growth and Retinoic Acid-induced Differentiation of P19 Embryonal Carcinoma Cells. J Biol Chem 272: 26545-26549

³⁹ Yang W, Dyck JRB, Fliegel L (1996) Regulation of NHE1 expression in L6 muscle cells. Biochim Biophys Acta 1306: 107-113

⁴⁰ Miller RT, Counillon L, Pages G, Lifton RP, Sardet C, Pouyssegur J (1991) Structure of the 5'-Flanking Regulatory Region and Gene for the Human Growth Factor-activatable Na/H Exchanger NHE1. J Biol Chem 266: 10813-10819

⁴¹ Kolyada AY, Lebedeva TV, Johns CA, Madias NE (1994) Proximal regulatory elements and nuclear activities required for transcription of the human Na⁺/H⁺ exchanger (NHE1) gene. Biochim Biophys Acta 1217: 54-64

⁴² Dyck JRB, Silva NLCL, Fliegel L (1995) Activation of the Na⁺/H⁺ Exchanger Gene by the Transcription Factor AP-2. J Biol Chem 270: 1375-1381

⁴³ Yang W, Dyck JRB, Wang H, Fliegel L (1996) Regulation of NHE1 promoter in mammalian myocardium. Am J Physiol 270: H259-H266

⁴⁴ Wang H, Yang W, Fliegel L (1997) Identification of an HMG-like protein involved in regulation of Na⁺/H⁺ exchanger expression. Mol Cell Biochem 176: 99-106

⁴⁵ Fernandez-Rachubinski F, Fliegel L (2001) COUP-TFI & COUP-TFII regulate expression of the NHE through a nuclear hormone responsive element with enhancer activity. Eur J Biochem 268: 620-634

⁴⁶ Zhang J, Hagopian-Donaldson S, Serbedzija G, Elsemore J, Plehn-Dujowich D, McMahon AP, Flavell RA, Williams T (1996) Neural tube, skeletal and body wall defects in mice lacking transcription factor AP-2. *Nature* 318: 238-241

⁴⁷ Imagawa M, Chiu R, Karin M (1987) Transcription Factor AP-2 Mediates Induction by Two Different Signal-Transduction Pathways: Protein Kinase and cAMP. *Cell* 51: 251-260

⁴⁸ Williams T, Admon A, Luscher B, Tjian R (1998) Cloning and expression of AP-2, a cell-type-specific transcription factor that activates inducible enhancer elements. *Genes Dev.* 2: 1557-1569

⁴⁹ Moser M, Imhof A, Pscherer A, Bauer R, Amselgruber W, Sinowitz F, Hofstatter F, Schule R, Buettner R (1995) Cloning & characterization of a second AP-2 transcription factor: AP-2 β . *Development* 121: 2779-2788

⁵⁰ Chazaud C, Oulad-Abdelghani M, Bouillet P, Decimo D, Chambon P, Dolle P (1996) AP-2.2, a novel gene related to AP-2, is expressed in the forebrain, limbs and face during mouse embryogenesis. *Mech Dev* 54: 83-94

⁵¹ Oulad-Abdelghani M, Bouillet P, Chazaud C, Dolle P, Chambon P (1996) AP-2.2: A novel AP-2-related transcription factor induced by retinoic acid during differentiation of P19 embryonic carcinoma cells. *Exp Cell Res* 225: 338-347

⁵² Schorle H, Meier P, Buchert M, Jaenisch R, Mitchel P (1996) Transcription factor AP-2 essential for cranial closure and craniofacial development. *Nature* 318: 235-238

⁵³ Nottoli T, Hagopian-Donaldson S, Zhang J, Perkins A, Williams T (1998) AP-2-null cells disrupt morphogenesis of the eye, face, and limbs in chimeric mice. *Proc Natl Acad Sci* 95: 13714-13719

⁵⁴ Moser M, Pscherer A, Roth C, Becker J, Mucher G, Zerres K, Dixkens C, Weis J, Guay-Woodford L, Buettner R, Fassler R (1997) Enhanced apoptotic cell death of renal epithelial cells in mice lacking transcription factor AP-2 β . *Gene Dev.* 11: 1938-1948

⁵⁵ Pereira FA, Tsai MJ, Tsai SY (2000) COUP-TF orphan nuclear receptors in development and differentiation. *Cell Mol Life Sci* 57: 1388-1398

- ⁵⁶ Qiu Y, Pereira FA, DeMayo FJ, Lydon JP, Tsai SY, Tsai MJ (1997) Null mutation of mCOUP-TF1 results in defects in morphogenesis of the glossopharyngeal ganglion, axonal projection, and arborization. *Genes Dev* 11: 1925-1937
- ⁵⁷ Pereira FA, Qiu Y, Zhou G, Tsai MJ, Tsai SY (1999) The orphan nuclear receptor COUP-TFII is required for angiogenesis and heart development. *Genes Dev* 13: 1037-1049
- ⁵⁸ Cox GA, Lutz CM, Yang C, Biemesderfer D, Bronson RT, Fu A, Aronson PS, Noebels JL, Frankel WN (1997) Sodium/Hydrogen Exchanger Gene Defect in Slow-Wave Epilepsy Mutant Mice. *Cell* 91: 139-148
- ⁵⁹ Bell S, Schreiner CM, Schultheis PJ, Miller ML, Evans RL, Vorhees CV, Shull G, Scott WJ (1999) Targeted disruption of the murine Nhel locus induces ataxia, growth retardation and seizures. *Am J Physiol* 276: C788-C795
- ⁶⁰ Wu D, Stassen JM, Seidler R, Doods H (2000) Effects of BIIB513 on ischemia-induced arrhythmias and myocardial infarction in anesthetized rats. *Basic Res Cardiol* 95: 449-456
- ⁶¹ Kusumoto K, Haist JV, Karmazyn M (2001) Na^+/H^+ exchange inhibition reduces hypertrophy and heart failure after myocardial infarction in rats. *Am J Physiol* 280: H738-H745
- ⁶² Avkiran M, Yasutake, M (1996) Role of the Sarcolemmal Na^+/H^+ Exchanger in Arrhythmogenesis During Reperfusion of Ischemic Myocardium. In *The Na^+/H^+ Exchanger*. Fliegel L, Ed., RG Landes Company, Texas, pp 173-187
- ⁶³ Karmazyn M, Gan XT, Humphreys RA, Yoshida H, Kusumoto K (1999) The Myocardial Na^+/H^+ Exchange Structure, Regulation and Its Role in Heart Disease. *Circ Res* 85: 777-786
- ⁶⁴ Silver RB, Mackins CJ, Smith NCE, Koritchneva IL, Lefkowitz K, Lovenberg TW, Levi R (2001) Coupling of histamine H_3 receptors to neuronal Na^+/H^+ exchange: A novel protective mechanism in myocardial ischemia. *Proc Natl Acad Sci* 98: 2855-2859
- ⁶⁵ Yoshida H, Karmazyn M (2000) Na^+/H^+ exchange inhibition attenuates hypertrophy and heart failure in 1-wk postinfarction rat myocardium. *Am J Physiol* 278: H300-H304

⁶⁶ Zoorob RJ, Arif AM, Morelli V (2000) Hypertension. Prim Care; Clinics in Office Practice 27: 589-614

⁶⁷ Orlov SN, Adragna NC, Adarichev VA, Hamet P (1999) Genetic and biochemical determinants of abnormal monovalent ion transport in primary hypertension. Am J Physiol 276: C511-C536

⁶⁸ Siczkowski M, Davies JE, Ng LL (1995) $\text{Na}^+ \text{-H}^+$ Exchanger Isoform 1 Phosphorylation in Normal Wistar-Kyoto and Spontaneously Hypertensive Rats. Circ Res 76: 825-831

⁶⁹ Phan VN, Kusuvara M, Lucchesi PA, Berk BC (1997) A 90-kD $\text{Na}^+ \text{-H}^+$ Exchanger Kinase has Increased Activity in Spontaneously Hypertensive Rat Vascular Smooth Muscle Cells. Hypertension 29: 1265-1272

⁷⁰ Kuro-o M, Hanaoka K, Hiroi Y, Noguchi T, Fujimori Y, Takewaki S, Hayasaka M, Katoh H, Miyagishi A, Nagai R, Yazaki Y, Nabeshima Y (1995) Salt-sensitive Hypertension in Transgenic Mice Overexpressing Na^+ -Proton Exchanger. Circ Res 76: 148-153

⁷¹ Hannan KM, Little PJ (1998) Mechanisms regulating the vascular smooth muscle Na/H exchanger (NHE1) in diabetes. Biochem Cell Biol 76: 751-759

⁷² Besson P, Fernandez-Rachubinski F, Yang W, Fliegel L (1998) Regulation of Na^+/H^+ exchanger gene expression: mitogenic-stimulation increases NHE1 promoter activity. Am J Physiol 274: C831-C839

⁷³ Williams B, Howard RL (1994) Glucose-induced Changes in Na^+/H^+ Antiport Activity and Gene Expression in Cultured Vascular Smooth Muscle Cells. J Clin Invest 93: 2623-2631

⁷⁴ Pierce GN, Slotin T, Fliegel L, Gilchrist JSC, Maddaford TG (1996) Expression and Activity of the Sodium-Hydrogen Exchanger in Cardiac Sarcolemma in Health and Disease. In The Na^+/H^+ Exchanger. Fliegel L, Ed., R.G.Landes Company, Texas, pp. 217-228

⁷⁵ Reshkin SJ, Bellizzi A, Caldeira S, Albarani V, Malanchi I, Poignee M, Alunni-Fabbroni M, Casavola V, Tommasino M (2000) Na^+/H^+ exchanger-dependent intracellular alkalinization is an early event in malignant transformation and plays an essential role in the development of subsequent transformation-associated phenotypes. FASEB J 14: 2185-2197

-
- ⁷⁶ Yamagata M, Tannock IF (1996) Therapeutic Potential of Inhibitors of Na⁺/H⁺ Exchange Activity in Tumor Selective Therapy. *In* The Na⁺/H⁺ Exchanger. Fliegel L, Ed., RG Landes Company, Texas, pp 269-291
- ⁷⁷ Shimomura O, Johnson FH, Saiga Y (1962) Extraction, purification, and properties of aequorin, a bioluminescent protein from the luminous hydromedusan, Aequorea. *J Cell Comp Physiol* 59: 223-39
- ⁷⁸ Tsien RY (1998) The Green Fluorescent Protein. *Annu Rev Biochem* 67: 509-44
- ⁷⁹ Ikawa M, Yamada S, Nakanishi T, Okabe M (1998) 'Green mice' and their potential usage in biological research. *FEBS Lett* 430: 83-87
- ⁸⁰ Ormo M, Cubitt A, Kallio K, Gross L, Tsien R, Remington S (1996) Crystal structure of the Aequorea victoria green fluorescent protein. *Science* 273: 1392-1395
- ⁸¹ Yang F, Moss LG, Phillips GN Jr (1996) The molecular structure of green fluorescent protein. *Nature Biotechnol* 14: 1219-1220
- ⁸² Ikawa M, Kominami K, Yoshimura Y, Tanaka K, Nishimune Y Okabe M (1995) Green fluorescent protein as a marker in transgenic mice. *Develop Growth Differ* 37: 455-459
- ⁸³ Fukumura D, Xavier R, Sugiura T, Chen Y, Park E, Lu N, Selig M, Nielsen G, Taksir T, Jain RK, Seed B (1998) Tumor Induction of VEGF Promoter Activity in Stromal Cells. *Cell* 94: 715-725
- ⁸⁴ Naramura M, Hu R, Gu H (1998) Mice with a Fluorescent Marker for Interleukin 2 Gene Activation. *Immunity* 9: 209-216
- ⁸⁵ Mesaeli N, Nakamura K, Zvaritch E, Dickie P, Dziak E, Krause K, Opas M, MacLennan D, Michalak M (1999) Calreticulin Is Essential for Cardiac Development. *J Cell Biol* 144: 857-868
- ⁸⁶ Cohn, M (1989) The way it was: a commentary by Melvin Cohn. *Biochim Biophys Acta* 1000: 109-112
- ⁸⁷ Jacob F, Monod J (1961) Genetic Regulatory Mechanisms in the Synthesis of Proteins. *J Mol Biol* 3: 318-356

- ⁸⁸ Torrente Y, Tremblay J, Pisati F, Belicchi M, Rossi B, Sironi M, Fortunato F, El Fahime M, Grazia D'Angelo M, Caron NJ, Constantin G, Paulin D, Scarlato G, Brezolin N (2001) Intraarterial Injection of Muscle-derived CD34⁺Sca-1⁺ Stem Cells Restores Dystrophin in *mdx* Mice. *J Cell Biol* 152: 335-348
- ⁸⁹ Shimizu-Albergue M, Ippolito DL, Beavo JA (2001) Downregulation of Fasting-Induced cAMP Response Element Mediated Gene Induction by Leptin in Neuropeptide Y Neurons of the Arcuate Nucleus. *J Neurosci* 21: 1238-1246
- ⁹⁰ Mazzalupo S, Coulombe PA (2001) A reporter transgene based on a human keratin 6 gene promoter is specifically expressed in the periderm of mouse embryos. *Mech Dev* 100: 65-69
- ⁹¹ Zhang JCL, Kim S, Helmke BP, Yu W, Du KL, Lu MM, Strobeck M, Yu Q, Parmacek MS (2001) Analysis of SM22 α -Deficient Mice Reveals Unanticipated Insights into Smooth Muscle Cell Differentiation and Function. *Mol Cell Biol* 21: 1336-1344
- ⁹² Igarashi P, Shashikant CS, Thomson RB, Whyte DA, Liu-Chen S, Ruddle FH, Aronson PS (1999) Ksp-cadherin gene promoter. II. Kidney-specific activity in transgenic mice. *Am J Physiol*. 277: F599-F610
- ⁹³ Hogan B, Beddington R, Costantini F, Lacy E (1994) Manipulating the Mouse Embryo: A Laboratory Manual, 2nd Edition. Cold Spring Harbor Laboratory Press, New York
- ⁹⁴ Argentin S, Sun YL, Lührmann I, Schmidt TJ, Drouin J, Nemer M (1991) Distal cis-acting promoter sequences mediate glucocorticoid stimulation of cardiac atrial natriuretic factor gene transcription. *J Biol Chem* 266: 23315-23322
- ⁹⁵ Hanley T, Merlie JP (1991) Transgene Detection in Unpurified Mouse Tail DNA by Polymerase Chain Reaction. *BioTechniques* 10: 56
- ⁹⁶ Hecker KH, Roux KH (1996) High and Low Annealing Temperatures Increase Both Specificity and Yield in Touchdown and Stepdown PCR. *BioTechniques* 20: 478-485
- ⁹⁷ de Vries JE, Vork MM, Roemen THM, de Jong YF, Cleutjens JPM, van der Vusse GJ, van Bilsen M (1997) Saturated but not mono-unsaturated fatty acids induce apoptotic cell death in neonatal rat ventricular myocytes. *J Lipid Res* 38: 1384-1394

⁹⁸ Talor, Z, Ng SC, Cragoe, EJ, Arruda, AL (1989) Methylisobutyl amiloride: a new probe to assess the number of Na-H Antiporters. *Life Sciences* 45: 517-523

⁹⁹ Dr. D. Singh, personal communication

¹⁰⁰ Takewaki S, Kuro-o M, Hiroi Y, Yamazaki T, Noguchi T, Miyagishi A, Nakahara K, Aikawa M, Manabe I, Yazaki Y, Nagai R (1995) Activation of Na⁺-H⁺ Antiporter (NHE1) Gene Expression during Growth, Hypertrophy and Proliferation of the Rabbit Cardiovascular System. *J Mol Cell Cardiol* 27: 729-742

¹⁰¹ Yoshida H, Karmazyn M (2000) Na⁺/H⁺ exchange inhibition attenuates hypertrophy and heart failure in 1-wk postinfarction rat myocardium. *Am J Physiol* 278: H300-H304

¹⁰² Kaufman, MH (1995) The Atlas of Mouse Development. Academic Press Limited, San Diego, CA

¹⁰³ Strazzabosco M, Poci C, Spirli C, Zsembery A, Granato A, Massimino ML, Crepaldi G (1995) Intracellular pH regulation in Hep G2 cells: effects of epidermal growth factor, transforming growth factor-alpha and insulin-like growth factor-II on Na⁺/H⁺ exchange activity. *Hepatology* 22: 588-597

¹⁰⁴ Garcia-Canero R, Trilla C, Perez de Diego J, Diaz-Gil JJ, Cobo JM (1999) Na⁺:H⁺ exchange inhibition induces intracellular acidosis and differentially impairs cell growth and viability of human and rat hepatocarcinoma cells. *Toxicol Lett* 106: 215-228

¹⁰⁵ Igarashi P, Shashikant CS, Thomson RB, Whyte DA, Liu-Chen S, Ruddle FH, Aronson PS (1999) Ksp-cadherin gene promoter. II. Kidney-specific activity in transgenic mice. *Am J Physiol* 277: F599-F610

¹⁰⁶ Rich IN, Brackmann I, Worthington-White D, Dewey MJ (1998) Activation of the Sodium/Hydrogen Exchanger Via the Fibronectin-Integrin Pathway Results in Hematopoietic Stimulation. *J Cell Physiol* 177: 109-122

¹⁰⁷ Palis J, Robertson S, Kennedy M, Wall C, Keller G (1999) Development of erythroid and myeloid progenitors in the yolk sac and embryo proper of the mouse. *Development* 126: 5073-5084

¹⁰⁸ Chiocchetti A, Tolosano E, Hirsch E, Silengo L, Altruda F (1997) Green fluorescent protein as a reporter of gene expression in transgenic mice. *Biochim Biophys Acta* 1352: 193-202

¹⁰⁹ Henning SJ (1981) Postnatal development: coordination of feeding, digestion & metabolism. Am J Physiol 241: G199-G214

¹¹⁰ Mitchell PJ, Timmons PM, Hebert JM, Rigby PW, Tjian R (1991) Transcription factor AP-2 is expressed in neural crest cell lineages during mouse embryogenesis. Genes Dev 5: 105-119

¹¹¹ Talbot D, Lorgin J, Schorle H (1999) Spatiotemporal Expression Pattern of Keratins in Skin of AP-2 α -deficient Mice. J Invest Dermatol 113: 816-820

University of Alberta Library



0 1620 1488 8562

B45615